Aalto-yliopisto
Insinööritieteiden
korkeakoulu

Eero Assmuth

Performance of roadside filtration systems in the treatment of stormwater

Master's thesis for the degree of Master of Science in Technology submitted for inspection

Espoo, 28 December 2017
Supervisor: Professor Harri Koivusalo
Instructors: D.Sc. Nora Sillanpää & M.Sc. Antti Auvinen

Aalto University
School of Engineering

Aalto University, P.O. BOX 11000, 00076
AALTO
www.aalto.fi

Abstract of master's thesis

Author	Eero Assmuth
Title of thesis	Performance of roadside filtration systems in the treatment of stormwater
Master programme	Water and Environmental Engineering **Code** ENG29
Thesis supervisor	Professor Harri Koivusalo
Thesis advisors	D.Sc. Nora Sillanpää & M.Sc. Antti Auvinen
Date 28.12.2017	**Number of pages** 67+26 **Language** English

Abstract

Urban stormwater is regarded as a remarkable source of pollutants entering water bodies. Therefore, stormwater management structures such as roadside sand filters have been developed in recent years. These filters can be amended with different materials such as biochar, but currently knowledge on filter performance is scarce, and especially studies under realistic field conditions are lacking. For this reason, this study focuses on accurate field experiments. To the author's knowledge, this is the first study to examine biochar amended stormwater filters in field conditions.

Two different full-scale roadside filters were investigated in Vantaa, Finland during summer 2017. One filter consists of sand and the other of sand and birch biochar. Rainfall and flow rates of the filter effluents were measured at the study site during the study period and plenty of water quality samples were gathered during three rain events. The samples were analyzed for 14–30 parameters. The laboratory results were analyzed with statistical methods, and event mean concentrations (*EMC*) and pollutant removal efficiencies were determined for the filters. Additionally, geochemical modelling (PHREEQC) was utilized in order to reveal the pollutant removal mechanisms occurring within the filters.

The results showed that both the untreated stormwater and the effluents from the filters expressed high temporal variability both during and between the examined rain events in terms of pollutant concentrations. Both filter types were observed to efficiently remove heavy metals and suspended solids from the stormwater. Also total phosphorus removal was efficient although both filters leached phosphate. Biochar amendment showed improved performance especially in nitrogen removal, whereas it impaired total organic carbon retention. Also the performance related to heavy metals and stormwater quantity was slightly better with the biochar amended filter.

Due to the high temporal variability, studying of similar filters clearly requires several samples per examined rain events, but also the number of studied events should be higher than in this study. Based on the results, biochar amendment seems to be an interesting option especially for areas with high nitrogen loadings. Also slightly improved heavy metal retention capacity and water holding capacity could be useful properties for some locations.

Keywords Stormwater filtration, Field study, Biochar amendment, PHREEQC modelling

Aalto-yliopisto
Insinööritieteiden
korkeakoulu

Aalto-yliopisto, PL 11000, 00076 AALTO
www.aalto.fi
Diplomityön tiivistelmä

Tekijä Eero Assmuth

Työn nimi Tienvarsisuodattimien suorituskyky huleveden käsittelyssä

Maisteriohjelma Water and Environmental Engineering **Koodi** ENG29

Työn valvoja Professori Harri Koivusalo

Työn ohjaajat TkT Nora Sillanpää & DI Antti Auvinen

Päivämäärä 28.12.2017 **Sivumäärä** 67+26 **Kieli** Englanti

Tiivistelmä

Hulevesi tiedostetaan merkittäväksi urbaanien vesistöjen saastuttajaksi. Huleveden hallintarakenteita, kuten tienvarsille sijoitettavia hiekkasuodattimia, on siksi kehitetty viime vuosina. Näitä suodattimia voidaan tehostaa erilaisilla materiaaleilla, kuten biohiilellä, mutta niiden suorituskyky tunnetaan heikosti ja erityisesti realistisissa kenttäolosuhteissa tehtyjä kokeita on vähän. Sen takia tämä tutkimus keskittyi tarkkoihin kenttäkokeisiin. Biohiilellä parannettuja huleveden hiekkasuodattimia tutkittiin tiettävästi ensimmäistä kertaa kenttäolosuhteissa.

Työssä tutkittiin kahta Vantaalla sijaitsevaa täysimittaista huleveden tienvarsisuodatinta kesällä 2017. Toinen suodatin koostuu hiekasta ja toinen hiekasta ja koivubiohiilestä. Sadantaa ja suodattimien virtaamia seurattiin kentällä tutkimuksen ajan, ja lukuisia vedenlaatunäytteitä kerättiin kolmen sadetapahtuman aikana. Vesinäytteistä analysoitiin 14–30 parametria. Laboratoriotuloksia analysoitiin tilastollisilla menetelmillä ja haitta-aineille määritettiin sadetapahtumien keskimääräiset pitoisuudet (*EMC*) ja suodattimien puhdistustehokkuudet. Lisäksi geokemiallista mallinnusta (PHREEQC) käytettiin haitta-aineiden puhdistumismekanismien selvittämiseen.

Tulokset osoittivat, että haitta-aineiden pitoisuudet vaihtelivat suuresti tutkittujen sadetapahtumien aikana ja niiden välillä sekä käsittelemättömässä hulevedessä että suodattimista purkautuvassa vedessä. Molemmat suodatintyypit poistivat hulevedestä tehokkaasti raskasmetalleja ja kiintoainetta. Myös kokonaisfosforin poistaminen oli tehokasta, vaikka molemmat suodattimet vuosivat fosfaattia. Biohiilen lisäys paransi suodattimen suorituskykyä erityisesti typen poistossa, mutta huononsi orgaanisen hiilen pidättymistä. Myös suorituskyky raskasmetallien ja huleveden määrän suhteen oli hieman parempaa suodattimella, johon oli lisätty biohiiltä.

Havaitusta suuresta ajallisesta vaihtelusta johtuen vastaavien suodattimien tutkiminen vaatii useita vesinäytteitä tutkittuja sadetapahtumia kohden. Myös tutkittujen sadetapahtumien määrän pitäisi olla suurempi kuin tässä tutkimuksessa. Tulosten perusteella biohiilen lisääminen hulevesisuodattimiin vaikuttaa mielenkiintoiselta vaihtoehdolta erityisesti alueilla, missä typpikuormitus on suurta. Myös hieman parempi raskasmetallien poistuminen ja veden pidätyskyky voisivat olla hyödyllisiä ominaisuuksia joissakin kohteissa.

Avainsanat Huleveden suodatus, Kenttätutkimus, Biohiili, PHREEQC mallinnus

Acknowledgements

This Master's thesis was conducted at the Aalto University School of Engineering in collaboration with the City of Vantaa. The work was done within the STORMFILTER project (*Engineered Infiltration Systems for Urban Stormwater Quality and Quantity, 2015-2017*) led by VTT (Technical Research Centre of Finland). The project involved Aalto University, University of Helsinki and 17 industrial and municipal partners. The project was funded by TEKES (Finnish Funding Agency for Innovation), industrial partners, VTT and Aalto University.

I am very grateful for the additional funding that Maa- ja vesitekniikan tuki ry (MVTT) provided for this thesis.

I would like to thank Professor Harri Koivusalo for supervising this thesis and for his valuable comments. Additionally, thank you for helping me with the installation of field instrumentation during the cold and sunny May.

I would like to express my deepest gratitude to my excellent instructors D.Sc. Nora Sillanpää from Aalto University and M.Sc. Antti Auvinen from the City of Vantaa. I am especially thankful for the long discussions with Nora and appreciate her encouragements during the work.

I wish to thank the City of Vantaa for collaboration. The city constructed the investigated filters and thus enabled the whole thesis.

I am most thankful for D.Sc. Laura Wendling from VTT for introducing me into geochemical modelling and for the very useful help and comments she provided.

I wish to thank the staff of the Water Laboratory of Aalto University, especially Aino Peltola, who taught me the laboratory analysis methods, and Antti Louhio for assembling the flow rate meters.

I would like to thank Professor Heikki Setälä from University of Helsinki for borrowing rain gauges for field measurements, and D.Sc. Tero Niemi from Aalto University for helping me with them.

Last, but not least, I want to thank my wife Moona Assmuth and my son Peetu for supporting me during this intensive project.

In Helsinki on 11 December 2017

Eero Assmuth

Table of contents

Abbreviations

A	Area
AADT	Annual average daily traffic
ADP	Antecedent dry period
Al	Aluminum
BOD	Biological oxygen demand
C	Concentration
Ca	Calcium
Cd	Cadmium
Cl	Chlorine
COD	Chemical oxygen demand
Cu	Copper
d	Rain depth
DEHP	Di(2-ethylhexyl) phthalate
DOC	Dissolved organic carbon
EC	Electrical conductivity
EMC	Event mean concentration
EMC_{eff}	EMC efficiency
EMV	Event mean value
Fe	Iron
FMI	Finnish Meteorological Institute
HCO_3	Bicarbonate
IAP	Ion activity product
K	Potassium
K_s	Solubility product
L	Pollutant load
LID	Low impact development
m_{eff}	Mass efficiency
Mg	Magnesium
Mn	Manganese
MTBE	Methyl tert-butyl ether
Na	Sodium
NH_4	Ammonium
Ni	Nickel
NO_2	Nitrite
NO_3	Nitrate
NOEL	No observable effects limit
NPEO	Nonylphenol ethoxylates and degradation products
PAH	Polycyclic aromatic hydrocarbon
Pb	Lead
PCB 28	Polychlorinated biphenyl 28
PCP	Pentachlorophenol
PO_4	Phosphate
Q	Flow rate
R^2	Coefficient of determination
r_s	Spearman correlation coefficient
SI	Saturation index
Si	Silicon

SO_4	Sulfate
SUDS	Sustainable urban drainage systems
t	Time
TN	Total nitrogen
TOC	Total organic carbon
TP	Total phosphorus
TSS	Total suspended solids
USGS	United States Geological Survey
V	Volume
VTT	Technical Research Centre of Finland
Zn	Zinc

1 Introduction

1.1 Background

The term *stormwater* means surface runoff generated by rainfall or snowmelt on impervious surfaces (Land Use and Building Act 132/1999; SKL 2012). Impervious surfaces are present everywhere in manmade areas, including streets, roofs and parking lots, and their amount is increasing due to urbanization (Sillanpää 2013; Solpuker et al. 2014).

In natural conditions, most of the precipitation over land areas is either infiltrated into the ground or evaporated and transpirated via plants, which keeps the amount of surface runoff small. On the contrary, in highly dense cities with large fraction of impervious surfaces preventing infiltration, most of the precipitation turns into stormwater runoff. Traditionally, this has been thought mainly as a quantity problem (Figure 1a), and the stormwater management has meant only conveyance of the peak flows to avoid flooding during heavy storms (Genç-Fuhrman et al. 2007; Valtanen et al. 2010). However, efficient drainage via a stormwater sewer network conveys stormwater to receiving waters quickly, which means that intensive rainfalls increase the flow rates of small streams rapidly (SKL 2012). On the other hand, the stream flow rates can be too low for the stream population during dry periods, because the precipitated water is not sufficiently delayed within the catchment area.

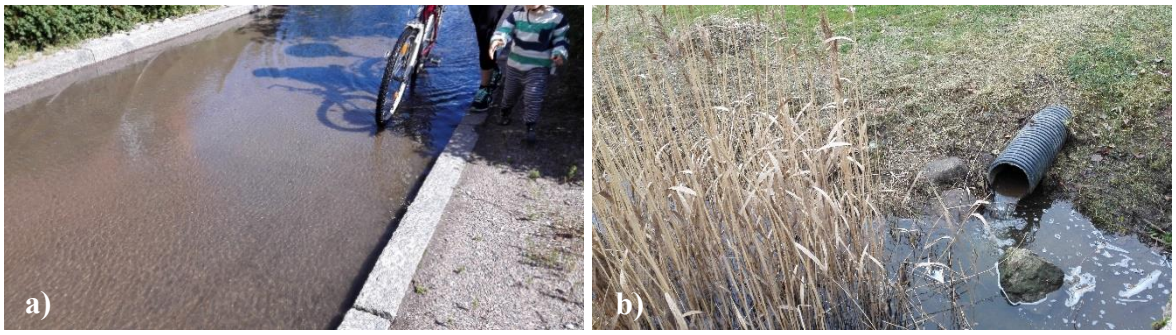

Figure 1. Small-scale quantity (a) and quality (b) problems related to stormwater. a) Stormwater flooding on a walkway long after rainfall. b) A stormwater sewer discharging into an urban stream habituated by endangered sea trout.

Around 1980s, stormwater has been recognized to have also major quality problems (Taebi & Droste 2004; Genç-Fuhrman et al. 2007; Valtanen et al. 2010), as runoff washes pollutants from the surfaces of urban areas (Figure 1b). Stormwater would in fact require treatment before discharging it into receiving waters (Sillanpää 2013; Reddy et al. 2014b; Valtanen 2015; Taka 2017). Therefore, stormwater being discharged untreated into surface waters and groundwater resources is currently understood as an environmental hazard, which possibly endangers human health (LeFevre et al. 2014; Reddy et al. 2014b). The problem is likely to expand, since ongoing urbanization increases not only the quantity but also the pollutant concentrations of stormwater (Sillanpää 2013).

In the Finnish legislation, demands on stormwater were first included in 2014 (Land Use and Building Act 132/1999). The new Section 13a of the law 1999/132 for instance states that stormwater should be infiltrated and retained at their source, and the harmful impacts on the environment should be avoided. In addition, the law mentions that the mitigation against climate change impacts must be considered in the management of stormwater.

Urban runoff degrades surface water quality, as stormwater may contain higher pollutant concentrations than effluents from wastewater treatment plants (Taebi & Droste 2004; LeFevre et al. 2014). For instance in the USA, stormwater from urban areas is the second most severe contributor to surface water pollution (Walker et al. 1999). These surface waters include urban streams, which have ecosystems sensitive to pollutants due to their small size. Moreover, polluted stormwater infiltrate into groundwater, which is a typical source of drinking water, thus hazarding public health in addition to the environment (Reddy et al. 2014b). Stormwater washes impurities e.g. from streets and parking lots and as a result, it contains all kinds of pollutants from human activities including significant amounts of heavy metals and PAHs (Walker et al. 1999; Reddy et al. 2014b).

Treatment of stormwater is already practiced to some extent, but for instance in Finland, most of the urban stormwater is conveyed to the nearest receiving water without any treatment (Valtanen et al. 2010). Fortunately, optional effective treatment methods, such as infiltration, biofiltration and sand filtration, are available. Currently, significant effort is directed towards managing the quality issues of stormwater by constructing different structures that reduce the amount of pollutants (Westerlund et al. 2003; Taebi & Droste 2004; Genç-Fuhrman et al. 2007).

Since the awareness of stormwater as a major pollutant has grown only relatively recently, the knowledge on stormwater characteristics and treatment methods is still limited and many studies conclude that further experiments are essential (Westerlund et al. 2003; Inha et al. 2013; Sillanpää 2013). Especially, there is a lack of stormwater treatment studies under realistic full-scale conditions (Genç-Fuhrman et al. 2007; Wu & Zhou 2009; Monrabal-Martinez et al. 2017), since the theoretical knowledge should be set against practical contexts (Sillanpää 2013).

1.2 Stormwater pollutants

Stormwater contains impurities, which are washed from the urban surfaces such as roads and roofs. Rainwater itself contains pollutants such as sulfates and ammonium (Valtanen et al. 2010). The impurities in stormwater include heavy metals, nutrients, suspended solids, pathogens, pesticides, petroleum hydrocarbons and polycyclic aromatic hydrocarbons (PAHs) and microplastics (Walker et al. 1999; LeFevre et al. 2014; Magnusson et al. 2016). The pollutants originate from several sources from both human activities and natural processes, including vehicles, salting of roads, building materials, industrial emissions, pesticides and atmospheric fallout (Walker et al. 1999; Valtanen et al. 2010; SKL 2012). In addition, stormwater may contain bacteria mainly from animal wastes and wastewater sewer overflows (SKL 2012). The composition of stormwater varies widely, depending e.g. on the location, preceding dry period, rain intensity, and human activities such as traffic volumes and land use (LeFevre et al. 2014).

The main nutrients in stormwater are nitrogen and phosphorus (LeFevre et al. 2014). They originate from sources such as fertilizers, died vegetation, detergents, animal feces and dry and wet deposition from the atmosphere (Valtanen et al. 2010; LeFevre et al. 2014). Also vehicular exhaust gases contain nutrients, such as different oxides of nitrogen (NO_x).

Stormwater generated on roads typically contains high concentrations of heavy metals originating mainly from vehicles (Prestes et al. 2006). Vehicular sources include the wearing of brakes, clutches and tires, corrosion of the road and combustion of fuel and lubricating oils (Walker et al. 1999; Genç-Fuhrman et al. 2007). In addition, deicers and grit used in wintertime road maintenance may contain traces of heavy metals (Galfi et al. 2017). Typical metals in stormwater are copper, nickel, chromium, zinc, iron, aluminum and lead (Genç-Fuhrman et al. 2007; Valtanen et al. 2010). Since heavy metals are not degradable in the environment and have negative effects on aquatic environments, they are important in stormwater treatment (Genç-Fuhrman et al. 2007).

In addition to the spatial variation, the pollutant concentrations of stormwater vary highly with time (Monrabal-Martinez et al. 2017). Concentrations vary between storms (eg. Prestes et al. 2006) but also remarkably during each rain event. For instance, heavy metal concentrations can vary up to several orders of magnitude (Genç-Fuhrman et al. 2007). Especially after a long dry weather period allowing pollutant accumulation on the urban surfaces, initial concentrations at the beginning of rainfall can be very high (Genç-Fuhrman et al. 2007). Also snowmelt can cause extreme pollutant loads due to accumulation into snowpack (Westerlund et al. 2003; Genç-Fuhrman et al. 2007).

Antecedent dry period (ADP) is a hydrological parameter often used to assess pollutant accumulation on urban surfaces, and thus the pollutant concentrations of stormwater. For instance, Tiefenthaler et al. (2002) observed pollutant accumulation during dry periods. However, according to Sillanpää & Koivusalo (2015), the amount of precipitation during preceding days may affect the concentrations even more than the length of ADP. The effects of both the length of ADP and the amount of precipitation during preceding days are not very clear in climates in which precipitation is evenly distributed year-round – for instance in Finland (Sillanpää & Koivusalo 2015). In addition, ADP and the amount of precipitation influence stormwater volumes through changes in depression storages within the catchment area (Kaczala et al. 2012).

Due to the high temporal variability, the determination of the pollutant concentrations in stormwater is a difficult task. A single water sample is not adequate to determine the concentrations as it describes the water properties at a specific moment of time. Instead, several samples should be taken during each examined rain event and the number of studied events should be relatively high. (Barbosa et al. 2012)

In the Finnish legislation, there are no regulatory limits for urban runoff quality (Inha et al. 2013). Therefore, Inha et al. (2013) used groundwater and surface water threshold values as well as drinking water quality requirements to assess the pollution of stormwater. Also other Finnish stormwater studies (e.g. Suihko 2016) apply reference values for surface waters. However, these limit values do not include all pollutants, which are typically present in stormwater. In addition, these limit values are not necessary applicable to stormwater because they can be unrealistically strict.

Since in Finland there is no legislation or official threshold values for stormwater pollutants, it is not clear which reference values should be used when comparing measured concentrations. Another question is which quality parameters are the most important ones. For instance, the City of Vantaa is currently applying threshold values for construction sites (City of Espoo 2015) for stormwater quality assessment. These limits include pH and

concentrations of suspended solids and oils. Eriksson et al. (2007) listed selected stormwater priority pollutants, which are targeted e.g. for comparison of different stormwater treatment methods (Table 1). Also Galfi et al. (2017) used Cd, Cr, Cu, Ni, Pb and Zn as indicators of anthropogenic activities, and applied Swedish recommended concentrations for comparison (Alm et al. 2010; Table 2). In addition, Galfi et al. (2017) studied the amount of Al, Ca, Fe, K, Mg and Na.

Table 1. Selected stormwater priority pollutants by Eriksson et al. (2007). Abbreviations are explained in the beginning of the study.

Basic parameters	Metals	PAHs	Herbicides	Miscellaneous
BOD	Zn	Benzo[a]pyrene	Terbutylazine	NPEO
COD	Cd	Naphthalene	Pendimethalin	PCP
TSS	Cr	Pyrene	Phenmedipham	DEHP
TN	Cu		Glyphosate	PCB 28
TP	Ni			MTBE
pH	Pb			
	Pt			

Setting the threshold values for stormwater seems to be complicated, since the concentrations vary widely depending on several factors, such as traffic volumes (e.g. Inha et al. 2013; LeFevre et al. 2014). Table 2 combines suggested limit values from several sources as well as measured values from roads similar to the road at the study site of this thesis (Section 2.1).

Table 2. Threshold values and typical concentrations of different pollutants in stormwater.

	Stockholm Vatten (2001) Low treatment need – High treatment need	**Travikverket (2011)** AADT 10000-15000	**Alm et al. (2010)** Recommended maximum annual concentration*	**EPA Ireland (2012)** Warning limit - Action limit	**Inha et al. (2013)** Road Kangasalantie AADT 10000
TSS [mg/l]	50 – 175	50 – 200	40 – 100	25 – 50	
TOC [mg/l]				30 – 40	
TN [mg/l N]	1.25 – 5	0.05 – 8	2.0 – 3.5		
NH_4 [mg/l N]					0.018 – 0.33
TP [mg/l P]	0.1 – 0.2	0.1 – 0.2	0.16 – 0.250		
Cd [µg/l]	0.3 – 1.5	0.2 – 1	0.4 – 0.5		
Cr [µg/l]	15 – 75		10 – 25		5 – 93
Cu [µg/l]	9 – 45	10 – 50	18 – 40		
Hg [µg/l]	0,04 – 0,2				
Pb [µg/l]	3 – 15	5 – 40	8 – 15		2 – 26
Ni [µg/l]	45 – 225		15 – 30		
Zn [µg/l]	60 – 300	50 – 300	75 – 150		55 – 510
pH				6 – 9	
EC [mS/m]					2.6 – 97
PAH [µg/l]	1 – 2	0.1 – 1			0.083 – 6.85

* Depending on the receiving water and discharge method.

Pollutants in stormwater are either in dissolved form or particulate form attached to suspended solids. Most of the contaminants in stormwater are in particulate form (Göbel et

al. 2007) and therefore it has been regarded to be the main form of pollutants. Recently, however, the importance of the dissolved pollutants is also understood, as they are more bioavailable and thus more readily influencing the receiving waters (Valtanen et al. 2010; Monrabal-Martinez 2017).

The pollutants mainly associated with suspended solids include Pb, Fe, Al, Cr, P and PAHs, whereas Cu, Cd, Ni, Zn and NO_3 are mainly in dissolved form (Walker et al. 1999; Prestes et al. 2006; Genç-Fuhrman et al. 2007; Valtanen et al. 2010; Huber, Welker & Helmreich 2016). This explains why e.g. Pb and Cr have very low mobility in sandy soils whereas nitrates have high mobility (Pitt 1996). Particulate substances attached to suspended solids are easier to remove from stormwater than dissolved ones. Particulate pollutants can be removed with simple methods such as settling in detention ponds and via infiltration systems (Genç-Fuhrman et al. 2007; Valtanen et al. 2010; Good et al. 2014). However, a large fraction of pollutants in particulate form are attached to very small suspended particles, such as particulate dust originating from incineration (Göbel et al 2007). They are challenging to be removed e.g. via settling and further treatment methods such as filtration are required.

Although the form (dissolved/particulate) of pollutant is important for its environmental effects and the required treatment methods, the total amount of the pollutant might be even more important to determine. The form may change as stormwater travel through the sewer network and treatment structures, as well as the receiving environment. For instance, particulate metals may dissolve in water bodies (Valtanen et al. 2010).

Nitrogen and phosphorus cause eutrophication and increase harmful algae growth in receiving surface waters (Valtanen et al. 2010; Li & Davis 2014). This causes loss of oxygen and fish mortality (e.g. Valtanen et al. 2010). In the City of Vantaa, for instance, one of the main aims behind the stormwater management is to protect the ecological status of streams discharging into River Vantaa and River Kerava, as they are habituated by endangered sea trout (Jormola et al. 2017). Heavy metals have toxic effects on aquatic biota, especially when in dissolved form (Valtanen et al. 2010). Heavy metals are non-biodegradable and thus can accumulate in the environment and cause long-term effects also for the humans (Genç-Fuhrman et al. 2007; Wu & Zhou 2009). Dissolution of heavy metals accumulated on the bottom of receiving waters accelerates under anaerobic conditions (Valtanen et al. 2010). Therefore, the environmental effects of heavy metals are linked with the effects of eutrophication due to nutrient releases. Other effects of stormwater on the environment are listed in Table 3.

Table 3. The effects of stormwater pollutants on the aquatic environment. Modified from Valtanen et al. (2010).

Pollutant	Effects on environment
Nutrients	Eutrophication, algae growth, loss of dissolved oxygen, increased dissolution of other pollutants
Suspended solids	Increase of turbidity, loss of dissolved oxygen
Metals	Toxicity of water and sediments, heavy metal accumulation on biota
PAHs and oils	Toxicity of water and sediments, accumulation on biota
Pesticides	Toxicity of water and sediments, accumulation on biota
Bacteria	Human health hazard (drinking water source, bathing waters)

1.3 Stormwater filters

During the last couple of decades, integrated approaches have been developed to manage stormwater issues. These approaches are often called low impact development structures (LIDs) or sustainable urban drainage systems (SUDS). These systems are developed to reduce problems related to stormwater quality and quantity, but also to improve the amenity of urban areas. The fundamental idea behind all LIDs is to mimic natural catchment area processes as opposed to stormwater conveyance via pipe networks. (Westerlund et al. 2003; Norris et al. 2013; Sillanpää 2013)

LIDs allow rainwater to infiltrate and evapotranspirate, which reduces the amount of stormwater, hinders flow peaks and improves stormwater quality. LIDs include permeable pavements, green roofs, settling structures, infiltration structures, sand filters and biofilters (Valtanen et al. 2010). Ideally, LIDs are decentralized, meaning stormwater is managed soon after the rainfall near the source, because large structures installed at the discharge points of conventional pipe networks are not as effective (Valtanen et al. 2010). It can be difficult to find space for numerous decentralized LIDs in densely built areas, but easier in completely new urban areas. Therefore, stormwater management should be taken into account already in the city plans of new areas (Ulvi 2016).

The development of LIDs has been intense especially in the USA and in the UK, where road stormwater treatment with LIDs is obligatory (Norris et al. 2013). However, the knowledge on the performance of different treatment methods is only emerging (Westerlund et al. 2003). LIDs have been built also in Finland, although stormwater control still mainly means the construction of new stormwater sewer networks. For instance, many open ditches allowing water to infiltrate are turned into conventional stormwater sewers also in existing residential areas in the capital area of Finland. This is against the new principles of integrated stormwater management.

There are also good examples of stormwater management in Finland. In Vantaa, for instance, a new residential area was built in Kivistö for a house fair in 2015, where stormwater management was integrated into the area. This includes green roofs and an infiltration pond in the central location of the area. The City of Vantaa has been also testing different kinds of stormwater treatment structures it the road area of Tikkurilantie (Lehikoinen 2015; Leinonen 2017), where also the test site of this study is located (Section 2.1). In addition, the City of Vantaa is planning to construct a full-scale sand-biochar filter structure in the road area of Länsimäentie (Suihko 2016) to protect the surrounding groundwater area (Figure 2).

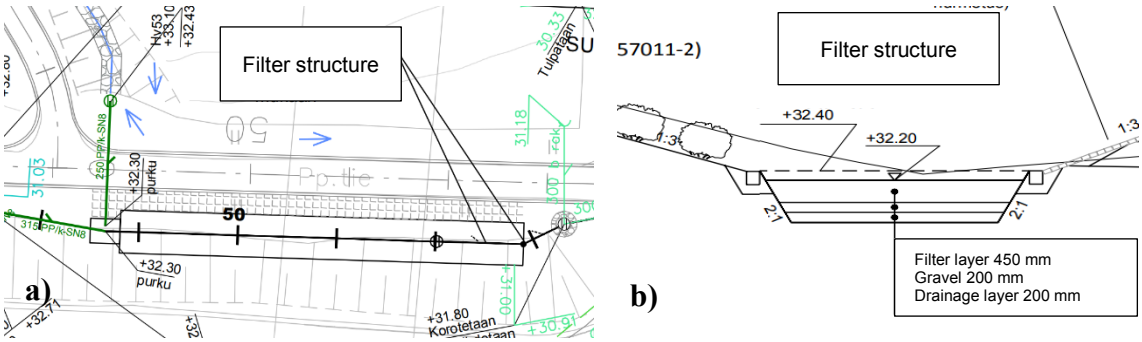

Figure 2. An example of a stormwater filtration structure. Blueprints of a sand-biochar filter at the road area of Länsimäentie, Vantaa. (Modified from images by City of Vantaa / A-Insinöörit)

Infiltration reduces the amount of stormwater and improves its quality. Infiltration structures can be used on their own, or they can be installed after a settling pond, for instance. Settling ponds reduce the amount of suspended solids entering infiltration systems, thus reducing their clogging. On the other hand, settling on its own is not a sufficient method to treat stormwater, as it is unable to remove the colloidal and dissolved fractions of pollutants (Genç-Fuhrman et al. 2007).

Infiltration structures – consisting of materials with relatively high hydraulic conductivity, such as sand – are used to infiltrate stormwater into subsurface soil layers and groundwater. Optionally, infiltrated water can be gathered with subsurface drains at the bottom of the structure and released into a stormwater network or directly into surface waters. In this case term filtration is typically used instead of infiltration. Even though released into a conventional pipe network, filtration reduces peak flows in the downstream network in addition to its water quality improving effects. (Valtanen et al. 2010)

It is noteworthy that infiltration or filtration of stormwater does not actually remove pollutants, but just immobilizes them. Infiltration accumulates pollutants into the filter itself, but possibly also in the surrounding ground (Boller 1997), if the filter is not isolated. Conventional stormwater conveyance mostly risks surface waters but the emerging infiltration creates a new pathway for pollutants also into soils and urban groundwater (Galfi et al. 2017). However, the pollutant deposition into a controllable soil volume can be seen as a better option compared with their release in the water bodies, as immobilization enables the harvesting of the substances in the future. The deposition of pollutants, such as heavy metals, will in any case occur somewhere in the environment as long as the generation of the contaminants is not reduced (Boller 1997).

According to Pitt et al. (1999), stormwater infiltration does not usually cause risk of groundwater contamination if infiltrated through surface soils, but the risk is higher if stormwater is conveyed directly into subsurface soil layers. This underlines the importance of the selected infiltration method and infiltration media.

If the infiltration of polluted stormwater is limited e.g. in groundwater areas, the bottom of the filters can be isolated from the surrounding soil using e.g. bentonite lining. Filters are typically dimensioned so that they are able to dry between rain events (Valtanen et al. 2010). The fundamental idea is that stormwater stays in the filter long enough to support the retention of pollutants, but short enough to enable the infiltration during the following rain event.

The simplest filter type consists of a pit in the ground, which is filled with sand. In road runoff treatment, they are usually located parallel to the road and called filter drains (Norris et al. 2013). Stormwater treatment with sand filters is mostly based on mechanical sieving and the same principle is applied in drinking water treatment (Norris et al. 2013). Sand filtration is efficient against pollutants in particulate form, but does not retain as much dissolved pollutants such as nitrogen and some of the heavy metals as discussed in Section 1.2. Therefore, filtration is sometimes improved with the addition of plants, known as biofiltration. The performance of sand filters can be amended also with the addition of other media, but the materials should be selected with care to ensure their effectiveness (Reddy et al. 2014b; Genç-Fuhrman et al. 2007). For instance Monrabal-Martinez et al. (2017) found good results, when a sand filter was amended with olivine or pine bark. Biochar is one

recently proposed option for sand filter amendment (Reddy et al. 2014a), but it is poorly studied to date.

If additional materials are included in sand filters, the pollutant retention is not based on only physical sieving, but other mechanisms may also occur. These mechanisms include particulate sedimentation, precipitation, adsorption and ion exchange, and biological assimilation (Norris et al. 2013; Huber et al. 2016). Several mechanisms occur at the same time and the fundamental knowledge on the processes is poor (Norris et al. 2013). It is noteworthy that even sand should not be considered as an inert material (Norris et al. 2013), unless it is composed of pure SiO_2 (quartz), which typically is not the case. Norris et al. (2013) found that the lithology of sand used in filters clearly influences the heavy metal retention, and natural weathering products of some minerals showed better performance than materials with chemical amendments.

The pollutant removal mechanisms of stormwater filters have been studied e.g. by means of geochemical modelling. PHREEQC program by USGS is a common tool for hydrogeochemical calculations (Appelo & Postma 2007). Different versions of PHREEQC were used in stormwater related studies by Bäckström et al. (2003), Genç-Fuhrman et al. (2007), Pennington et al. (2008), Norris et al. (2013), Paus et al. (2013), Solpuker et al. (2014), Huber et al. (2016), Islam et al. (2016) and Wendling et al. (2017b). However, most of these studies were conducted in laboratory, as opposed to the realistic field conditions. PHREEQC uses databases containing thermodynamic equilibrium data, and it can be used to assess precipitation of minerals (Pennington et al. 2008).

Biochar has been seen as one potential material to improve the efficiency of LIDs, as it has high internal porosity and surface area, and thus ability to adsorb substances (Reddy et al. 2014a). Biochar has high carbon content (Chan et al. 2008) and it is the product of thermal decomposition (pyrolysis) in which biomass is heated at low temperature (less than 700 °C) with limited amount of oxygen (Chan et al. 2008; Tian et al. 2014). Gases produced in pyrolysis can be used in energy production (Mattila et al. 2012). The biomass can originate from various sources, such as trees, nut shells, poultry litter, corncobs and manure (Manyà 2012; Tian et al. 2014). The properties of biochar depend on both the biomass origin and the manufacturing process (Manyà 2012; Kuoppamäki et al. 2016). In addition to its other proposedly beneficial properties, biochar acts as a long-term carbon sink as the biomass removes carbon dioxide from the atmosphere (Manyà 2012; Mattila et al. 2012).

Kuoppamäki et al. (2016) found that some biochar products reduced nutrients leaching from green roof applications. However, they noticed that another biochar product – made from the same material, but by another manufacturer – showed opposite effects. Therefore Kuoppamäki et al. (2016) underlined the need for studies on biochar properties to gain understanding about the pollutant removing principles. Additionally Kuoppamäki et al. (2016) noticed that biochar had positive effects on stormwater quantity due to its water retention capacity.

A column test by Reddy et al. (2014a) showed promising results on the performance of biochar in stormwater filtration. They observed high reductions especially in TSS (86%), NO_3 (86%), PAHs (68%), Cu (65%) and Pb (75%), whereas the filtration was not as effective on Cd, Cr, Ni and Zn but still remarkable (17–47%). Tian et al. (2014) observed a clear reduction of NH_4 in their laboratory experiments utilizing biochar, but underlined the need

for pilot-scale tests. Moreover, biochar has been observed to remove bacteria (Escherichia coli) from stormwater (Mohanty et al. 2014; Reddy et al. 2014a).

Monrabal-Martinez et al. (2017) used charcoal as a filter amendment material and found promising results especially on Cu, Pb and Zn removal. However, the used charcoal was manufactured from anthracite coal, and thus cannot be directly compared with biochar, although they share some similar properties.

According to column tests by Wendling et al. (2017a) biochar amended sand filtration was effective to reduce Cu, Pb and Zn from stormwater. Based on their tests, biochar made of spruce outperformed the biochar made of birch in removal of Cu, Pb, Zn and P. Moreover, biochar made of birch showed substantial release of phosphorus, suggesting birch biochar was acting as a source instead of a sink, but the results strongly depended on stormwater concentrations. Wendling et al. (2017a) concluded that birch biochar is assumed to initially release phosphorus, indicating its usage may need to be limited near ecologically sensitive receiving waters. However, after the initial release, also birch biochar was observed to remove phosphorus. Additionally, Wendling et al. (2017a) concluded that the retention of metals and phosphorus was based on physical mechanisms or both physical and chemical mechanisms.

Similar to concentrations of untreated stormwater (Section 1.2), the concentrations of filtered stormwater are time dependent, although filters typically retard the changes. For instance, in a lysimeter study investigating biofilters, phosphate and nitrate concentrations were noticed to clearly change in the filter effluents within a couple of hours, even though the lysimeters were fed with artificial stormwater of constant concentration (Valtanen et al. 2017). This complicates the assessment of stormwater filter performance.

As almost all engineered structures, stormwater filters require maintenance. Sand filters typically last more than 20 years, but their maintenance costs are relatively high (Valtanen et al. 2010). Paus et al. (2013) concluded that biofilters remove metals efficiently more than 25 years. The maintenance frequency can be reduced by pretreatment of stormwater. For instance, a pre-settling basin before the actual filter reduces the amount of suspended matter entering the filter, thus reducing the clogging of filter top layers (Monrabal-Martinez et al. 2017). The clogging of the filter surface prevents the adsorption processes within the filter, and some water may overflow from the filters due to decreased hydraulic conductivity. Clogging layer typically forms in the filter structure at the boundary of the actual filter material and surrounding ground (Siriwardene et al. 2007). The City of Vantaa, for example, assesses the functioning of stormwater treatment structures by testing the hydraulic conductivity of the filters.

City of Tampere, Finland, recently introduced operation and maintenance manuals for stormwater treatment structures, including maintenance schedule and main information about the treatment structures (Heinonen 2016). However, determination of the required maintenance frequency is challenging and would benefit if the long-term operating properties of the filters were precisely known. Based on such information, the maintenance frequency could be optimized, which would likely reduce the costs and improve the filter performance. Knowledge on the long-term functioning of stormwater filters – especially on biochar amended ones – is lacking, which complicates the planning of sufficient maintenance. The retention of pollutants is a result of their accumulation into the filter

media, requiring removal at some point. Monrabal-Martinez et al. (2017) reported highly varying expected service lives for filters with different amendments depending on the target pollutants. Wendling et al. (2017b) expected 5–10 years of lifetime for different filter materials – including biochar – depending on filter dimensioning based on their laboratory studies.

1.4 Objectives of the study

There is a need for stormwater filter studies under realistic field conditions. Especially the knowledge on biochar amended filters is scarce, since they are only studied in laboratory conditions to date.

This study focuses on the treatment of road stormwater using sand and sand-biochar filters. The main objectives of the study are listed as follows:

1. To assess the impact of the filtration systems on road stormwater quality and quantity.
   Similar field studies on road runoff have not been conducted in Finland.

2. To determine if biochar amendment improves the treatment performance of a sand filter.
   To the author's knowledge, similar field scale studies on the performance of biochar filters do not exist.

3. To describe the behavior of the filters during several rain events as precisely as possible.
   Earlier studies have shown rapid changes in stormwater quality and quantity, but detailed information on stormwater filters is scarce.

4. To develop reliable and efficient methods for monitoring of stormwater treatment systems.
   The methods are needed both in research and in practical use by e.g. municipalities. This includes seeking of quality parameters, which could be used as indicators of the treatment performance.

5. To gain knowledge on the operating principle of the filters.
   Understanding the pollutant removal mechanisms may enable systematic development of stormwater filters rather than development by trial and error.

The study was conducted as field experiments under specific field and weather conditions, indicating that the results cannot be straightforwardly generalized to similar filters under different conditions.

2 Materials & Methods

The study period for this thesis was from May 17 to September 27, 2017. The pilot site in Vantaa, Finland was monitored during this period including continuous rainfall measurements. More precisely investigated rainfall-runoff events took place in June and July, 2017. All field measurements were conducted by the author. After collecting the data from the field site, results were analyzed with the methods illustrated in Figure 3.

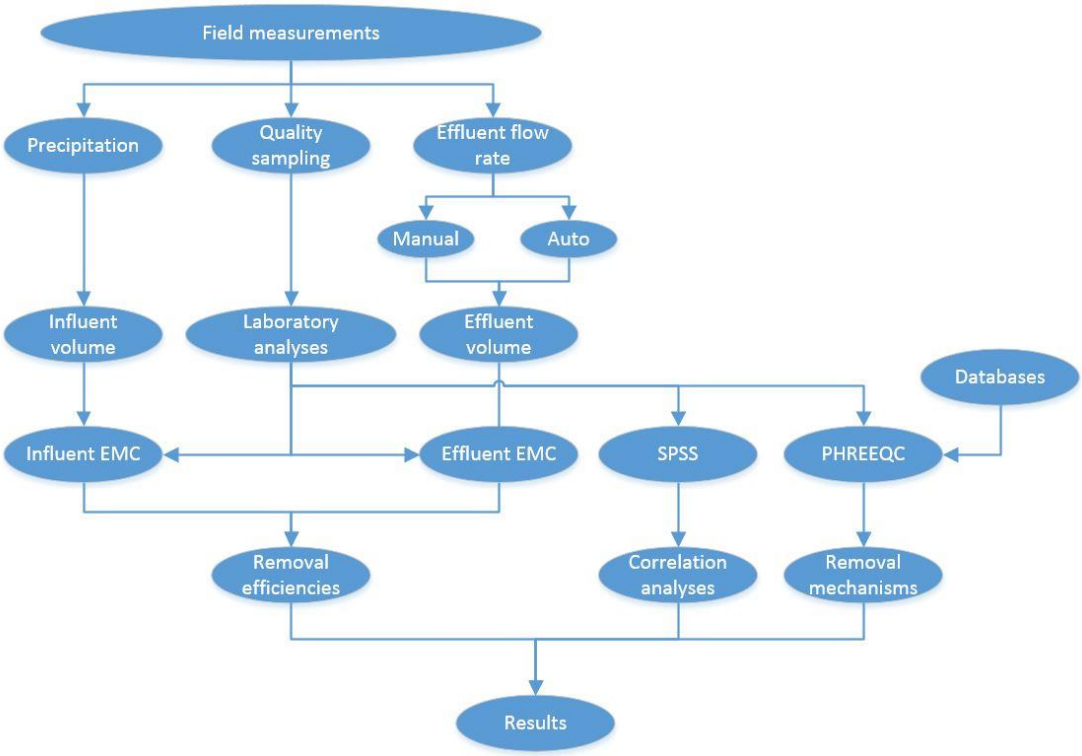

Figure 3. The materials and methods of the study in flowchart format.

2.1 Site description

The study investigated two different stormwater treatment filters, located at Tikkurilantie road area in Vantaa, Finland (60°18'52" N, 24°52'52" E; Figure 4). The site is located ca. 17 km north from the center of Helsinki, the capital city.

The extension of road Tikkurilantie, where the study site is located, was built in 2013. The satellite image in Figure 4b shows how the site is surrounded by agricultural fields and some storage houses with no residential buildings nearby. The road crosses River Vantaa ca. 250 meters from the investigated filters. The study site is ca. one km away from the Helsinki-Vantaa Airport area.

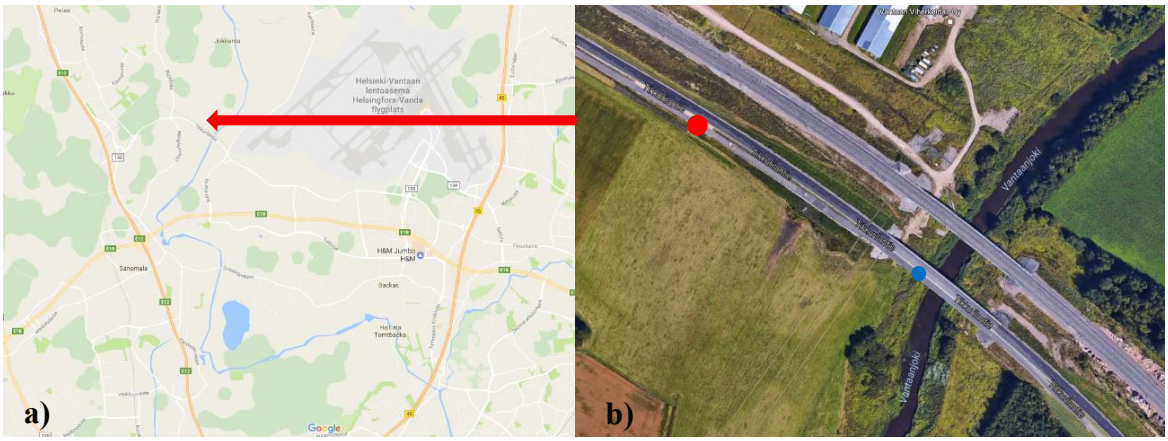

Figure 4. Location of the study site in Vantaa (a) and in Tikkurilantie (b). Red arrow points to the site location in larger scale, while the location of the filters in the satellite image is pointed by a red dot. Blue dot indicates the location of the untreated stormwater sampling. (Google Maps 2017)

The same road area has been used for earlier stormwater studies (Lehikoinen 2015; Leinonen 2017), which provided existing data on stormwater properties of the area since 2013. However, these studies did not investigate the particular filters in question but were conducted a few hundred meters north-west from the site of this study.

On average, total annual precipitation in Vantaa is 682 mm, while the average temperature is 5.3 °C (Pirinen et al. 2012). On average, late summer and autumn have the most precipitation (Figure 5). The year 2017 was quite similar to the average in terms of precipitation and temperature. However, May and July in 2017 had notably less precipitation compared with the average, while June had slightly more.

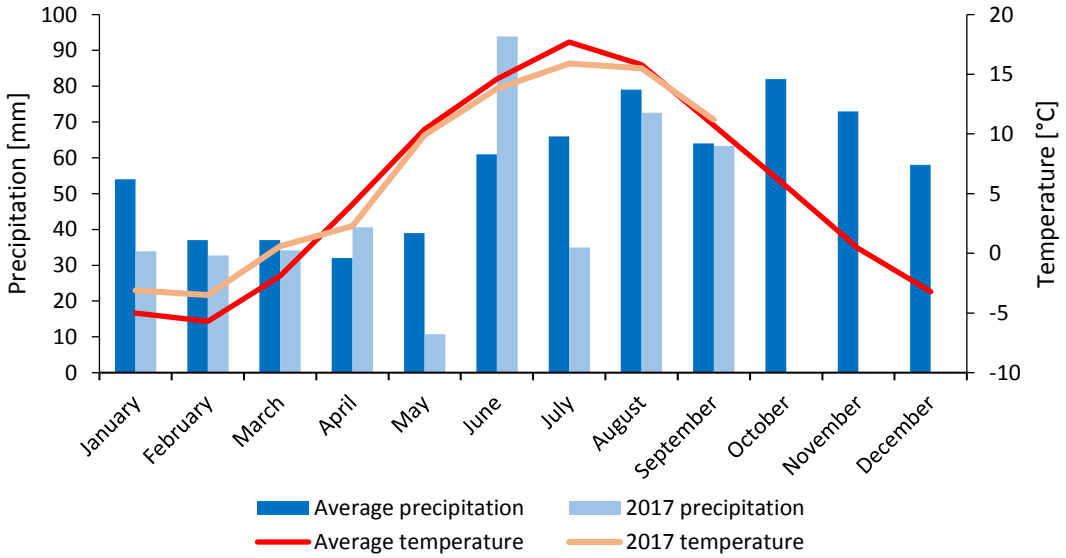

Figure 5. Monthly temperatures and precipitation in Vantaa on average (Pirinen et al. 2012; y. 1981-2010) and in 2017 (Finnish Meteorological Institute 2017). Measured at Helsinki-Vantaa Airport, ca. 4.5 km from the study site.

The annual average daily traffic (AADT) of the road Tikkurilantie at the site location was 7610 vehicles per day in 2016, and the share of heavy traffic was 16% (Rytkönen / City of Vantaa, personal communication August 17, 2017). The speed limit at the site is 60 km/h.

Based on the traffic properties, Tikkurilantie is comparable to road Kangasalantie in the study by Inha et al. (2013) with AADT of 10 000 and speed limit of 60 km/h (Section 1.2).

The study site has two pilot stormwater filters: a sand filter and a sand filter amended with a birch biochar layer (Figure 6). Both filters were built in January 2017 (Figure 7), meaning they had been operable ca. five months before the start of the study period. Both filters are 10 m long and 3.4 m wide, thus having a filter area of 34 m^2. The catchment areas of the filters consist of asphalt road and pedestrian and bicycle way with a total area of ca. 100 m^2 per each filter.

Figure 6. a) Upper parts of the sand filter (left) and sand-biochar filter (right) highlighted. The manholes in front connect the subsurface drains and outlet pipes which convey water under the walkway to the left. Gravel part of the walkway was covered with new asphalt before the beginning of the study. b) Drain outlets from the sand filter (left) and sand-biochar filter (right) discharging into the ditch next to the road.

The dimensioning of the filters was based on the City of Vantaa design rainfall intensities, which were 150 l/s/ha for base calculation and 167 l/s/ha for flood calculation. Theoretical catchment area of the filters used for the dimensioning was 15 m x 10 m per filtration unit, which forms maximum 2.25 l/s base flow and 2.51 l/s flood flow. As a result, the filtration units with an area of 34 m^2 should have a minimum hydraulic conductivity of 6.6 x 10^{-5} m/s (base) and 7.4 x 10^{-5} m/s (flood). Laboratory tests in July 2016 by VTT confirmed that biochar can be used as a filter material, since the hydraulic conductivity was sufficiently high (average 2.11 x 10^{-4} m/s).

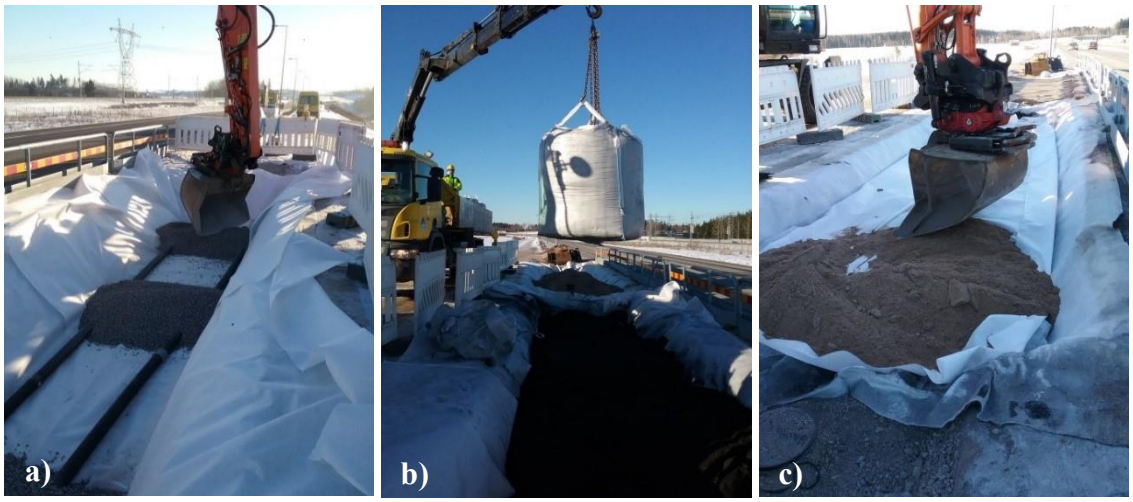

Figure 7. Construction of the filters in January 2017. a) Underdrains and subsurface drainage gravel at the bottom of the filter. b) Addition of the biochar layer. c) Addition of the surface sand layer. (Images by City of Vantaa)

The filters are located next to each other, and a bentonite mat was installed to separate them to prevent water leaking from one filter to another (Figures 8 and 10b). In addition, the bentonite lining around the filters prevents water infiltrating from the filters to the surrounding ground, allowing infiltration of water only into the subsurface drains (Figures 7a and 8). Subsurface drains at the bottom of the filters lead the water to the effluent pipes, which discharge under the walkway to the ditch next to the road (Figures 6b and 9). This was essential for precise monitoring of the filter effluents.

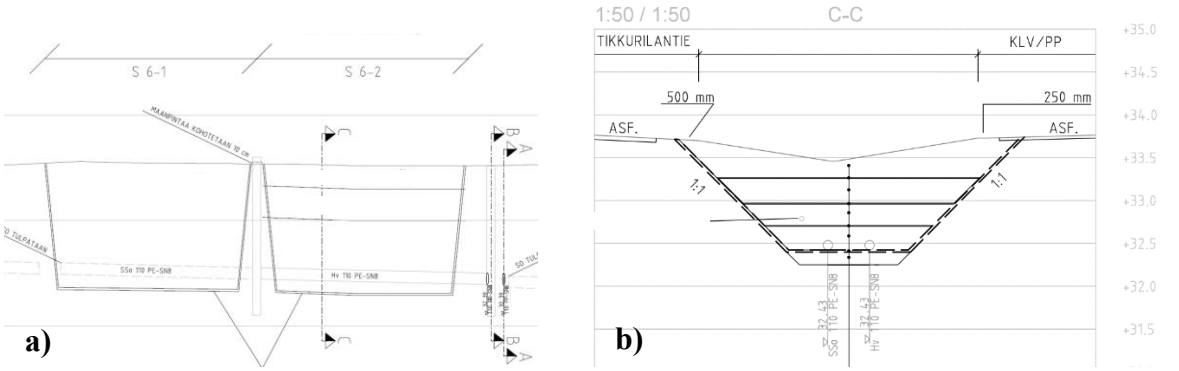

Figure 8. a) Sectional view of the sand filter (left) and sand-biochar filter (right). Bentonite lining separates the filters from each other and from surrounding ground. b) Cross-section of the sand-biochar filter (Section C-C in Figure 8a). 300 mm biochar layer is the second layer from the top. Subsurface drains are installed at the bottom of the filter, and bentonite lining covers the sides of the filter. Structure of the sand filter is similar but it has not a biochar layer. (Modified from images by City of Vantaa / Pöyry)

The two filters were planned and constructed to be as identical as possible, apart from the addition of the biochar layer in the other filter. This enabled detailed comparison between the filters, and assessment of the biochar influence on the filter performance. The filters consist of several layers (Table 4). The layers are separated from each other with filter fabric to prevent biochar washing away from the filter with the filtrating water. The biochar layer is placed under the sand layer in order to keep biochar immobilized. Otherwise there would be a risk of biochar washing away from the surface of the filter with water overflow, since biochar has smaller density than water. The biochar used in the sand-biochar filter is manufactured from birch (*Betula*) by RPK Hiili Oy using pyrolysis (Figure 10a).

Table 4. Layer structure of the studied filters.

Sand-biochar filter		**Sand filter**	
Layer	**Depth [mm]**	**Layer**	**Depth [mm]**
Sand 0.2–2 mm	200	Sand 0.2–2 mm	800
Filter fabric N2		Filter fabric N2	
Birch biochar	300	Subsurface drain gravel 8–16 mm	250
Filter fabric N2		Bentonite mat	
Sand 0.2–2 mm	300	Sub-base KaM 0–32 mm	150
Filter fabric N2			
Subsurface drain gravel 8–16 mm	250		
Bentonite mat			
Sub-base KaM 0–32 mm	150		

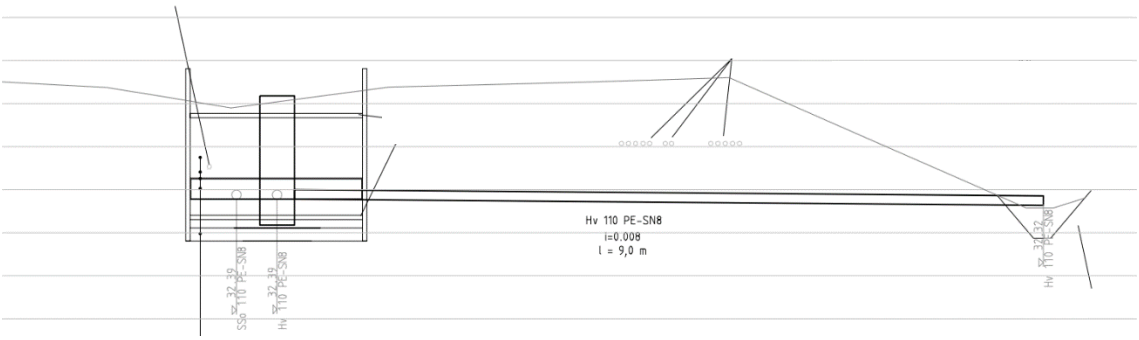

Figure 9. Cross-sectional view of the road (Section B-B in Figure 8a). Effluent pipe starting from the manhole in the filter is discharging under the walkway to the ditch. (Modified from images by City of Vantaa / Pöyry)

Sand used in both filters is washed and 0.2–2 mm in grain size, and it is manufactured by Seepsula Oy. The sand originates from Hausjärvi, Finland, and it consists of light gneiss (54 %), reddish granite (27%), and dark mica slate (19%) with no iron or sulfur compounds nor limestone (VTT Expert Services 2017).

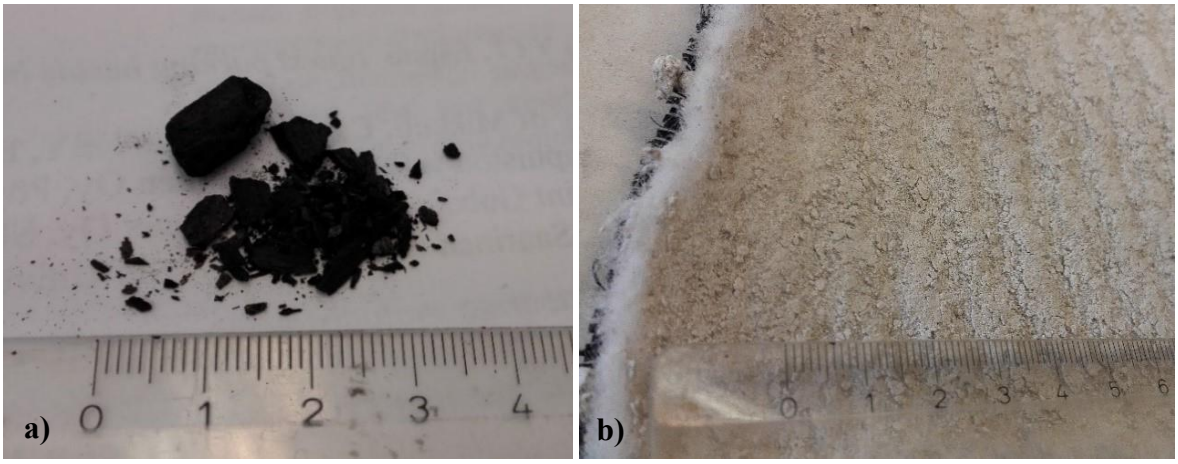

Figure 10. a) Birch biochar used in the sand-biochar filter. Centimeter ruler for scale. b) Bentonite mat used for the lining of the filters. Centimeter ruler for scale.

To assess the treatment performance of the filters, it is necessary to know the quality of the water input, i.e. the influent. Influent samples were taken from a downspout of a bridge of the same road ca. 250 m away from the filters (Figures 4 and 11). Likewise the filters, the downspout collects stormwater from the road and from the pedestrian and bicycle way. Inha et al. (2013) recommended this sampling method for road stormwater collection, since it is reliable and simple.

Figure 11. The downspout (a) of a bridge (b) used for untreated stormwater sampling. Location of the inlet of the downspout is denoted with red arrow. The actual test site is ca. 250 m away.

Flow rate for the influent stormwater was estimated using precipitation data from the site (Section 2.2.2) and approximate catchment areas of the filters.

2.2 Measurements

2.2.1 Flow rate measurements

Flow rates of the filter effluents were measured both automatically and manually. The manual measurements were conducted during the studied rain events to produce reliable and accurate data. The automatic measurements supplemented the manual flow rate data. The flow rates were monitored manually also occasionally between rain events during the study period.

Ultrasonic water meters were used for automatic flow rate monitoring of both filters. Diehl Hydrus (DN 50 mm) water meters were installed at the end of the outlet pipes, and the data was remotely gathered with Wikon Waterbox transmitters. The water meters and the transmitters were installed inside a protective casing in a U-shaped water-sealing trap structure to ensure that the meters were constantly full of water without air (Figure 12). The casings were equipped with small hatches to give access to the meter device and transmitter. Water samples and manual flow rate measurements were taken from the outlet of the meters.

Figure 12. Installation of the automatic effluent flow rate meter for the sand-biochar filter. The flow rate meter, its transmitter (not shown) and pipes (grey) are placed inside the bigger red pipe, which protects the devices. Water samples and manual flow rate measurements were taken from the outlet. Note that the outlet is higher than the water meter to ensure it is constantly full of water.

Due to technical difficulties, the automatic flow metering was used only to supplement the gaps in the manual flow rate measurements of the studied events and to observe the most intensive rain events (intensive enough to produce measurable effluent flow rate) during the whole study period. Additionally, automatic meters provided data on effluent temperature.

Manual measurements were conducted with a 1000-ml measuring glass and a stopwatch. Starting time of the measurement, volume of water (ca. 200–1000 ml) and the required time for the volume were written down with an accuracy of 1 min, 5 ml and 1 s, respectively. The flow rate Q is:

$$Q = \frac{V}{t} \tag{1}$$

where V is the measured volume of water and t the measured time. The center point of each measurement was used as a time stamp for the flow rate measurement, since many of the measurements took more than one minute.

Several manual effluent flow rate measurements were recorded during each studied rain event in order to fill the lack of proper automatic measurements. The interval between the measurements was mainly ca. 5–60 minutes. The amount of the realized flow rate measurements is shown in Table 9 in Section 3.1.

2.2.2 Precipitation measurements

Information on precipitation at the site was used for the assessment of the influent flow rate. Precipitation was measured on site, since rain gauge at the site is the most accurate source of rainfall data for small catchment areas (Niemi 2017). The measured rainfall was compared with precipitation data by a meteorological station of FMI (Finnish Meteorological Institute) ca. 5 km away from the site.

Rainfall was measured with two IM523 rain gauges produced by Metos (Pessl Instruments GmbH) and a Decagon EM50 digital data logger. The rain gauges used have a double spoon tipping bucket, which tips and is registered when filled with 4 ml of water, corresponding to

0.2 mm of precipitation. The gauges were installed next to the studied filters at the height of 2 m (Figure 13).

Figure 13. Rain gauges at the test site used for continuous precipitation monitoring.

One gauge was used for actual rainfall measurements and the other one was used as a backup system. The backup gauge was faulty and measured only every other flip, so its measurements were doubled to verify the order of magnitude of the measurements by the actual gauge.

2.3 Sampling

During the studied rainfall-runoff events, influent (stormwater from the bridge downspout; Section 2.1) and the filter effluents were sampled for quality analyses. The samples from each point were collected manually with a point-specific 3-l plastic can (Figure 14). The sample number and beginning and ending times were written down with one minute accuracy. Since most of the samples (especially the effluent samples) took more than one minute to collect, the center point was used as a time stamp for each sample. Approximately 2 l of water was collected for each sample, and the water was then divided into the sample bottles (Table 5). For some samples additional analyses were to be done in a separate laboratory (Section 2.4). For these samples, a larger volume of water was collected to the cans and was divided also into additional sample bottles.

Table 5. Sample bottles.

Basic samples Analyzed by Aalto University	**Additional samples (Events 2 & 3)** Analyzed by Metropolilab Oy
Plastic bottle 1000 ml	Plastic bottle 100 ml*
Plastic bottle 500 ml	Plastic bottle 100 ml **
Glass bottle 250 ml (known as TOC bottle)	Plastic bottle 250 ml **

* 8-9 samples per sampling point (untreated stormwater, sand-biochar filter and sand filter) per event.
** Two samples per filter effluent per event.

Sampling was planned to cover entirely each selected rain event. The effluents were sampled mostly in ca. 15–60 minute intervals, whereas the influent samples were gathered in ca. 3–10 minute intervals during intensive rain peaks.

Figure 14. a) Data gathering in progress on June 8, 2017. b) 3-litre cans were used for sample gathering, and 1000-ml measuring glasses for manual flow rate measurements.

In addition to frequent sampling during the event, Hatt et al. (2009) took one sample later, even more than 18 hours after the last one. The same principle was practiced in two of the rainfall-runoff events of this study to obtain values at the end or after the event. For practical reasons, it was not possible to collect samples manually with short intervals constantly during periods longer than approximately 14 hours.

As discussed earlier in Sections 1.2 and 1.3, the pollutant concentrations may change rapidly during rain events. Therefore, it was planned to collect as many samples as possible in order to get precise data to cover the whole rainfall-runoff event. However, practical reasons limited the total amount per each event to ca. 40 samples. These reasons included the capacity of the analyzing laboratory, the sample collecting author and his vehicle. The amount of the realized samples is shown in Table 9 in Section 3.1.

2.4 Laboratory analyses

Table 6 presents the analyses conducted by Aalto University Water Laboratory. Samples for these analyses were stored in a cold room at +4 °C temperature before the analyses. The analyses were started as soon as possible – the next morning after the rain event – in order to minimize the effect of storage.

Analyses included pollutants and parameters widely used in stormwater studies. They were supplemented with parameters necessary for geochemical modelling (Section 2.6).

Some of the samples of the rain events on July 20 (Event 2) and July 11–12 (Event 3) were analyzed for additional substances by Metropolilab Oy (Table 7). Samples for these analyses were stored in a cool box and delivered to the laboratory within 12 hours from the last sample of each rain event.

Table 6. Laboratory analyses conducted by Aalto University.

Parameter	Standard	Equipment
pH *	SFS-EN ISO 10523, 2012	WTW inoLab pH 720, probe: Sentix 81 Plus
Alkalinity *	SFS-EN ISO 9963-1, 1996	Metrohm Dosimat 775; WTW inoLab pH 720, probe: Sentix 81 Plus
Electrical conductivity *	SFS-EN 27888, 1994	Orion Research Conductility Meter MOD.101, Probe Orion 990101
Turbidity *	SFS-EN ISO 7027, 2000	Hach 2100AN IS Turbidimeter
Total suspended solids (TSS)*	SFS-EN 872, 2005	Glass fiber filter Whatman GF/C
UV-absorbance, 254 nm	Eaton et al. (2005; p. 5-71)	Schimadzu UV 1201-spektrofotometer
Ammonium (NH_4)	ISO 7150/1-1984	Schimadzu UV 1201-spektrofotometer
Total nitrogen (TN)	SFS-EN-ISO 11905-1, 1998	Lange Ganimede N
Nitrite & Nitrate (NO_2+NO_3)	SFS-EN ISO 13395, 1997	Foss Tecator, FIAstar 5000 Analyzer; Sampler 5027
Total phosphorus (TP)	SFS-EN ISO 6878, 2004; SFS-EN-ISO 15681-1, 2005	Foss FIAstar 5000 Analyzer
Phosphate (PO_4)	SFS-EN ISO 15681-1, 2005	Foss FIAstar 5000 Analyzer
Total organic carbon (TOC)	SFS-EN 1484, 1997	Total organic carbon analyzer Shimadzu TOC-V_{CPH} + ASI-V
Dissolved organic carbon (DOC)	SFS-EN 1484, 1997	Total organic carbon analyzer Shimadzu TOC-V_{CPH} + ASI-V; Whatman ME25 Membrane filter 0.45 µm
Redox potential *	Eaton et al. (2005; p. 2-77)	WTW inoLab pH 720; Radiometer Redox-electrode P101; Kalomeli reference electrode REF 401

* Analyzed by the author.

Table 7. Additional laboratory analyses for Events 2 and 3 conducted by Metropolilab Oy.

Parameter	Standard	Uncertainty [%]
Cadmium (Cd)	SFS-EN ISO 17294-2:2005	15
Copper (Cu)	SFS-EN ISO 17294-2:2005; SFS-EN ISO 11885:2009	20
Lead (Pb)	SFS-EN ISO 17294-2:2005	20
Nickel (Ni)	SFS-EN ISO 17294-2:2005	25
Zink (Zn)	SFS-EN ISO 17294-2:2005 SFS-EN ISO 11885:2009	25 20
Manganese (Mn) *	SFS-EN ISO 11885:2009	20
Silicon (Si) *	SFS-EN ISO 11885:2009	20
Iron (Fe) *	SFS-EN ISO 11885:2009	20
Sulfate (SO_4) *	Internal method	10
Chloride (Cl) *	Internal method	10
Calcium (Ca) *	SFS-EN ISO 11885:2009	20
Magnesium (Mg) *	SFS-EN ISO 11885:2009	20
Potassium (K) *	SFS-EN ISO 11885:2009	20
Sodium (Na) *	SFS-EN ISO 11885:2009	20
Aluminum (Al) *	SFS-EN ISO 11885:2009	20
Total organic carbon (TOC) *	SFS-EN 1484:1997	15

* Two samples per filter effluent per event.

2.5 Data analysis

2.5.1 Event mean concentrations

Event mean concentration (*EMC*) is a concentration value weighted by the flow rate. It is widely used in stormwater studies (e.g. Westerlund et al. 2003; Davis & McCuen 2005; Kaczala 2012; Galfi et al. 2017), since it takes into account the influence of flow rate and water volume and is thus more representative than normal concentration average.

*EMC*s were determined with the following equation:

$$EMC = \frac{\sum_{t=1}^{t=T} Q_t C_t}{\sum_{t=1}^{t=T} Q_t} \quad (2)$$

where Q_t is the flow rate and C_t is the concentration at time t (Davis & McCuen 2005; Kaczala et al. 2012).

*EMC*s were calculated using both interpolation method and block method (e.g. Westerlund et al. 2003). In the interpolation method, the Equation 2 was applied in minute basis. For each minute of an event, both pollutant concentrations and flow rates were linearly interpolated based on the existing measured values. In the block method, *EMC*s were calculated based on blocks that have constant concentrations between two samples, instead of using interpolated minute based values. This means that the resolution of the block method was the same as the intervals between the samples.

The choice of beginning and ending times of rainfall-runoff events is always a subjective decision. This was especially so for the effluent discharges: the flow rates were above zero also before the rainfall events and stayed elevated compared with the pre-event situation still after the last measurements. Also rain characteristics and sampling intervals and duration varied between the studied events (Section 3.2). Therefore, *EMC*s for the studied storms were calculated using different methods (Table 8), and average *EMC*s were calculated based on these values for each storm.

Table 8. Methods used to determine event mean concentrations (EMC) and event mean values (EMV; Section 2.5.2). Average EMCs and EMVs were calculated for each event based on the values provided by these methods.

	Event 1	Event 2	Event 3
1	From first to last measurement; interpolation method	From first to last measurement; interpolation method	From first to last measurement; interpolation method
2	From fist measurements until the flow rate at pre-event level (interpolated); interpolation method	During the period when the flow rates were elevated. End part flow rates interpolated to zero. Concentrations assumed constant after the last measurements.	During the period when the flow rates were elevated. End part flow rates interpolated to zero. Concentrations assumed constant after the last measurement.
3	During clear flow rate peak; interpolation method	From first to last measurement; block method	From first to last measurement; block method
4	From first to last measurement; block method		

2.5.2 Event mean values

The principle of *EMC* (Section 2.5.1) was applied also for the other laboratory results than concentrations. Flow weighted averages were calculated for parameters including pH, turbidity, redox potential, alkalinity, electrical conductivity and UV-absorbance. In this study, these averages are referred to event mean values (*EMV*) and were determined as:

$$EMV = \frac{\sum_{t=1}^{t=T} Q_t x_t}{\sum_{t=1}^{t=T} Q_t} \quad (3)$$

where Q_t is the flow rate and x_t is the measured value at time t.

Due to incomplete data, *EMV*s were calculated in several different manners for each event (Table 8), and average *EMV*s were calculated based on them, using the same approach as for the *EMC*s (Section 2.5.1).

2.5.3 Removal efficiencies

Filter performance can be described with different effectiveness parameters, *EMC efficiency* and *mass efficiency* being the most used ones (Law et al. 2008). *EMC efficiencies* (EMC_{eff}) were calculated as a ratio of reduced *EMC* and influent *EMC* (Law et al. 2008):

$$EMC_{eff} = \frac{EMC_{in} - EMC_{out}}{EMC_{in}} 100\% \quad (4)$$

where EMC_{in} is the event mean concentration of the influent and EMC_{out} is the event mean concentration of the effluent (Equation 2 in Section 2.5.1)

If the filter is reducing water volume (due to infiltration and evapotranspiration), it can be reducing pollutant loads as well, although the concentrations may be higher due to smaller volume. In these cases *mass efficiency* is more representing value than *EMC efficiency*, as it takes into account also the water losses in the filter. *Mass efficiencies* (m_{eff}) were determined by the following equation:

$$m_{eff} = \frac{L_{in} - L_{out}}{L_{in}} 100\% \quad (5)$$

where L_{in} is pollutant load of the influent and L_{out} pollutant load of the effluent. (Law et al. 2008)

Pollutant load L was determined as:

$$L = (EMC)\, V \quad (6)$$

where *EMC* is event mean concentration and V volume of water during the event (Law et al. 2008).

The influent volume was estimated based on the measured precipitation and the catchment areas of the filters (both assumed 100 m^2). It was assumed that 90% of the rain fallen on the catchment areas enters the filters. Thus, the influent volume V_{in} becomes:

$$V_{in} = 0.9Ad \quad (7)$$

where A is the catchment area and d the rain depth.

The effluent volume was calculated based on the measured flow rates assuming they changed linearly between the measurements. Thus, the effluent water volume V_{out} becomes:

$$V_{out} = \sum_{t=1}^{t=T} V_t = \sum_{t=1}^{t=T} Q_t \, t_0 \quad (8)$$

where V_t is the water volume and Q_t flow rate at time t and t_0 calculation interval (1 min). The effluent volumes were calculated using the period that flow rates were assumed to be elevated compared with pre-event situation (method 2 in Table 8).

2.5.4 Correlation between measured parameters

The Spearman correlations (r_s) between the analyzed parameters were determined separately for the untreated stormwater, sand-biochar filter and sand filter samples. Since the aim was to observe relationships between the parameters of the same sampling point, parameters were not divided into different rain events. This means that the correlations between the parameters were based on all analyzed values of this study – i.e. for most parameters N was 44, 40 and 38 for the untreated stormwater, sand-biochar filter effluent and sand filter effluent, respectively (Table 9 in Section 3.1; Appendix 6). The most strongly correlated parameters were plotted against each other and a coefficient of determination value (R^2) was determined.

The flow rates were included in the correlation analysis for the filter effluents. As the flow rate measurements were not conducted in the same intervals as the quality samples, corresponding flow rates were linearly interpolated based on the existing measurements.

2.6 Geochemical modelling

Geochemical modelling was utilized for Event 2 and 3 in order to specify the mechanisms involved in the pollutant reduction in the filters. The geochemical modelling was conducted with PHREEQC Interactive software (version 3.3.312.12704) by USGS. Instructions for the program are presented by Appelo & Postma (2007) and Parkhurst & Appelo (2013).

PHREEQC modelling applies thermodynamic principles to predict equilibrium reactions, which are controlling the concentrations of dissolved components within a solution (Wendling et al. 2017b). PHREEQC was used to model saturation indices (*SI*) of different mineral phases in the sand filter and sand-biochar filter effluents based on the measured concentrations and databases containing mineral information. The input values for the model are given in Appendix 4. Saturation index (*SI*) describe the saturation state of a mineral phase, and it is defined as:

$$SI = \log\left(\frac{IAP}{K_s}\right) \quad (9)$$

where IAP is the ion activity product and K_s is the solubility product (Appelo & Postma 2007; Genç-Fuhrman et al. 2007; Islam et al. 2016).

Positive *SI* indicates the solution (water) is oversaturated in respect of the mineral phase, whereas negative *SI* indicates the mineral phase is undersaturated (Appelo & Postma 2007; Wendling et al. 2017b). *SI* near zero (ca. -0.5 to 0.5) indicates the mineral is at equilibrium or at approximate equilibrium with the solution (Wendling et al. 2017b). Oversaturation of a mineral predicts its precipitation from the solution, while undersaturation suggests possible mineral solubility if the given mineral is present in solid phase and in contact with the solution (Appelo & Postma 2007; Islam et al. 2016; Wendling et al. 2017b).

Two database files provided with the PHREEQC software were used as a source for the K_s values: phreeqc.dat (Parkhurst & Appelo 2013) and wateq4f.dat (Ball & Nordstrom 1991). In total, 89 mineral phases were included in the geochemical modelling of this study (Appendix 5).

The PHREEQC modelling was applied for a total of four sand-biochar filter samples and four sand filter samples – i.e. two samples per filter per event (Appendix 4). As the model input concentrations were set to the measured concentrations of the filter effluents (immediately after exiting the filters), the modelling results were assumed to describe the saturation conditions within the filters. Thus, modelled *SI*s were used to predict the pollutant removal mechanisms in the studied filters.

PHREEQC requires input alkalinity in unit of mg/l of HCO_3. Therefore, the measured alkalinity values in mmol/l were converted by multiplying them by 61 (SFS-EN ISO 9963-1 1996).

3 Results & Discussion

3.1 Characteristics of the study period

During the study period (summer 2017), total measured precipitation at the site was 281 mm. Figure 15 shows that most rainfalls caused so small effluent flow rates that they were not detected by the automatic metering, since the used instrumentation was not suitable for low flows. Therefore, it was important that the flow rates were frequently measured manually during the examined events. Based on the occasional manual measurements between the rain events, the flow rates varied between 1 and 5 l/h suggesting that the filter structures were not completely dry at any time.

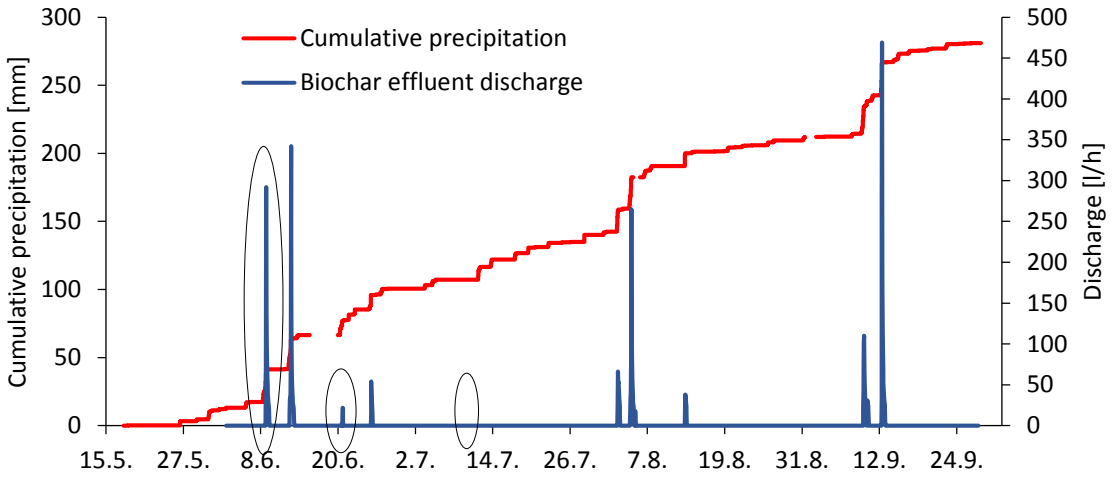

Figure 15. Cumulative precipitation at the site and the flow rate of the sand-biochar filter by the automatic metering during the study period. The flow rate curve of the sand filter was similar. Studied rain events are shown with black circles. Gaps in the precipitation curve indicate missing data. Note that only discharges generated by major rainfalls were detected by the automatic metering.

In June-August, total measured precipitation at the site was 201.0 mm. During the short gaps in the measured site data (Figure 15), rainfall of 10.8 mm was measured by FMI, indicating that total precipitation at the site in June-August was approximately 212 mm. During the same period, precipitation measured by FMI only ca. 4.5 km away from the site was 201.5 mm (Figure 5). It seems that during a period of three months, differences in rainfall within a 5 km distance were averaged out.

There was higher variability in precipitation at different locations in smaller temporal scale and rain dynamics during the storms varied between the site and the FMI station. For example, the storm in June 20 (Event 2) produced 5 mm of precipitation according to measurements by FMI, whereas at the study site the measured rainfall was 10.6 mm (Table 9). Visual observations support that rainfall only couple of hundred meters away was likely to be different than at the site. This suggests that rain gauge measurement at the site is necessary for precise stormwater investigation such as practiced in this study, which is consistent with Niemi (2017).

The precipitation measurements and the rain gauge at the site can be assumed to be relatively reliable, since the backup gauge produced similar results. The total precipitation during the

study period by the backup gauge was 284 mm, which is only 1% apart from the actual measurement.

As the studied storms varied significantly in terms of rain characteristics and measured concentrations and flow rates (Table 9), they are studied separately in Section 3.2.

Table 9. Measured characteristics of the studied rain events.

	Event 1	**Event 2**	**Event 3**
Date	June 8-9	June 20	July 11-12
Rain duration	06:49-23:49 (17.0 h)	05:18-22:42 (17.4 h)	17:25-02:33 (9.1 h)
Precipitation [mm]	23.8	10.6	9.4
Average rain intensity [mm/h]	1.4	1.0	1.0
Max rain intensity [mm/10 min]	2	2.6	1.2
Max rain intensity [mm/5 min]	1.4	1.8	0.8
Antecedent dry period (ADP) [days] *	2	0 **	6
Cumulative precip. in preceding 10 days [mm]	14.2	32.1 **	6.6
Samples taken between	11:06-07:42 (20.6 h)	09:59-18:51 (8.9 h)	16:33-09:07 (16.6 h)
Number of samples (biochar; sand; influent; total)	15; 14; 11; 40	12; 12; 17; 41	13; 12; 16; 41
Number of additional samples (biochar; sand; influent; total)	-	9; 9; 8; 26	9; 8; 8; 25
Manual flow rate measurements	10:58-07:55 (21.0 h)	06:48-19:10 (12.4 h)	15:56-16:04 (24.1 h)
Number of manual flow rate measurements (biochar; sand; total)	52; 51; 103	42; 39; 81	34; 34; 68
Max effluent flow rates [l/h] (biochar; sand)	428; 576	32; 64	14; 17

* Days with less than 1 mm of precipitation (Sillanpää 2013).
** Precipitation data in June 16-19 by FMI (Helsinki-Vantaa Airport), due to gap in the field data.

The studied rainfall events lasted relatively long, which was challenging for the manual field measurements (Table 9). The studied rain events were longer than the median reported by Sillanpää (2013; median rain duration 3–8 h). It is noteworthy that the studied storms actually consisted of several shorter rain events instead of continuous rainfall (Section 3.2). Moreover, the studied events were biased towards larger storms, since they were chosen based on the forecasts predicting enough rainfall for measurable flow rates. Similar observation was reported by Li & Davis (2014). The median storm depth at residential areas in Espoo, Finland is 3–7 mm (Sillanpää 2013). In terms of pollutant mass loads, intermediate storms (5–26 mm) have a crucial role as they produce the majority of the long-term pollutant loads (Tuomela 2017). Although frequent, smaller rain events do not generate large amounts of runoff or pollutant loads. Tuomela (2017) concluded that design storms with 10–26 mm of rain depth should be used in the dimensioning of stormwater management systems instead of the currently mostly used 10 mm. Thus, the examined rain events in this study were quite representative in terms of stormwater quality assessment.

Although the quantities of the samples from the influent and effluents were approximately the same (Table 9), the samples were not taken at the same times or in same intervals. The reasons for this were the following: 1) Increased effluent flow rates occurred some time after the rainfall. Before increased effluent discharge, the flow rate measurements and samples were taken more seldom, representing the base flow situation. 2) Runoff from the bridge downspout was much more intense, but lasted only a short time after the rainfall, whereas the filter outflow occurred during a much longer period. 3) Changes in the concentrations of stormwater were supposedly much more rapid than in the effluents requiring more frequent sampling.

3.2 Dynamics of the events

3.2.1 Event 1

Event 1 (June 8, 2017) was the heaviest studied storm in terms of event precipitation (23.8 mm; Table 9 in Section 3.1). However, the rain occurred during a prolonged period and its intensity was mostly low. Rainfall was intense (≥ 0.4 mm / 5 min) during 1.5 hours (Figure 16).

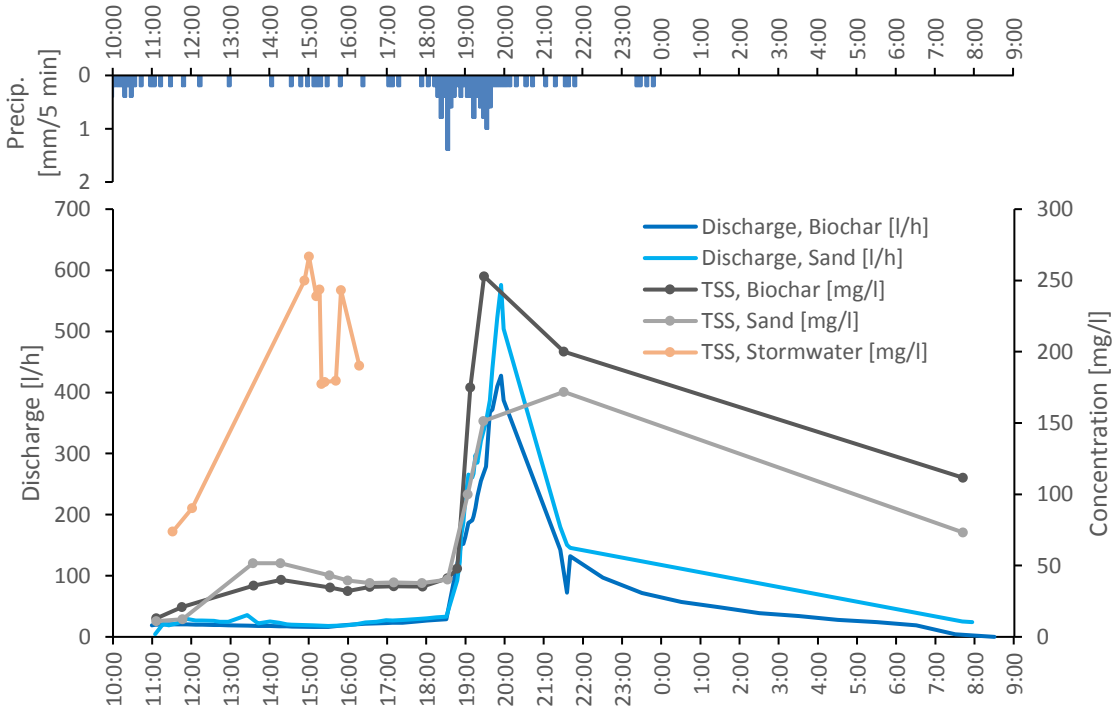

Figure 16. Concentrations of total suspended solids, effluent flow rates and rainfall during Event 1 (June 8, 2017). Similar figures showing the dynamics of all analyzed pollutants are presented in Appendix 1.

Flow rates of both effluents (the sand-biochar filter and the sand filter) started to quickly increase approximately 10 minutes after the intensive rain peak and reached maximum values of ca. 400 and 600 l/h for the sand-biochar and sand filter, respectively, being ca. 30 times higher than before the peak (Figure 16). When the effluent discharges were at their highest, stormwater started to accumulate on the surface of the filters (Figure 17). This could mean that the filters were saturated with water during the prolonged rainfall and also because

of the relatively wet antecedent period (Table 9). Therefore the intensive rain pulse produced rapid effluent flow rate peaks.

Figure 17. The filters during the rain event in June 8 (19:14). Temporary ponding was observed on top of the filters due to intensive rainfall.

The concentrations of the effluent total suspended solids (TSS) increased together with the flow rates (Figure 16). The same was observed for turbidity, ammonium (NH_4) and total phosphorus (TP) (Appendix 1). However, some analyzed quality parameters behaved in a different manner during the event. For instance, total organic carbon (TOC) of the sand-biochar filter started to rise simultaneously with the flow peak, whereas TOC of the sand filter decreased (Appendix 1).

The sampling of the influent stormwater was unsuccessful, because no stormwater samples were gathered during the most intensive rainfall (18:13–20:09; Figure 16). This relatively short rain impulse produced 45% of the total precipitation of the event. For instance, the lighter rainfall during the beginning of the event increased TSS concentration of the untreated stormwater ca. three-fold, but the concentration during the intense rain is unknown. The sampling of the filter effluents was more successful, despite the fact that more samples could have been taken during the flow peak – which generated most of the total effluent volume – and during the end of the event.

3.2.2 Event 2

Event 2 (June 20, 2017) consisted of several short rain peaks during ca. 18 hours (Figure 18) with a total precipitation of 10.6 mm (Table 9). Several rain peaks clearly resulted in effluent flow rate curves with a gradual increase. The rainfall was very intensive (≥ 1 mm / 5 min) only during 10 minutes at ca. 15:30, which also produced the most rapid increase in the effluent flow rates.

TSS concentration of the untreated stormwater varied strongly during the event and reached its maximum during the most intensive rain pulse (Figure 18). Also the TSS concentrations of the filter effluents changed during the event but these changes were much smaller than those observed in the influent stormwater. TSS, turbidity, NH_4 and TOC concentrations behaved similarly throughout the event indicating a positive correlation between the flow rates and the concentrations. However, TN and alkalinity revealed an opposite relationship since the concentrations diminished as the flow rate increased (Appendix 2).

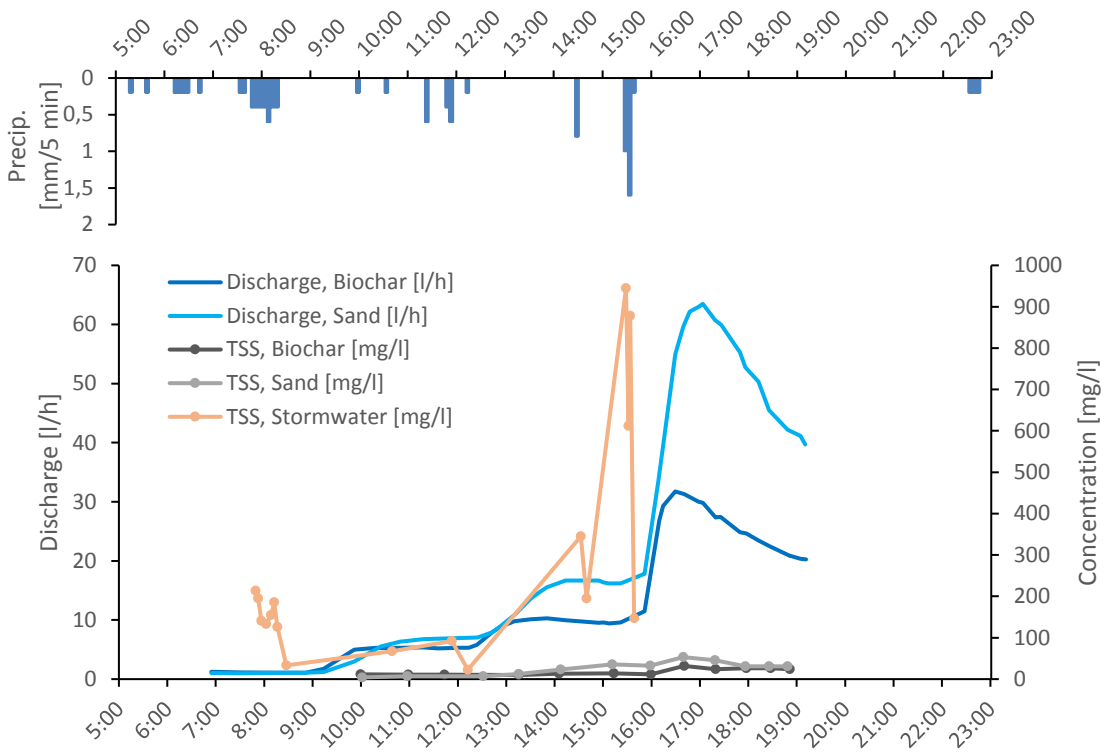

Figure 18. Concentrations of total suspended solids, effluent flow rates and rainfall during Event 2 (June 20, 2017). Similar figures showing the dynamics of all analyzed pollutants are presented in Appendix 2.

The sampling of Event 2 was successful in capturing the water quality changes during the most intense parts of the rainfall and runoff (Figure 18). However, the quality samples and discharge measurements were finished when the flow rates were still elevated compared with the pre-event situation. Unlike in the other two events, no extra measurements were taken at the following day.

In Event 2, the effluent from the sand filter had twice as high maximum flow rate as the sand-biochar filter. Almost during the whole event, the measured flow rates were higher from the sand filter. The same order occurred also during the other two studied storms, but the differences in the flow rates were not as remarkable as in Event 2 (Section 3.6). During Event 2, it was observed that a vehicle had driven over the filters and damaged the structure revealing the edge of the filter fabric or bentonite mat at the location of the sand-biochar filter (Figure 19), which likely affected the runoff from the road surface to enter the filter. This means that some of the influent stormwater infiltrated into the ground surrounding the filter.

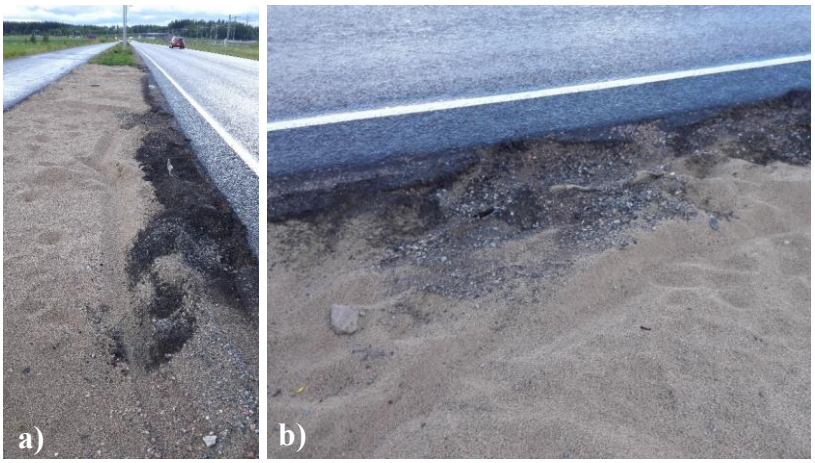

Figure 19. Vehicle had driven over the filters and damaged the structure revealing the edge of the filter fabric or bentonite mat. Some of the stormwater from the road surface may have infiltrated to the ground outside the filter.

The smaller runoff volume that entered the sand-biochar filter than the sand filter should not have major effect on the observed effluent concentrations, although greater share of the sand-biochar filter influent was generated on the walkway, which possibly had different amounts of pollutants than the motor road.

3.2.3 Event 3

Event 3 (July 11, 2017) was shorter than the previous two. In total, it lasted ca. 9 hours and 9.4 mm of precipitation was measured. However, most of the precipitation (79%) fell within 2.5 hours (17:25–19:53), thus making the storm more intensive and easier to sample (Figure 20).

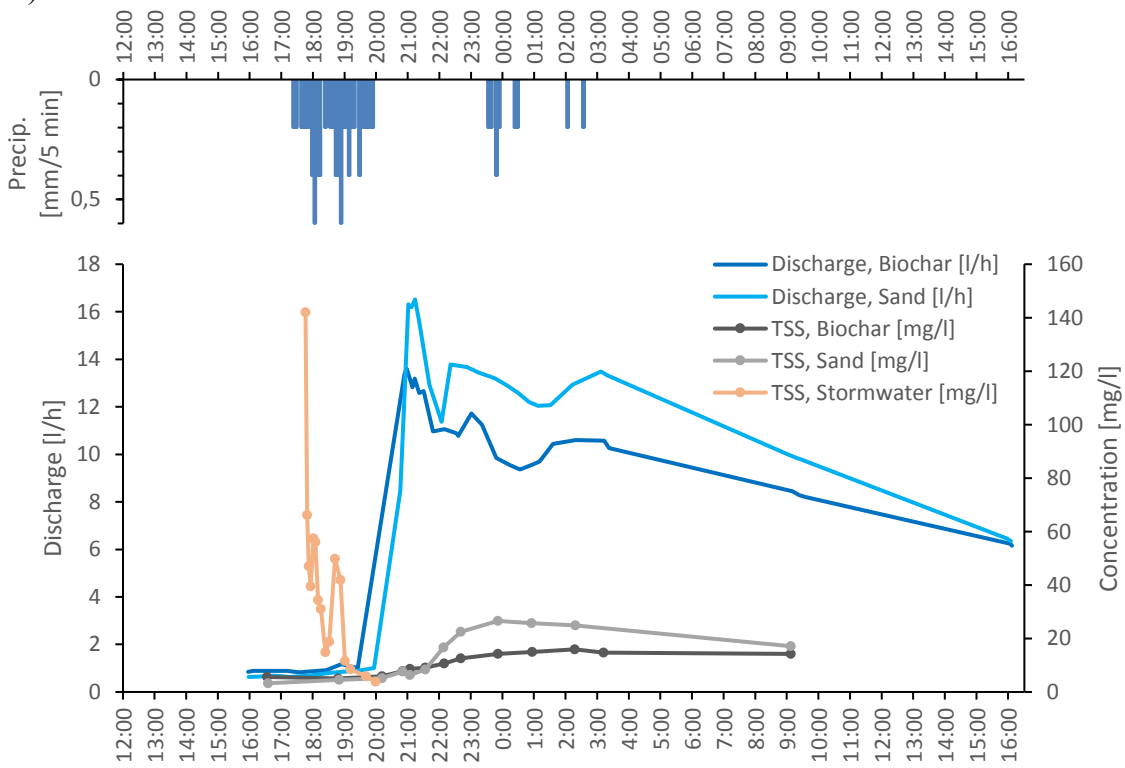

Figure 20. Concentrations of total suspended solids, effluent flow rates and rainfall during Event 3 (July 11, 2017). Similar figures showing the dynamics of all analyzed pollutants are presented in Appendix 3.

With the exception of the lack of stormwater samples during the lighter rainfall and too few effluent samples during the end of the event, the sampling of Event 3 was successful (Figure 20). Therefore, the determined *EMC*s and their comparison between the stormwater, sand-biochar filter and sand filter, can be seen as reliable.

During the intensive rainfall (Figure 20), stormwater was sampled with short intervals and the whole rain pulse was covered. During the rain peak, TSS concentration decreased rapidly. This change was noticed also in the stormwater color at the sampling site, as the water from the downspout was very dark grey at the beginning and started to clear during the event.

Figure 20 shows rapid rises in the flow rates of the effluents, starting ca. 1.5 h after the beginning of the rain. It is noteworthy, however, that the flow rates were much lower than in the previous two events. The flow rates stayed elevated compared with the pre-event situation still ca. 23 hours after the beginning of the rainfall when the last manual flow rate measurements were conducted. When the flow rates were at their highest, quality samples were gathered with ca. 30–60 minutes intervals. The end part of the event (after ca. 03:00) was covered with only one quality sample and couple of flow rate measurements per filter. However, due to the moderate slow changes in concentrations and flow rates at the end of the event, it is unlikely that any clear changes were missed during the measurement gaps.

The lighter rain (23:31–02:31) was not covered with stormwater samples due to intensive effluent measurements (Figure 20). Despite its relatively small contribution to the total precipitation of the event (21%), it is evident that it caused new peaks in the effluent flow rates approximately at 03:00.

3.3 Correlation between measured parameters

Spearman correlation analysis was used to detect similarities in the behavior of different pollutants and to find possible indicator parameters, which could be used to predict other parameters. This section presents the main results from the correlation analysis. All determined Spearman correlation coefficients (r_s) are presented in Appendix 6.

TSS strongly correlated with TP in the untreated stormwater (r_s = 0.979). Correlation analysis yielded also relatively high correlations for TSS and TP in the sand-biochar filter and sand filter effluents (r_s = 0.806 and 0.843, respectively), but Figures 21b and 22c reveal that the correlation is not clear. The difference between the stormwater and the filter effluents is partly due to the higher ranges of TSS and TP in the stormwater (Figure 21a): if only TSS values below 200 mg/l are considered, the correlation in the untreated stormwater is not as strong (r_s = 0.956 and R^2 = 0.88; not shown), but still clearly higher than in the effluents. These results suggest that TSS can be quite accurately used as a surrogate constituent for TP in untreated stormwater but not in filtered water. In addition, the result suggests that phosphorus was mainly associated with suspended solids in the untreated stormwater as opposed to being in dissolved form, which is consistent with e.g. Valtanen et al. (2010) as discussed in Section 1.2.

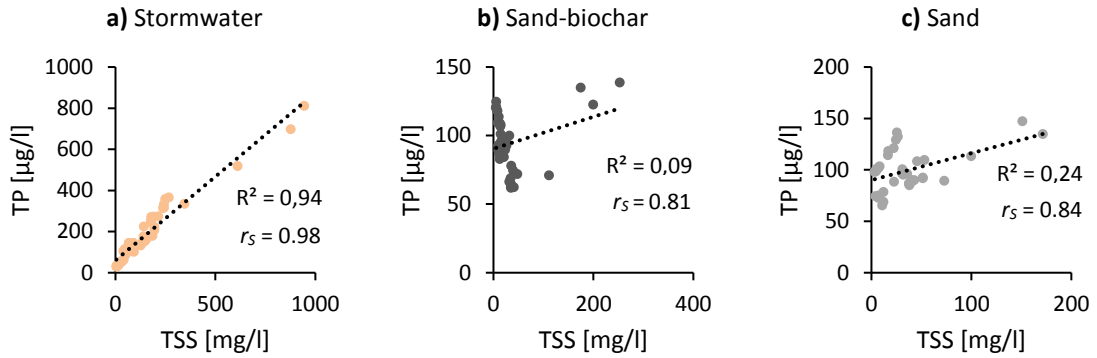

Figure 21. TSS vs. TP of all the analyzed samples for the untreated stormwater (a), sand-biochar filter effluent (b) and sand filter effluent (c). Also Spearman correlation coefficients (r_s), linear trend lines and their coefficients of determination (R^2) are shown.

Based on the Spearman correlation coefficients (Table 10), there was clear correlation between TSS and heavy metals in the untreated stormwater, which is in line with Galfi et al. (2017). Figure 22 reveals that the especially Pb strongly correlated with TSS ($R^2 = 0.95$), whereas the linkage with Zn was weak ($R^2 = 0.35$). The results indicate that measurement of only TSS can be quite accurately used to predict Pb and Ni concentrations of untreated stormwater in road areas. Also Kaczala et al. (2012) found that TSS is potential surrogate for Pb and Ni. However, the wide ranges in the concentrations may skew the correlations, since it is possible that only couple of very high values increase the strength of the correlation. Therefore, conclusions on the use of surrogate parameters should not be drawn too far based on just correlation coefficients. Although correlation does not identify causation, the results suggest that the metals in the stormwater – except Zn – were mostly attached to suspended solids as opposed to being in dissolved form. Pb being associated with suspended solids is supported by Prestes et al. (2006) and Genç-Fuhrman et al. (2007), but according to Prestes et al. (2006), Cd and Cu are typically in dissolved form. Weak correlation between Zn and TSS agrees with earlier studies showing that Zn is mostly in dissolved form (Section 1.2). The correlation between stormwater TSS and heavy metals suggests that efficient removal of TSS reduces efficiently also metals from stormwater (especially Pb, N and Cd), as concluded also by Kaczala et al. (2012). The results in Section 3.7 support this finding.

Table 10. Spearman correlation coefficients (r_s) between TSS and heavy metals.

	N	Cd	Cu	Pb	Ni	Zn
Stormwater TSS	16	0.891**	0.830**	0.922**	0.876**	0.739**
Sand-biochar TSS	18	0.471*	-0.769**	0.253	0.355	-0.204
Sand TSS	17	-0.165	-0.711**	0.778**	0.755**	-0.708**

* Correlation is significant at the 0.05 level (2-tailed).
** Correlation is significant at the 0.01 level (2-tailed).

The correlations between TSS and heavy metals were not clear after the filtration with the sand-biochar and sand filters (Table 10). For Cu and Zn, the results were even quite opposite, as the correlations were highly negative, indicating that high TSS was linked with low metal concentrations. In fact, none of the analyzed parameters correlated well with all of the included metals in the filter effluents (Appendix 6). This was most likely because metals were not equally retained in the filters (Sections 3.4 and 3.7). Whereas the metal contents in

the untreated stormwater were strongly dictated by the amount of particulate matter, the metals in the filter effluents were likely more soluble or bound with particles with different particle size distribution than in the influent. The results suggest that use of surrogate analyses for heavy metals is unreliable for treated stormwater.

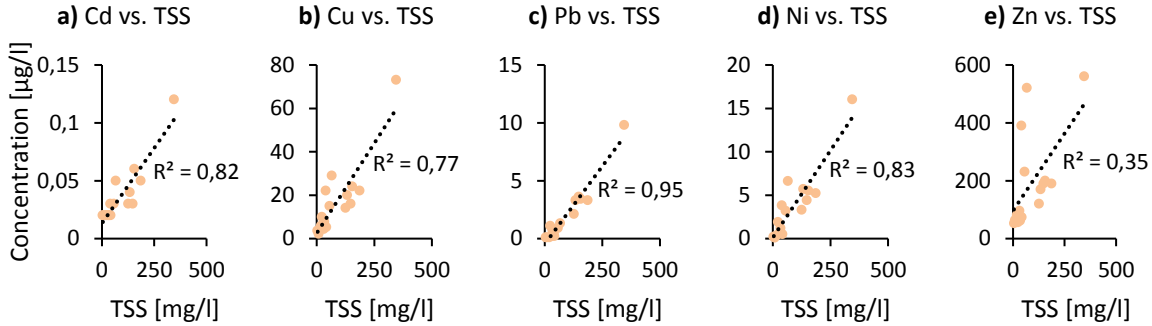

Figure 22. TSS compared with Cd (a), Cu (b), Pb (c), Ni (d) and Zn (e) in the untreated stormwater. Also linear trend lines and their coefficients of determination (R^2) are shown. Spearman correlation coefficients are given in Table 10.

Turbidity expressed correlation with TSS especially in the filter effluents (Figure 23). The correlation being lower in the stormwater than in the filter effluents indicates that TSS in the effluents consisted of smaller particles, which have greater impact on turbidity measurements than the larger particles abundant in the stormwater. The visual observations from the field and laboratory that particles were significantly larger in the untreated stormwater support this suggestion. This suggests that the filters removed the larger particles from the stormwater, whereas smaller particles – originating from the stormwater or the filters themselves – were present in the effluents. The amount of TSS is not totally descriptive of the water quality, since the smallest particles are known to convey a large share of the pollutants (Section 1.2). Therefore, based on the results, shares of the different sized particles should be considered in forthcoming studies instead of just TSS monitoring.

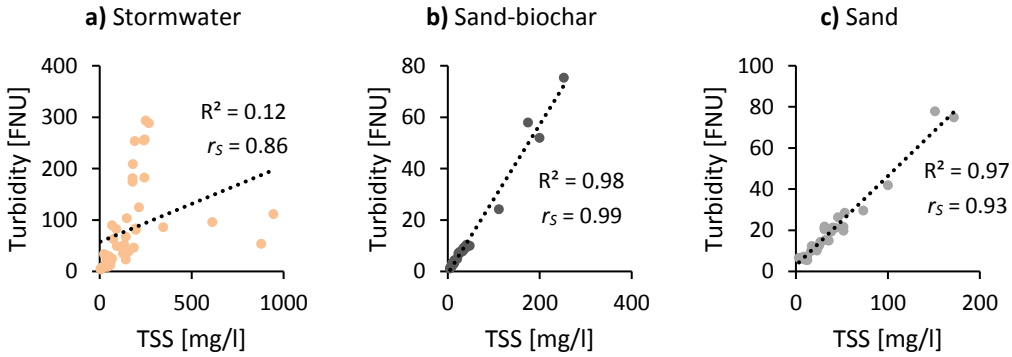

Figure 23. TSS vs. turbidity of all the analyzed samples for the untreated stormwater (a), sand-biochar filter effluent (b) and sand filter effluent (c). Also Spearman correlation coefficients (r_s), linear trend lines and their coefficients of determination (R^2) are shown.

The correlation analysis showed linkage between pH and Cu in the sand-biochar filter effluent (r_s = 0.819). This correlation turned out to be almost opposite for the sand filter effluent (r_s = -0.716), indicating that Cu concentrations were high when pH was lower. The

result suggests that different processes may occur within the two filter types. Cu is most soluble at low pH (Oorts 2013), and thus most challenging to capture. This may explain the negative correlation of the sand filter, whereas the different behavior in the sand-biochar filter effluent suggests that even dissolved Cu can be retained by the biochar. There were no clear correlations between pH and metals in the untreated stormwater, which is in line with Kaczala et al. (2012).

UV-absorbance is widely used for assessing the amount of organic material in water (e.g. Dobbs et al. 1972; McElmurry et al. 2013). In this study, UV-absorbance showed strong correlation in the untreated stormwater with TOC (r_s = 0.969), dissolved organic carbon (DOC; r_s = 0.956) and electrical conductivity (EC; r_s = 0.814). The same was not observed in the filter effluents (Appendix 6). For instance, the correlation between UV-absorbance and TOC was clearly weaker in the filter effluents than in the untreated stormwater (Figure 24). In the case of UV-absorbance and TOC, the higher correlation in the untreated stormwater is only slightly affected by the wider range of the values. For instance, if only the UV-absorbance values below 0.5 abs/cm are considered, correlation is still clearly stronger (r_s = 0.93 and R^2 = 0.87; not shown) than in the filter effluents. These results indicate that UV-absorbance is reliable surrogate for TOC only in untreated stormwater.

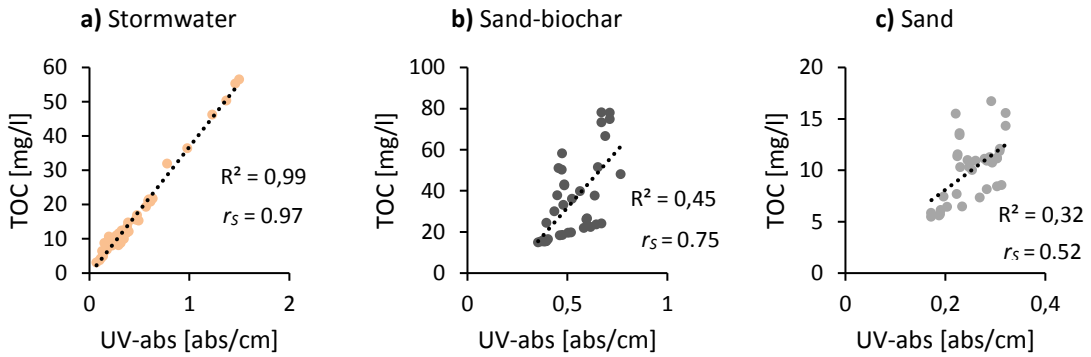

Figure 24. UV-absorbance vs. TOC of all the analyzed samples for the untreated stormwater (a), sand-biochar filter effluent (b) and sand filter effluent (c). Also Spearman correlation coefficients (r_s), linear trend lines and their coefficients of determination (R^2) are shown.

Based on the determined Spearman correlations, the sand-biochar filter effluent flow rate correlated with TOC (r_s = 0.810), whereas in the sand filter effluent this correlation was weak (r_s = 0.447). However, Figure 25a reveals that there was no clear connection between the flow rate and TOC either in the sand-biochar filter. Still, figures in Appendices 1 and 2 show that in Events 1 and 2, TOC of the sand-biochar filter seemed to increase as a consequence of the flow peak.

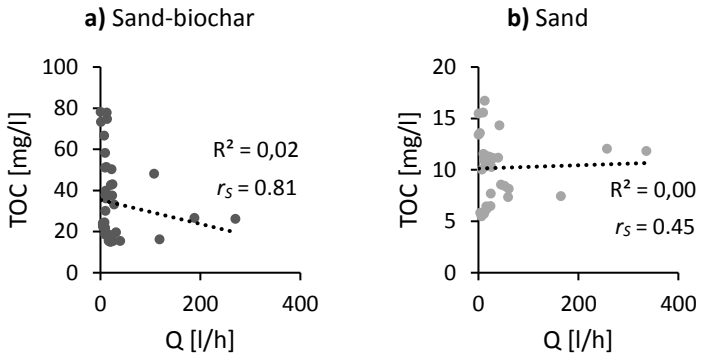

Figure 25. Flow rate (Q) vs. TOC of all the analyzed samples for sand-biochar filter effluent (a) and sand filter effluent (b). Also Spearman correlation coefficients (r_s), linear trend lines and their coefficients of determination (R^2) are shown.

Overall, the results showed that filtration of stormwater changes the relationships between the parameters. Therefore, useful surrogate parameters are not necessarily applicable to treated stormwater. Additionally, it is clear that Spearman correlation alone is not a reliable method to assess the correlations between the measured parameters.

3.4 Event mean concentrations

The determined *EMC*s varied widely between the untreated stormwater and the two filter types but also between the events (Figures 26 and 29). All the methods used to determine *EMC*s (Section 2.5.1) yielded very similar results. It indicates that the specific method – including the assumed beginning and ending times of the event – does not remarkably affect the *EMC*s. Therefore, only the averages of these different *EMC* methods are given.

3.4.1 Suspended solids & Nutrients

Total suspended solids

TSS *EMC* of the influent stormwater had more than 10-fold variability between the events (Figure 26). It is noteworthy that TSS had the same order of magnitude in all the three sampling points in Events 1 and 3 indicating only minor treatment effect, whereas in Event 2, TSS of the influent was more than ten times higher than TSS of the filter effluents. More importantly, both the sand-biochar and sand filters had high TSS values in Event 1 compared with the limits by Stockholm Vatten (2001; Table 2 in Section 1.2), and the sand-biochar filter exceeded even the higher threshold. This suggests the filters were not able to satisfactorily remove TSS from the stormwater during the intensive storm with more than 20 mm of rainfall. If stricter TSS threshold values – such as *no observable effect limit* (NOEL) of 25 mg/l (Ellis & Mitchell 2006) – were applied, the performances would have been unsatisfactory also in Events 2 and 3. Compared with this NOEL value, TSS *EMC* of the stormwater in Event 2 was very high.

The stormwater TSS *EMC*s were higher compared with the roads with slightly more traffic (Trafikverket 2011; Table 2 in Section 1.2). It should be noted that the actual measured stormwater TSS concentrations varied even more, as they were between 4 and 950 mg/l in the analyzed samples (Section 3.2). High variability in the untreated stormwater TSS during and between the rain events was consistent with the results from urban areas by Sillanpää (2013). Based on the current results, TSS clearly varied between the events also in the filter effluents.

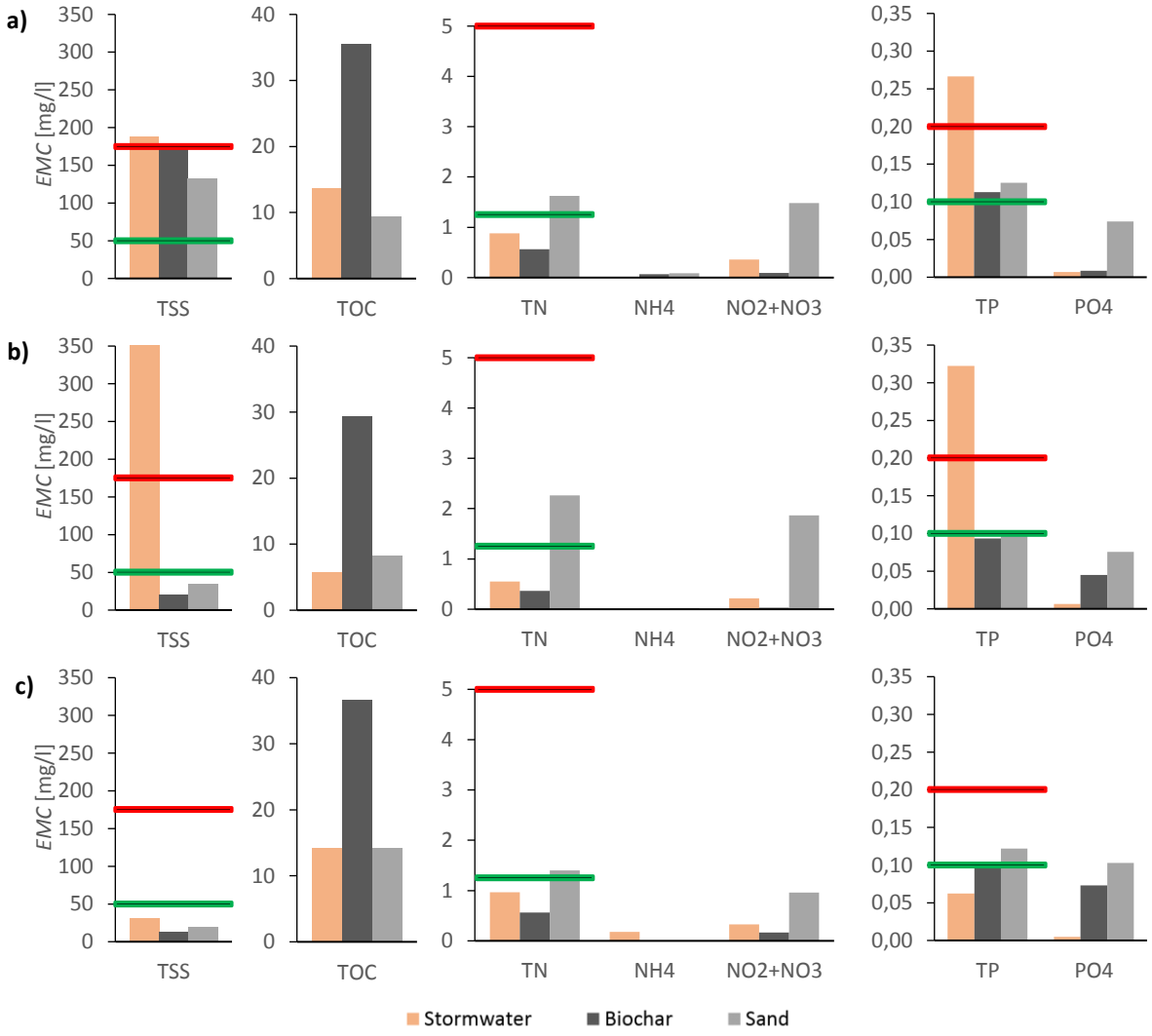

Figure 26. EMCs for suspended solids and nutrients in Events 1 (a), 2 (b) and 3 (c). Green lines indicate the lower thresholds and red lines the higher thresholds by Stockholm Vatten (2001). Note that NH_4 value for stormwater is missing in Events 1 and 2.

Total organic carbon

TOC showed similar behavior in all of the studied events (Figure 26). The sand filter had similar TOC *EMC*s as the untreated stormwater, whereas TOC of the sand-biochar filter was clearly higher than in the untreated stormwater in all of the events. The sand-biochar filter effluent exceeded the lower TOC limit value by EPA Ireland (2012; Table 2 in Section 1.2), whereas the sand-filter effluent and the untreated stormwater were clearly below the limit.

Nitrogen

TN *EMC*s were higher in the sand filter effluent than in the stormwater and exceeded the lower the lower limit by Stockholm Vatten (2001) in all of the events, suggesting the sand filter was leaching nitrogen (Figure 26). However, TN concentrations were still relatively low, if compared e.g. with construction sites with ca. 20 mg/l TN concentrations and the common TN levels in mature residential areas (Sillanpää 2013). Interestingly, most of the increased TN was due to increase in nitrite and nitrate (NO_2+NO_3) concentrations as they accounted for the most of TN in the sand filter effluent (Figure 27). In all of the analyzed sand filter effluent samples, Spearman correlation between TN and NO_2+NO_3 was as high

as 0.99 (Appendix 6). In contrast, the sand-biochar filter expressed lower TN and NO_2+NO_3 *EMC*s than the untreated stormwater, and far less of TN was in form of NO_2+NO_3 than in the sand filter effluent.

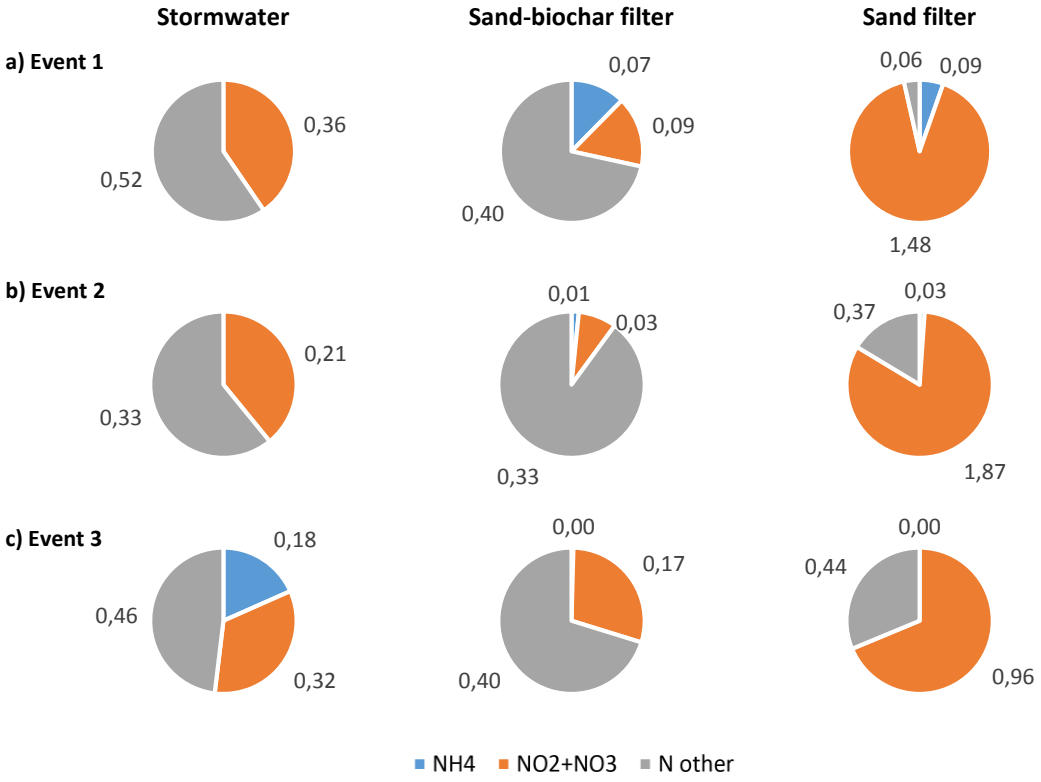

Figure 27. Shares of ammonium (NH_4), nitrite & nitrate (NO_2+NO_3) and other forms of nitrogen (N other) of the total nitrogen EMC in Events 1 (a), 2 (b) and 3 (c). Values in mg/l N. Note that value for stormwater NH_4 is missing in Events 1 and 2.

Based on Figure 27, the amount of organic nitrogen (*N other*) was similar in the untreated stormwater and in both filter effluents in Events 2 and 3, but the sand filter was not able to retain NO_2+NO_3 to the same extent as the sand-biochar filter. Thus, it is possible that more organic nitrogen (present in the filters due to both stormwater and filter media) transforms into NO_2 and NO_3 in the sand filter. The different behavior in Event 1 could be related to the different rain characteristics or the sampling (Section 3.2.1).

Nitrite and nitrate (NO_2+NO_3) were determined together for practical reasons, instead of analyzing them separately. However, it can be assumed that the samples contained mostly NO_3, since NO_2 transforms into NO_3 under aerobic conditions. Although the amount of NO_3 in the sand filter effluent was elevated compared with the untreated stormwater, the concentrations were still relatively low compared e.g. with construction sites, which are known to have much higher NO_3 concentrations (Sillanpää 2013).

Both the sand filter and sand-biochar filter effluents contained only small amounts of NH_4 (Figure 27). NH_4 content in the stormwater in Event 3 was approximately 0.2 mg/l, which is similar than the results from the road Kangasalantie by Inha et al. (2013; Table 2 in Section 1.2). NH_4 of the untreated stormwater was not determined for Events 1 and 2 due to practical problems in the laboratory.

Phosphorus

The results showed that in general, both filters decreased TP *EMC*s but increased *EMC*s of PO_4 (Figure 26). The *EMC*s of TP were similar in Event 1 and 2, in which both filters lowered almost equally the stormwater TP *EMC*, which exceeded the higher limit by Stockholm Vatten (2001). Event 3 was different, as the effluents had similar TP *EMC*s as during the previous events, but the stormwater had low TP content. In fact, stormwater TP was only ca. half of the effluent TPs. Relatively high fraction of TP in the filter effluents was in form of PO_4, whereas the influent stormwater had only small amounts of PO_4 (Figure 28). Especially in the sand filter effluent, most of the phosphorus was in form of PO_4, which is dissolved in the water and thus most easily bioavailable and important to remove (Erickson et al. 2011). These results suggest that most of the stormwater TP was in particulate form, whereas the effluents contained higher fraction of dissolved phosphorus.

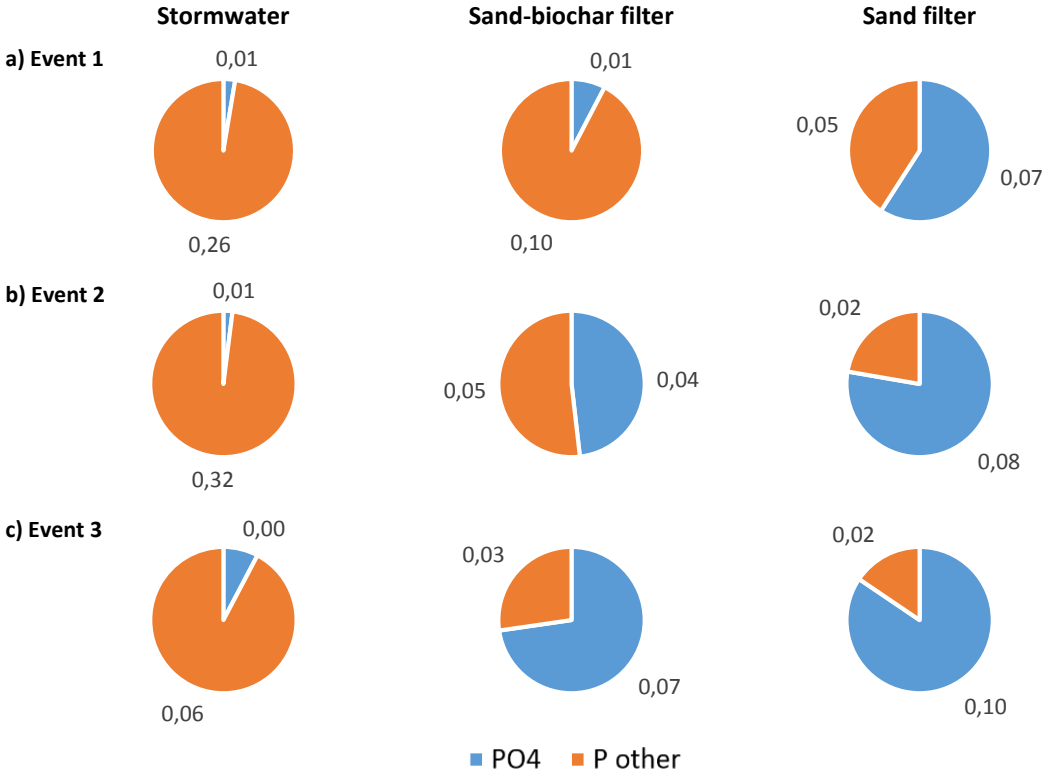

Figure 28. Shares of phosphate (PO_4) and other forms of phosphorus (P other) of the total phosphorus EMC in Events 1 (a), 2 (b) and 3 (c). Values in mg/l P.

3.4.2 Metals

Heavy metals were analyzed for Events 2 and 3. The untreated stormwater was relatively clean in terms of heavy metals, as the higher limit value by Stockholm Vatten (2001) was not exceeded for any of the included metals (Figure 29). Stormwater Ni *EMC*s, for instance, were similar than background Ni concentrations in forest streams (Lidman et al. 2014; 0.4–2.1 µg/l). However, the exceedances of the lower limit (Stockholm Vatten 2001) in Cu, Pb and Zn *EMC*s indicate that there is a need for stormwater treatment also at roads with moderate amounts of traffic. Cu *EMC*s were up to 10-fold higher than the background concentrations reported by Lidman et al. (2014; 0.46–1.8 µg/l). The effluents from both filters had heavy metal *EMC*s below the lower limit by Stockholm Vatten (2001).

In the studied events, the order of metals in the untreated stormwater based on their concentrations was Zn > Cu > Ni > Pb > Cd (Figure 29), which is slightly against the typical rank reported by Walker et al. (1999) (Zn > Pb > Cu > Ni > Cd). Higher amounts of Pb reported by Walker et al. (1999) could be partly due to lead used in gasoline in the past. However, Pb content of the sampled stormwater was relatively low, although the lower limit by Stockholm Vatten (2001) was exceeded. This underlines that the selection of threshold and reference values easily affects the interpretation of the concentrations. Especially Cd and Ni *EMC*s were very low compared with the threshold values.

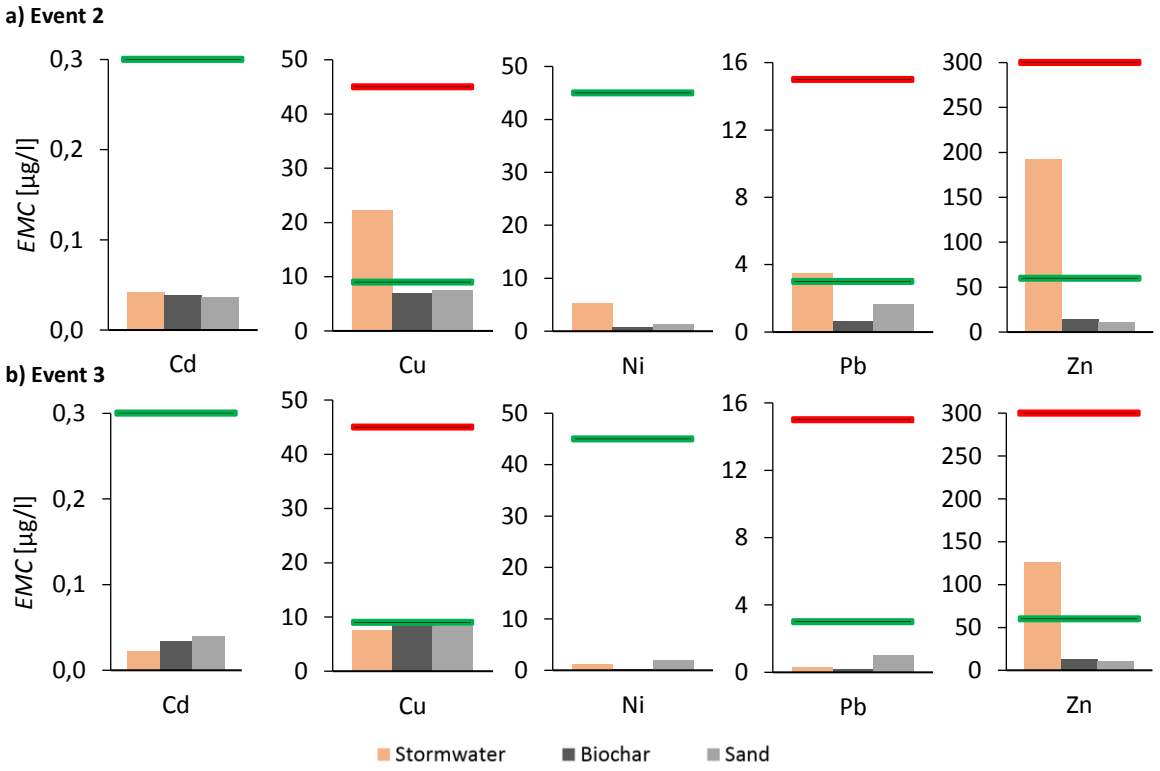

Figure 29. Heavy metal EMCs of Events 2 (a) and 3 (b). Green lines indicate the lower thresholds and red lines the higher thresholds by Stockholm Vatten (2001).

The influent stormwater had similar amounts of Zn and Pb than reported by Trafikverket (2011) and Inha et al. (2013) (Table 2 in Section 1.2). The range of stormwater Zn (10–560 µg/l) was actually very similar to the one determined by Inha et al. (55–510 µg/l). Pb showed greater variability (0.1–52 µg/l) than reported by Inha et al. (2013; 2–26 µg/l).

The determined metal *EMC*s were similar for both filter types (Figure 29). The clearest difference between the two filters was observed in Pb concentrations: the sand filter effluent had higher Pb *EMC*s than the sand-biochar filter effluent. Moreover, Pb *EMC* in the sand filter effluent was higher than in the untreated stormwater in Event 3. In fact, Pb concentration of the sand filter was higher than in the untreated stormwater throughout Event 3 (Appendix 3). However, Pb *EMC*s were low also in the sand filter effluent compared e.g. to residential areas (Valtanen et al. 2014). This indicates that higher Pb concentrations in the sand filter effluent did not necessarily have practical importance.

It seems that the effluent metal *EMC*s were relatively constant between the events and only the *EMC*s of the influent stormwater varied. It would have been interesting to see if the metal

*EMC*s were as low in Event 1 with the highest rain depth and flow rates, but it was lacking metal analyses.

3.5 Event mean values

There were clear differences between the untreated stormwater and the effluents from the two filter types with respect to the analyzed quality parameters and their event mean values (*EMV*) (Figure 30). Most of the *EMV*s were almost identical between the studied events, as turbidity was the only one showing clear variability. In Events 1 and 2, turbidity was the highest in the untreated stormwater, which was also visibly observed, as the untreated stormwater was dark grey and highly turbid, and the effluents from the filters were relatively clear and transparent (Figure 31). In Event 3, turbidity was the highest in the sand filter effluent, but still very low, since the magnitude of turbidities was clearly lower in Events 2 and 3 than in Event 1. It seems that high turbidity was related to heavy rainfall and thus high flow rates.

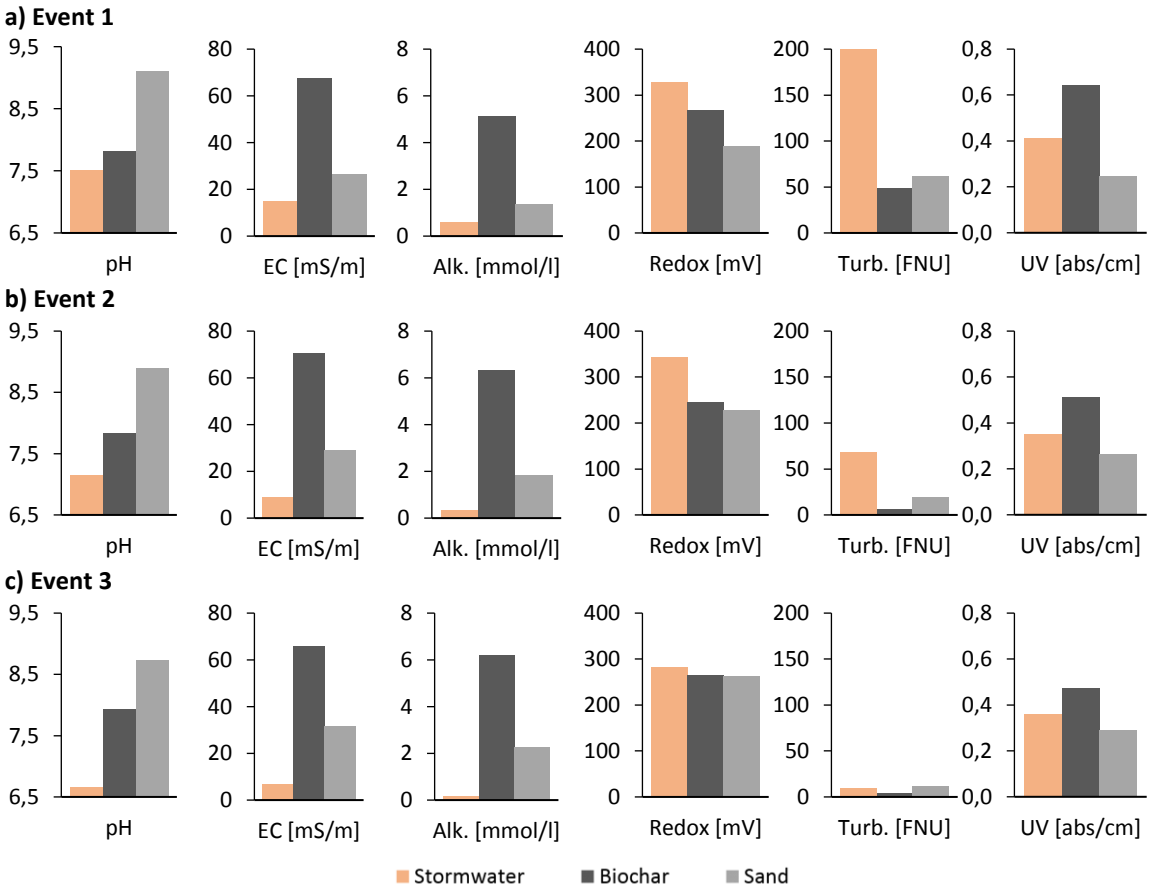

Figure 30. Event mean values (EMV) of pH, electrical conductivity (EC), alkalinity (Alk.), redox potential (Redox), turbidity (Turb.) and UV-absorbance (UV) in Events 1 (a), 2 (b) and 3 (c).

Event mean pH in the sand filter effluent was higher than in the sand-biochar filter effluent and in the untreated stormwater in all studied events (Figure 30). More interestingly, the sand filter pH increased during the events whereas pH of the sand-biochar filter decreased (Appendices 1–3). However, both filters increased the basicity of the untreated stormwater. Also in the column tests by Wendling et al. (2017a) birch biochar filtration was observed to

increase pH of the influent stormwater. Event mean pH of the sand filter and sand-biochar filter was relatively constant between the events, whereas pH of the stormwater showed some variability. However, stormwater pH was close to neutral in all the studied events, and unlike most of the studied parameters, it stayed relatively constant during the events as well (Appendices 1–3). The event mean pHs of the stormwater were slightly lower than reported by Galfi et al. (2017; event mean pH 6.9–8.4).

Figure 31. Color of the filter effluents and untreated stormwater. Sampled waters in 1-liter bottles from the sand filter (left), the sand-biochar filter (middle) and the untreated stormwater (right). The effluent from the sand filter was the most transparent and colorless, while the effluent from the sand-biochar filter was slightly yellowish and stormwater dark grey. The colors were similar throughout the study, although the shades varied.

EC and alkalinity acted similarly (Figure 30). In both, the sand-biochar filter had the highest average values. EC and alkalinity levels were closely associated also during the events in the untreated stormwater (r_s = 0.895) and sand-biochar filter effluent (r_s = 0.946) but not in the sand filter effluent (r_s = 0.579) (Appendix 6). In Event 1 with the highest effluent flow rates, both EC and alkalinity of the sand-biochar filter increased during the flow peak, whereas in the sand filter effluent they decreased continuously (Appendix 1). In Event 1, also TOC of the sand-biochar filter behaved almost identically as EC and alkalinity. The same behavior was not observed in Events 2 and 3. This suggests that elevated discharge through the sand-biochar filter was able to release dissolved substances from the biochar layer and thus also increase EC and alkalinity. Since there was no clear correlation between EC and analyzed pollutants (Appendix 6), more detailed nature of these dissolved substances is unclear.

Electrical conductivity of the untreated stormwater was in the same order of magnitude than observed by Inha et al. (2013) from a road with similar amount of traffic (2.6–97 mS/m). Compared with this range, ECs of the untreated stormwater in this study were somewhat lower (2.9–20 mS/m). The reason for this is likely that Inha et al. (2013) studied stormwater properties also during winter when road salt is applied to the road for antiskid reasons. They found clear relationship between the salting and EC.

The earlier discussion (Sections 3.2 and 3.4) about the uncertainty in the stormwater sampling in Event 1 applies also for the *EMV*s shown in Figure 30. The *EMV*s were determined in the same manner as the *EMC* values (Section 2.5.2). Therefore, the comparison between the untreated stormwater and the filter effluents is less reliable than the comparison between the two filters, which were sampled almost identically.

3.6 Mass balance

The calculated volumes of the filter influents and effluents were not equal, i.e. all water which was assumed to enter the filters did not exit them during the events (Table 11). Especially the effluent volumes from the sand-biochar filter were low and smaller than from the sand filter in all the events, which was result from the lower flow rates as discussed in Section 3.2. The biochar layer was likely able to retain the water and release it during longer period, as biochar is known to have high water holding capacity (Section 1.3). In addition, the water retaining in the biochar layer likely enabled larger share of the water to evaporate after the rainfall, thus reducing the amount of water exiting via the subsurface drainage. Similar results from biochar amended green roofs were reported by Kuoppamäki et al. (2016). These results suggest that the biochar amendment improved the filter performance in reducing the quantity of stormwater.

Table 11. Mass balance of the rainfall-runoff events.

Volumes [liter]	**Event 1**	**Event 2**	**Event 3**
Influent (for both filters)	2142	954	846
Sand-biochar filter effluent	1415	177	243
Sand filter effluent	1697	298	253
Sand-biochar filter effluent / influent	66 %	19 %	29 %
Sand filter effluent / influent	79 %	31 %	30 %

The improved water holding capacity could be a useful feature in locations where the rapid discharge of stormwater is an issue. On the other hand, water staying in the filter for longer period is potentially problematic during winter time as it may freeze and reduce the hydraulic conductivity of the filter. Therefore, further studies under winter conditions are recommended.

Also the higher number of filter fabric layers in the sand-biochar filter (Section 2.1) was probably able to hinder the flow through the sand-biochar filter. In addition, small differences in the catchment areas and other errors could have affected the results. The sand-biochar effluent volume compared with the influent was especially low in Event 2, which may be related to the damaging of the filter edge (Figure 19 in Section 3.2.2).

Four different possible reasons were identified for the observed difference between the assumed influent and effluent volumes: 1) The discharges from the filters during the end of the events were not taken into account for long enough. As the flow rate measurements were finished when the discharges were still elevated compared with pre-event situation, the tails of the events were linearly interpolated, which does not necessarily correspond to the reality. It is possible that the flow rates stayed elevated during periods of days, meaning the effluent volumes would approach the influent volumes after a prolonged period. 2) The size of the catchment areas of the filters may have been assessed wrongly. However, the error should not be large enough to produce the observed error in the mass balance, indicating other reasons occurred simultaneously. 3) It was assumed that 90% of rainfall on the catchment areas entered the filters (Section 2.5.3). This assumption may not be valid. Greater share of the stormwater may have e.g. evaporated or infiltrated through the asphalt cracks. 4) It is

possible that not all the water exited the filters via the discharge pipes. Although the filters were isolated from the surrounding ground with a bentonite mat (Section 2.1), it is likely that at least some water leaked from the filters to surrounding soil.

During the entire study period, it was noticed that the flow rates of the filter effluents were never zero but varied approximately between 1 and 5 l/h also during longer dry periods. This supports the assumption of slow discharge of the water (especially in case of the sand-biochar filter), but possibly also means that water from the surrounding ground infiltrated into the filters. Therefore, it is impossible to determine exactly, which water enters and exits the filters at which time. Thus, it was accepted that the mass balances of the rainfall-runoff events were not closed and this was taken into account in the filter performance assessment (Section 3.7).

3.7 Removal efficiency

The two methods used to assess filter performance – *EMC efficiency* and *mass efficiency* – yielded varying or even conflicting results (Tables 12 and 13). *EMC efficiencies* were clearly lower and many of them were negative, since *EMC*s of many pollutants were higher in the effluents than in the influent, especially in Event 3 with the lowest influent *EMC*s (Section 3.4). *Mass efficiencies* seemed to provide more reliable measure for the treatment performance.

Comparison of removal efficiencies based on *EMC*s is not strictly valid, as the filters reduced the amount of water (Section 3.6). Law et al. (2008) stated that performance of a structure that is reducing water (via infiltration and evapotranspiration) should be described by *mass efficiency*, since the filter can reduce pollutant loads, even when the effluent concentrations may be higher due to decreased water volumes. On the other hand, if most of the reduced water volume was a result of infiltration of water (and pollutants within) into surrounding ground, the pollutants would still be released into the environment and *mass efficiency* could give too optimistic results. Therefore, the pollutant reducing capacity should not be reported with a single value (Law et al. 2008). However, as the observed water deficit was clear (Section 3.6), *mass efficiency* gave more reliable results. *Mass efficiency* also took into account the higher water holding capacity of the sand-biochar filter.

Table 12. EMC efficiencies (%) of the sand-biochar filter (B) and sand filter (S). Negative value indicates increase in EMC. Bolded value indicates that EMC of the influent stormwater exceeded the lower limit by Stockholm Vatten (2001; Figures 26 and 29 in Section 3.4).

		TSS	TOC	TN	NH_4	NO_2+ NO_3	TP	PO_4	Turb.	Cd	Cu	Ni	Pb	Zn
Event 1	**B**	**5**	-159	36	-	75	**58**	-23	76	-	-	-	-	-
	S	**29**	31	-85	-	-316	**53**	-950	69	-	-	-	-	-
Event 2	**B**	**94**	-409	33	-	86	**71**	-597	92	11	**69**	86	**82**	**93**
	S	**90**	-43	-312	-	-769	**70**	-1076	71	14	**67**	75	**54**	**94**
Event 3	**B**	58	-157	42	99	49	-61	-1418	63	-48	-14	83	42	**90**
	S	38	0	-45	100	-197	-95	-2034	-22	-75	-11	-73	-265	**91**

Comparison of *EMC efficiencies* revealed clear differences between the two filter types, although there was high variability between the studied events (Table 12). The most notable differences were in TOC, nitrogen compounds, Pb and Ni. The sand-biochar filter demonstrated better performance on the decreasing of turbidity, even though the sand filter was also efficient in Events 1 and 2.

Table 13. Mass efficiencies (%) of the sand-biochar filter (B) and sand filter (S). Negative value indicates increase in the pollutant load. Bolded value indicates that EMC of the influent stormwater exceeded the lower limit by Stockholm Vatten (2001; Figures 26 and 29 in Section 3.4).

		TSS	TOC	TN	NH_4	NO_2+ NO_3	TP	PO_4	Cd	Cu	Ni	Pb	Zn
Event 1	**B**	**37**	-71	58	-	83	**78**	19	-	-	-	-	-
	S	**44**	46	-46	-	-230	**63**	-732	-	-	-	-	-
Event 2	**B**	**99**	28	88	-	97	**95**	-29	83	**94**	97	**97**	**99**
	S	**97**	66	-28	-	-171	**91**	-267	73	**90**	92	**85**	**98**
Event 3	**B**	88	26	83	100	85	54	-335	58	67	95	83	**97**
	S	81	70	57	100	11	42	-539	48	67	48	-9	**97**

The efficiencies were higher when the *EMC*s of the influent stormwater were higher (Tables 12 and 13). When the influent concentrations were already low, the filters were not able to remove the pollutants to same extent. However, in these cases high efficiency was not needed. For instance, Pb *mass efficiency* of the sand filter in Event 3 was negative, although its *EMC* was clearly below the threshold (Figure 29 in Section 3.4.2) and in this sense the performance was sufficient. These results highlight that low efficiency percentage does not necessarily indicate poor filter performance whereas high percentage does not necessarily indicate that pollutant retention is sufficient in terms of threshold values.

3.7.1 Suspended solids & Nutrients

Total suspended solids

Based on the *mass efficiencies* (Table 13), the filters performed almost equally well in the reduction of TSS, especially in Events 2 and 3 with less rainfall. However, compared with the threshold values, the performances were poor in Event 1 (Figure 26a in Section 3.4.1). As both filters acted similarly, it seems that the biochar layer did not have clear effect on TSS loads. Thus, TSS was likely retained mostly in the surface sand layers before reaching the biochar layer. The filters likely retained efficiently the largest particles, while the smallest ones were not removed from the stormwater, as visibly observed from the water samples. It is possible that the filters themselves released very small particles in their effluents, since in the laboratory the effluent samples quickly clogged 0.45 µm membrane filters whereas the stormwater samples did not.

Total organic carbon

Based on the two efficiency methods, the performance related to TOC was clearly better in the sand filter than in the sand-biochar filter (Tables 12 and 13). In fact, the sand-biochar filter had negative *mass efficiency* for TOC in Event 1 with the highest rain depth, indicating that the sand-biochar filter was increasing the carbon load i.e. acting as a source instead of a sink. This likely means that some carbon from the biochar layer was washed away during the event. In Events 1 and 2, TOC concentration in the sand-biochar filter effluent increased

with increasing flow rates (Appendices 1 and 2), suggesting high flows were able to release carbon from the biochar layer.

In all samples from all three sampling points, TOC was almost equal to DOC, demonstrating that carbon was mostly in dissolved form (r_s = 0.911–0.994; Appendix 6). It seems that the lower performances of the sand-biochar filter with respect to TSS and TOC were related, i.e. carbon release was seen also in elevated TSS concentrations. This could explain the visually observed smaller particles in the effluent than in the stormwater: TSS particles in the influent and effluent had different origin.

Phosphorus

The results in Tables 12 and 13 reveal that the performance of both filters with respect to PO_4 was consistently poor. In contrast to this, Valtanen et al. (2017) reported more than 90% *mass efficiencies* for PO_4 in their test columns without vegetation. These columns consisted of both sand and organic matter, but still the difference to this study is large. Based on the current study, it is evident that both filters were leaching PO_4, even though TP retention was good or excellent. This indicates that influent phosphorus transformed into dissolved form (PO_4) within the filters. Efficient TP reduction was consistent with the results by Inha et al. (2013) showing efficient phosphorus retention via filtration, although the type of filtration in their study was not specified. Based on the *mass efficiencies*, the sand-biochar filter had slightly better performance on TP removal than the sand filter. As discussed in Section 1.2, the amount of TP is even more important than of PO_4, since the form of phosphorus can change in the receiving environment. Therefore, both filters were almost equally promising in retaining phosphorus, although the sand filter leached more PO_4 than the sand-biochar filter.

Wendling et al. (2017a) reported initial leaching of phosphorus from birch biochar as discussed in Section 1.3. Similar leaching was not observed in this study. It is possible that initial leaching of TP occurred from the sand-biochar filter soon after it was constructed but after ca. 5 months and ca. 150 mm of precipitation (Figure 5 in Section 2.1) the filter was clearly removing TP. As the performance of the sand-biochar filters was slightly higher than of the sand filter (Table 13), the biochar layer actually improved TP removal.

Nitrogen

The results (Table 12 and 13) showed that the sand-biochar filter had good ability to retain TN from the stormwater. It was consistent for each event using both efficiency methods. The retention of NO_3 (and NO_2) by the sand-biochar filter was even higher than in vegetated biofilters studied by Valtanen et al. (2017). Instead, the sand filter showed poor performance in this study with respect to nitrogen, as leaching of TN was observed in Events 1 and 2 based on the *mass efficiencies*. The leaching of NO_3 (and NO_2) was at higher level than from the non-vegetated biofilters reported by Valtanen et al. (2017).

Leaching of nitrogen is widely reported from recently constructed stormwater structures and from construction sites (e.g. Treese et al. 2012; Sillanpää 2013; Valtanen et al. 2017). Based on this study and Valtanen et al. (2017), it seems that new structures need some amendment to prevent initial leaching of nitrogen. Biochar amendment is an interesting option to reduce the nitrogen release, especially if no vegetation – that would retain nitrogen once grown – is used in the treatment structure. The nitrogen binding performance of biochar could be applied to sites with high nitrogen loading, such as construction sites. However, it is unclear,

how well biochar amendment would perform under higher nitrogen loading. According to Treese et al. (2012), the amount of organic material in the filter should not be unnecessary high. Determination of suitable amount of biochar would require further laboratory and field experiments. In the location of this study, the increased nitrogen removal by the sand-biochar filter was not as beneficial, since the nitrogen concentrations were relatively low also in the sand filter effluent.

3.7.2 Metals

Based on the removal efficiencies (Tables 12 and 13), the filters retained efficiently most of the analyzed metals. The almost complete removal of Zn was consistent for both filters in both events with both efficiency methods. This was inconsistent with Inha et al. (2013) who reported that Zn was not efficiently removed with (unspecified) filtration. However, Valtanen et al. (2017) reported Zn removal percentages of 94–96 for non-vegetated filters consisting of both sand and organic soil.

Based on the *mass efficiencies* (Table 13), the sand-biochar filter slightly outperformed the sand filter in the removal of Cd, Cu, Pb and Ni. Birch biochar expressed good capacity in Cu and Pb removal also in the column tests by Wendling et al. (2017a; 82 and 80%, respectively). Cu removal of both filters was similar or lower than in the non-vegetated filters studied by Valtanen et al. (2017; 92–95 %).

Removal efficiencies of metals varied between Events 2 and 3 (Tables 12 and 13) even though they were similar storms in terms of total precipitation (Section 3.1), indicating that higher number of storms should be studied. However, the rank between the filters based on the *mass efficiencies* stayed the same for all metals in both events.

Clear retention of Pb by the sand-biochar filter (Table 13) was consistent with the (unspecified) filtration results by Inha et al. (2013). The results showed that the sand filter was leaching Pb in Event 3, since both removal efficiencies were negative, whereas in Event 2 Pb was efficiently removed also by the sand filter. It should be noted that Pb concentrations were low and also the sand filter was clearly below limit values (Section 3.4.2).

3.8 Other analyzed pollutants

The study included limited number of extra analyzed substances from the filter effluents, which were determined mostly for the geochemical modelling. The results shown in Table 14 were used as an input for PHREEQC modelling along with other measured values (Section 2.6; Appendix 4).

Table 14 lists the values of the individual measurements. It should be noted, that the values describe only the concentrations at the given times, and do not cover the entire events. Reduction analysis was not conducted, since these substances were not analyzed from the untreated stormwater. Based on the results, the sand filter effluent had ca. 5 times higher Al and Fe concentrations than the sand-biochar filter. Also Si was more abundant in the sand filter effluent. In contrast, the sand-biochar filter effluent had more Ca, Cl, K, Mg and Na.

Table 14. Concentrations of the other analyzed parameters in Events 2 and 3. Values in mg/l.

	Event 2				Event 3			
	Biochar		Sand		Biochar		Sand	
[mg/l] Time	16:40	18:51	16:39	18:48	20:50	22:41	20:50	22:41
Al	1.1	1.4	5.2	4.1	0.46	0.92	2.6	4.4
Ca	21	18	2.8	2.4	22	18	3	3.3
Cl	18	15	10	16	24	17	9.9	11
Fe	0.23	0.3	1.5	1.1	0.11	0.15	0.54	0.88
K	37	33	2	1.8	61	52	1.9	1.9
Mg	4.7	3.9	1.5	1.2	6.1	4.9	0.93	1.3
Mn	0.05	0.054	0.025	0.018	0.009	0.007	0.008	0.014
Na	120	91	59	55	170	130	61	66
SO_4	7.2	6.5	7.8	7.7	9.2	8.6	8.8	7.8
Si	7.6	7.6	14	12	7.8	8.2	9.5	13

3.9 Mechanisms of pollutant removal

This section provides the results of the geochemical modelling and discussion about the pollutant removal mechanisms. Modelling with PHREEQC program was applied to Events 2 and 3 (Section 2.6). To enable analysis of the numerous saturation indices (*SI*), mineral phases included in the model are divided into groups (Sections 3.9.1–3.9.10). The elements monitored both from the influent and the filter effluents (Cd, Cu, Ni, Pb, Zn, P and N) are presented first. Combined hydro-, polluto- and hyteographs of these substances for both events are presented in Appendix 2–3 to enable comparison between the modelled *SI*s and the rainfall-runoff event dynamics. The main mechanisms are summarized for all studied pollutants in Section 3.9.11.

All modelled *SI*s are provided in Appendix 5. The number of included mineral phases (89) is higher than in most stormwater studies applying PHREEQC (e.g. Bäckström et al. 2003; Genç-Fuhrman et al. 2007; Huber et al. 2016). The reason for this was the high number of analyzed pollutants (Section 2.4): it was reasonable to include all mineral phases containing analyzed contaminants to enable comparison between the observed reductions and geochemical modelling results.

3.9.1 Cadmium

The PHREEQC modelling indicated that all Cd-containing minerals were undersaturated during the studied rain events in both filters, as they had negative saturation indices (Appendix 5). Otavite ($CdCO_3$) exhibited the highest degree of saturation compared with other Cd-containing minerals in all modelled samples but remained clearly undersaturated (*SI* = -2.6 to -2.0). Genç-Fuhrman et al. (2007) reported opposite results, as many of the studied columns were saturated with respect to cadmium.

Based on the negative *SI*s indicating undersaturation in the effluents form both filters, none of the modelled cadmium minerals were likely to precipitate as a pure phase within the filters. Despite the low concentrations, both filters were observed to remove Cd from the stormwater (Section 3.7). As Cd in stormwater is mostly in dissolved form (Section 1.2), the observed removal was likely based on sorption reactions and physical sieving was not an

important mechanisms. The measured Cd concentrations were very low, so it is possible that precipitation reactions would occur with higher influent concentrations. The very low concentrations also indicate that the observed removal was questionable.

3.9.2 Copper

According to PHREEQC modelling, cupric ferrite ($CuFe_2O_4$) and cuprous ferrite ($CuFeO_2$) were the only Cu-containing minerals, which were oversaturated in the filter effluents. These mineral phases had clearly positive saturation indices (Table 15).

Table 15. Some of the modelled saturation indices of copper-containing mineral phases. Values indicating approximate equilibrium or supersaturation (≥ -0.5) are shown in bold text. All modelled Cu phases are presented in Appendix 5.

		Event 2				Event 3			
		Biochar		Sand		Biochar		Sand	
Mineral	**Formula**	**16:40**	**18:51**	**16:39**	**18:48**	**20:50**	**22:41**	**20:50**	**22:41**
$Cu(OH)_2$	$Cu(OH)_2$	-2.8	-2.7	-2.3	-2.3	-2.3	-2.4	-2.0	-2.1
$Cu_2(OH)_3NO_3$	$Cu_2(OH)_3NO_3$	-10.6	-10.5	-9.2	-9.0	-9.7	-9.6	-8.0	-8.7
CuOCuSO4	$CuOCuSO_4$	-19.8	-19.6	-21.3	-21.1	-19.5	-19.4	-18.8	-20.0
Cuprite	Cu_2O	-3.8	-3.6	-5.5	-5.3	-4.0	-3.9	-3.4	-4.5
Cupric ferrite	$CuFe_2O_4$	**14.7**	**14.9**	**16.7**	**16.5**	**14.5**	**14.6**	**16.3**	**16.5**
Cuprous ferrite	$CuFeO_2$	**13.7**	**13.9**	**13.7**	**13.7**	**13.3**	**13.4**	**14.3**	**13.9**
$CuSO_4$	$CuSO_4$	-17.1	-16.9	-19.0	-18.8	-17.2	-17.1	-16.9	-18.0
Dioptase	$CuSiO_3$:H2O	-4.0	-3.9	-3.4	-3.4	-3.6	-3.7	-3.2	-3.2

Copper may form mineral precipitates in alkaline environments (Wendling et al. 2017b). Although the mineral copper hydroxide ($Cu(OH)_2$) was undersaturated based on the modelling results, it usually dominates under neutral and alkaline circumstances (Wendling et al. 2017b), which occurred in both filter effluents. Cuprous ferrite ($Cu_2Fe_2O_4$) can form and be stable in soils saturated with water (Wendling et al. 2017b). Therefore, both cupric and cuprous ferrite were possible to form within the filters, but also formation of copper hydroxide ($Cu(OH)_2$) was possible. Also in the batch experiments by Genç-Fuhrman et al. (2007), copper was likely precipitating within many tested sorbents, including sand and granular activated carbon.

Copper is most soluble when soil pH is low and organic matter content is low (Oorts 2013). Initial pH of the filter effluents were ca. 8, but interestingly pH of the sand filter effluent increased during the events up to ca. 9, while Cu concentration decreased (Section 3.3). The lower pH in the sand-biochar effluent suggests that Cu in the sand-biochar filter was more soluble than in the sand filter.

In an organic-rich environment copper forms stable complexes with dissolved organic matter (Oorts 2013). Even trace amounts of organic matter are enough to bind Cu. For instance, Pennington et al. (2008) reported that copper was bound to small organic particles, such as pieces of fungi or moss, in stormwater generated on copper roofs. This likely means that Cu was retained by the organic matter of the biochar layer in the sand-biochar filter, as well as by existing traces of organic matter within the sand of both filters.

Cu can also strongly adsorb to Mn and Fe oxide minerals in inorganic soils (Dixon & Weed 1989). The typical order of Cu adsorption in soils is: Mn oxides > organic matter > Fe oxides > clay minerals (Oorts 2013). The sand used in the filters contains practically no iron (Section 2.1), but based on the results in Section 3.8, Fe was still present in both filter effluents (likely due to the influent stormwater). Also Mn was present in the filter effluents (Section 3.8). Therefore, Cu was likely adsorbed onto Mn oxides of the sand, onto organic matter and onto Fe oxides. As both filters acted similarly, the effect of the biochar layer on Cu removal was small, and most Cu reduction was due to the sand.

As Cu in stormwater is mostly in dissolved form (Section 1.2), the clear reduction of copper observed in the filters (Section 3.7) was likely due to a combination of the precipitation of Cu minerals and the adsorption of Cu onto Mn oxides, organic matter and Fe oxides. The result suggesting that the efficient Cu reduction was partly based on precipitation reactions is important, because precipitation indicates long-term immobilization. Precipitated Cu minerals are not likely to be re-released from the filters during time, i.e. the removal can be assumed relatively permanent.

The filters were acting in a similar manner with respect to Cu in the examined rain events, based on the *SI*s and the measured effluent Cu concentrations (Section 3.4). This indicates that the lower observed removal of Cu in Event 3 (Section 3.7) was mostly due to the differences in the influent concentrations, as opposed to actual differences in the filter performance.

3.9.3 Lead

All Pb containing minerals included in the PHREEQC modelling were undersaturated both in the sand filter and the sand-biochar filter effluents during the studied events (Appendix 5), which means that precipitation of Pb within the filters was unlikely.

According to Steinnes (2013), Pb strongly bounds with organic matter and iron oxides. Pb can form insoluble complexes with organic matter when pH is above 4 (Steinnes 2013). Since the filter effluents had pHs of ca. 8–9, Pb likely attached strongly on organic matter and thus, was retained relatively permanently. Lead is quite immobile in soils, especially if its concentration is low as in the present study (Steinnes 2013).

Based on the modelled Pb mineral phases and their negative *SI*s, Pb ions did not likely precipitate in the filters. Thus, the clear observed reduction of lead in the sand-biochar filter in both events and in the sand filter in Event 2 (Section 3.7) was likely due to metal retention on organic matter and reactive mineral surfaces and physical sieving. As Pb in stormwater is known to be mostly in particulate form (Section 1.2), physical sieving was likely important removal mechanism. As the sand-biochar filter showed better removal performance (Section 3.7), it is likely that the organic matter of the biochar layer had some role in the Pb reduction and was able to bind lead more permanently. This could explain the observed leaching of lead from the sand filter in Event 3 (Section 3.7).

3.9.4 Nickel

All mineral phases containing Ni included in the PHREEQC model had negative *SI*s (Appendix 5), which indicates that Ni did not likely form mineral precipitates within the filters. The results of Event 2, in which Ni was reduced to the same extent in both sand and

sand-biochar filters (Section 3.7), suggest the reduction was likely due to physical sieving process, i.e. Ni-humic complexes were physically filtered out.

The differences in the reduction percentages in Event 3 (Section 3.7) suggest that other mechanisms than physical sieving occurred simultaneously. As the modelled *SI*s did not predict precipitation reactions in either of the filters, it can be assumed that the better retention in the sand-biochar filter was due to surface sorption reactions within the biochar layer. However, it should be noted that Ni concentrations were low (Section 3.4.2), indicating the differences between the filters did not have clear practical importance and the results of laboratory analyses can be uncertain.

3.9.5 Zinc

PHREEQC modelling of Zn-containing minerals revealed differences between the sand filter and the sand-biochar filter (Table 16). The results predicted that willemite (Zn_2SiO_4) was at approximate equilibrium in the sand filter effluent during both events, whereas in the sand-biochar filter effluent it was clearly undersaturated based on the modelled *SI*s. In addition, $ZnSiO_3$ was oversaturated in both filter effluents, although the *SI*s of the sand filter effluent were higher.

Table 16. Modelled saturation indices of zinc-containing mineral phases. Values indicating approximate equilibrium or supersaturation (≥ -0.5) are shown in bold text.

		June 20				Event 3			
		Biochar		Sand		Biochar		Sand	
Mineral	**Formula**	**16:40**	**18:51**	**16:39**	**18:48**	**20:50**	**22:41**	**20:50**	**22:41**
Smithsonite	$ZnCO_3$	-2.7	-2.6	-2.8	-2.8	-2.7	-2.5	-2.0	-2.5
Willemite	Zn_2SiO_4	-4.0	-3.7	**0.0**	**0.0**	-3.5	-3.1	**-0.5**	**-0.4**
$Zn(OH)_2$	$Zn(OH)_2$	-3.6	-3.4	-1.7	-1.6	-3.5	-3.3	-2.0	-2.0
$ZnSiO_3$	$ZnSiO_3$	**0.9**	**1.0**	**3.0**	**3.0**	**1.2**	**1.4**	**2.7**	**2.8**

PHREEQC simulation suggested that precipitation was a potential mechanism to explain the observed high retention of Zn in both studied events. Precipitation of Zn_2SiO_4 was possible in the sand filter and $ZnSiO_3$ was thermodynamically possible mineral phase to precipitate in both filters. However, according to Mertens & Smolders (2013), Zn solubility is almost always controlled by sorption reactions and Zn precipitates form only if Zn concentration is very high. This is consistent with Genç-Fuhrman et al. (2007) who reported that Zn removal via precipitation occurred in a sand column, when initial Zn concentration was 3400 µg/l, which is more than ten times higher than in the present study. Likewise Cu and Pb, Zn sorbs on organic matter and oxyhydroxides of Mn, Fe and Al (Mertens & Smolders 2013).

Since both filters removed Zn from the stormwater almost equally well (Section 3.7), it seems that biochar did not affect the performance. If the retention was mostly based on sorption on organic matter, the sand-biochar filter with higher organic content should have clearly outperformed the sand filter. Therefore, it is likely that the observed Zn reduction was based either on sorption to Mn, Fe and Al mineral surfaces or mechanical filtration, or combination of both. This suggests that Zn was not retained as permanently as if it was precipitated, and its re-release is possible, as concluded also by Wendling et al. (2017b) who studied treatment of stormwater with layered structure including spruce biochar.

3.9.6 Phosphorus

Hydroxyapatite ($Ca_5(PO_4)_3OH$) was the only mineral phase containing phosphorus that was at or approaching thermodynamic equilibrium in the filter effluents (Table 17). Similar observation was reported by Wendling et al. (2017b). In Event 2 of this study, hydroxyapatite in the sand-biochar filter effluent was slightly undersaturated, whereas in the sand filter effluent it was at approximate equilibrium. In Event 3, hydroxyapatite was at approximate equilibrium in the sand-biochar filter effluent and reaching equilibrium during the event in the sand filter effluent. All other phosphorus-containing phases were highly undersaturated, indicating their precipitation in the filters was very unlikely.

Table 17. Modelled saturation indices of phosphorus-containing mineral phases. Values indicating approximate equilibrium or supersaturation (≥ -0.5) are shown in bold text.

		June 20				Event 3			
		Biochar		Sand		Biochar		Sand	
Mineral name	**Formula**	**16:40**	**18:51**	**16:39**	**18:48**	**20:50**	**22:41**	**20:50**	**22:41**
$Cd_3(PO_4)_2$	$Cd_3(PO_4)_2$	-17.1	-17.2	-14.6	-14.8	-17.5	-17.2	-15.3	-14.6
$Cu_3(PO_4)_2$	$Cu_3(PO_4)_2$	-11.8	-11.4	-15.1	-14.8	-12.1	-11.9	-11.1	-13.1
$Cu_3(PO_4)_2{:}3H_2O$	$Cu_3(PO_4)_2{:}3H_2O$	-13.5	-13.1	-16.8	-16.5	-13.8	-13.6	-12.9	-14.9
Hydroxyapatite	$Ca_5(PO_4)_3OH$	-1.2	-1.9	**0.2**	**-0.4**	**0.6**	**-0.2**	-2.6	**-0.4**
$Ni_3(PO_4)_2$	$Ni_3(PO_4)_2$	-19.0	-19.2	-16.8	-16.8	-20.7	-20.5	-17.7	-17.7
Struvite	$MgNH_4PO_4{:}6H_2O$	-33.7	-34.1	-32.2	-32.7	-33.0	-1000	-1000	-1000
Tsumebite	$Pb_2CuPO_4(OH)_3{:}3H_2O$	-8.3	-8.1	-5.2	-5.3	-10.1	-9.3	-5.9	-5.8
Vivianite	$Fe_3(PO_4)_2{:}8H_2O$	-4.1	-3.4	-9.9	-9.9	-7.8	-6.6	-6.0	-8.5

According to the PHREEQC modelling results, hydroxyapatite was likely the mineral phase controlling phosphorus concentrations in the solutions within the filters and observed phosphorus reduction can be due to hydroxyapatite precipitation. Both filter effluents contained notable amounts of Ca (Section 3.8), which indicates there was excess Ca in the filters enabling the formation of hydroxyapatite. However, the extent of TP reduction by both the sand-biochar and sand filters was similar in Event 2 (Section 3.7) but the modelled *SI*s of hydroxyapatite suggest precipitation only in the sand filter. In Event 3, the modelled *SI*s were almost opposite but the observed TP reduction was again similar in both filters. Therefore, additional mechanisms than precipitation must have been involved in the phosphorus reduction.

Phosphate is known to form strong chemical bonds with iron oxides (Wendling et al. 2017b). The oversaturation of several iron oxide minerals (Table 19) suggests that PO_4 could have been removed via sorption to iron oxide mineral surfaces. Also PO_4 binding with calcium is possible (Wendling et al. 2017b). Calcium was especially abundant in the sand-biochar filter effluent (Section 3.8). However, although TP was efficiently removed, PO_4 actually increased in the filters (Section 3.7), suggesting these mechanisms were not efficient in phosphorus retention.

Most phosphorus in the stormwater was supposedly in particulate form (Sections 1.3 and 3.4.1) and no reduction was observed in the (dissolved) PO_4 (Section 3.7). Therefore, most TP reduction was related to particulate phosphorus and physical sieving was likely the most important TP removal mechanism within the filters, although precipitation as hydroxyapatite and sorption e.g. to iron oxide mineral surfaces may have also occurred to some extent. This

suggestion is supported by the finding that the differences between the two filters were notably smaller in relation to TP than PO_4: the biochar layer enabled the occurrence of mechanisms to reduce the dissolved PO_4, but both filters were able to remove particulate phosphorus via physical sieving through the sand.

3.9.7 Nitrogen

$Cu_2(OH)_3NO_3$ (Table 15) and struvite (Appendix 5) were the only nitrogen-containing mineral phases included in the PHREEQC model. They were both highly undersaturated, which indicates that their precipitation was not causing the clearly observed reduction of TN in the sand-biochar filter (Section 3.7). The biochar layer was reducing especially the amount of NO_3, which is mainly in dissolved form (Section 1.2). This suggests that the nitrogen removal was not based on just physical sieving, but other mechanisms occurred within the biochar layer.

It is interesting that the sand-biochar filter was so efficient in NO_3 removal, although the biochar layer is placed under only 20 cm deep sand layer (Section 2.1). This indicates that the observed NO_3 leaching form the sand filter occurred in the topmost sand layer and the sand placed deeper did not release notable amounts of NO_3. In this sense, the biochar layer was placed deep enough to capture NO_3 leaching from the sand and originating from the influent stormwater.

3.9.8 Aluminum

Based on the PHREEQC modelling, most of the mineral phases containing aluminum were oversaturated or at approximate equilibrium (Table 18). Alunite ($KAl_3(SO_4)_2(OH)_6$) was inconsistent as its *SI*s in the sand-biochar filter effluent during Event 2 were positive, whereas in the other samples they were clearly negative.

Table 18. Modelled saturation indices of aluminum-containing mineral phases. Values indicating approximate equilibrium or supersaturation (≥ -0.5) are shown in bold text.

		June 20				Event 3			
		Biochar		Sand		Biochar		Sand	
Mineral name	**Formula**	**16:40**	**18:51**	**16:39**	**18:48**	**20:50**	**22:41**	**20:50**	**22:41**
$Al(OH)_3$ (amorph)	$Al(OH)_3(am)$	**0.1**	**0.3**	**-0.4**	**-0.5**	-0.8	**-0.3**	**-0.1**	**-0.3**
Albite	$NaAlSi_3O_8$	**1.3**	**1.3**	**2.3**	**2.0**	**0.8**	**1.1**	**1.4**	**2.1**
Alunite	$KAl_3(SO_4)_2(OH)_6$	**1.4**	**2.1**	-5.1	-5.1	-2.8	-1.2	-2.0	-4.2
Anorthite	$CaAl_2Si_2O_8$	**0.6**	**0.8**	**1.6**	**1.2**	**-0.3**	**0.3**	**0.7**	**1.4**
Basaluminite	$Al_4SO_4(OH)_{10}:5H_2O$	**4.2**	**5.0**	**-0.5**	**-0.5**	-1.1	**0.9**	**1.9**	**0.0**
Ca-Montmorillonite	$Ca_{0.165}Al_{2.33}$-$Si_{3.67}O_{10}(OH)_2$	**7.2**	**7.6**	**7.0**	**6.6**	**5.0**	**6.0**	**6.9**	**7.0**
Gibbsite	$Al(OH)_3$	**2.9**	**3.1**	**2.4**	**2.3**	**2.0**	**2.4**	**2.7**	**2.5**
HydrotalciteMgAl (Meixnerite)	$Mg_6Al_2(OH)_{16}(OH)_2$	**41.6**	**40.7**	**52.5**	**51.2**	**43.8**	**42.7**	**41.9**	**47.7**
Illite	$K_{0.6}Mg_{0.25}Al_{2.3}$-$Si_{3.5}O_{10}(OH)_2$	**7.0**	**7.3**	**7.0**	**6.6**	**5.3**	**6.2**	**6.3**	**6.8**
Jurbanite	$AlSO_4OH$	-5.0	-4.7	-7.9	-7.8	-6.7	-6.1	-6.0	-7.2
Kaolinite	$Al_2Si_2O_5(OH)_4$	**7.8**	**8.1**	**7.1**	**6.9**	**5.8**	**6.7**	**7.5**	**7.3**
K-feldspar	$KAlSi_3O_8$	**3.3**	**3.3**	**3.3**	**3.0**	**2.8**	**3.1**	**2.4**	**3.0**
K-mica	$KAl_3Si_3O_{10}(OH)_2$	**14.6**	**15.1**	**13.6**	**13.2**	**12.3**	**13.5**	**13.4**	**13.5**

Amorphous $Al(OH)_3$ was likely the mineral phase controlling aluminum solubility, although it was at approximate equilibrium based on the modelled *SI*s (Table 18), since poorly crystalline minerals form more rapidly than similar crystalline minerals (Wendling et al. 2017b). The modelled *SI*s indicate that with time, amorphous $Al(OH)_3$ would likely become more crystalline and form gibbsite (Wendling et al. 2017b), which is the most common $Al(OH)_3$ polymorph in nature (Dixon & Weed 1989). The relevance of $Al(OH)_3$ is increased by the fact that its surface can act as a sorbent for other metals (Mertens & Smolders 2013), which could partially explain e.g. the observed reduction of Zn.

Also precipitation of basaluminite and alunite was likely, since they typically control aluminum solubility in waters containing SO_4 (Wendling et al. 2017b) and the effluents expressed notable amounts of SO_4 (Section 3.8). These two mineral phases potentially acted as a sink for sulfur, but SO_4 measurements from the influent stormwater were not available to confirm this.

Since there were no aluminum measurements from the influent stormwater, comparison of geochemical modelling results and possible reduction of Al is not possible. However, Al concentrations were lower in the sand-biochar filter effluent than in the sand filter effluent (Section 3.8), which could be explained by the differences in the precipitation reactions.

3.9.9 Iron

Fe-containing mineral phases expressed both clearly undersaturated and highly supersaturated values in the PHREEQC modelling (Table 19). Based on the modelled *SI*s, precipitation of cupric ferrite and cuprous ferrite, hydrotalcite-MgFe, schwertmannite, hematite, goethite and amorphous $Fe(OH)_3$ was thermodynamically possible in both the sand-biochar and sand filters. Also siderite ($FeCO_3$) was at approximate equilibrium in the biochar effluent in Event 2, but undersaturated in the rest of the modelled samples. Many iron-containing phases were oversaturated also in the field study by Bäckström et al. (2003).

Table 19. Modelled saturation indices of iron-containing mineral phases. Values indicating approximate equilibrium or supersaturation (≥ -0.5) are shown in bold text.

		June 20				Event 3			
		Biochar		Sand		Biochar		Sand	
Mineral	**Formula**	**16:40**	**18:51**	**16:39**	**18:48**	**20:50**	**22:41**	**20:50**	**22:41**
Cupric ferrite	$CuFe_2O_4$	**14.7**	**14.9**	**16.7**	**16.5**	**14.5**	**14.6**	**16.3**	**16.5**
Cuprous ferrite	$CuFeO_2$	**13.7**	**13.9**	**13.7**	**13.7**	**13.3**	**13.4**	**14.3**	**13.9**
$Fe(OH)_3$ (amorphous)	$Fe(OH)_3(am)$	**2.8**	**2.8**	**3.6**	**3.5**	**2.3**	**2.5**	**3.1**	**3.2**
Goethite	FeOOH	**8.3**	**8.3**	**9.1**	**9.0**	**8.0**	**8.1**	**8.7**	**8.8**
Hematite	Fe_2O_3	**18.5**	**18.6**	**20.1**	**19.9**	**17.9**	**18.2**	**19.3**	**19.7**
Hydrotalcite MgFe	$Mg_6Fe_2(OH)_{16}(OH)_2$	**33.6**	**32.4**	**47.2**	**45.7**	**37.2**	**35.5**	**35.3**	**41.8**
Jarosite-K	$KFe_3(SO_4)_2(OH)_6$	-2.8	-2.5	-5.1	-5.3	-4.8	-4.1	-4.1	-5.1
Jarosite-Na	$NaFe_3(SO_4)_2(OH)_6$	-6.0	-5.8	-7.3	-7.5	-8.0	-7.4	-6.3	-7.2
Melanterite	$FeSO_4{:}7H_2O$	-8.3	-8.1	-11.1	-11.0	-9.9	-9.4	-9.3	-10.5
Schwertmannite	$Fe_8O_8(OH)6SO_4$	**23.6**	**24.2**	**27.6**	**26.8**	**19.4**	**20.7**	**25.2**	**25.6**
Siderite	$FeCO_3$	**-0.5**	**-0.4**	-2.9	-3.0	-1.4	-1.2	-1.6	-2.3
Vivianite	$Fe_3(PO_4)_2{:}8H_2O$	-4.1	-3.4	-9.9	-9.9	-7.8	-6.6	-6.0	-8.5

Formation of hydrotalcite-MgFe was unlikely during the short retention time within the filters, as it forms only during prolonged periods (Wendling et al. 2013). In addition, schwertmannite forms only when pH is remarkably lower and sulfate concentrations higher than in the present study (Bigham et al. 1996). Precipitation of both cupric ferrite ($CuFe_2O_4$) and cuprous ferrite ($CuFeO_2$) was possible as discussed earlier under Cu minerals (Section 3.9.2).

Despite the relatively lower modelled *SI*s of amorphous $Fe(OH)_3$ (Table 19), it was the most likely iron mineral phase to precipitate within the filters, since it is poorly crystalline and thus forms most rapidly (Wendling et al. 2013; Wendling et al. 2017b). Taking into account the short retention time of the filters, amorphous $Fe(OH)_3$ likely controlled Fe concentrations in the filters. Based on the positive modelled *SI*s of goethite and hematite, amorphous $Fe(OH)_3$ may turn into more crystalline forms, such as goethite or hematite (Wendling et al. 2013).

The likely formation of $Fe(OH)_3$ is important, since it is able to sorb other metals (e.g. Green-Pedersen et al. 1997; Tiberg et al. 2013) and phosphate (e.g. Arai & Sparks 2001), thus preventing their re-release. Presence of $Fe(OH)_3$ could e.g. partially explain the observed removal of Cu and Zn. For instance, Wendling et al. (2017b) reported that Fe treatment of biochar increased removal of PO_4 and Zn. The poor observed PO_4 retention in this study (Section 3.7) suggests that the amount of precipitated $Fe(OH)_3$ was, however, limited.

It is impossible to compare the modelling results and reduction of Fe, since iron was not analyzed from the untreated stormwater samples. However, there was ca. 5 times less Fe in the sand-biochar filter effluent than in the sand filter effluent (Section 3.8), suggesting that biochar addition improved Fe reduction. As the differences in modelled *SI*s are minor, this improvement cannot be explained just by precipitation reactions, which suggests that also other Fe removing mechanisms than precipitation occurred in the sand-biochar filter.

3.9.10 Manganese

All Mn-containing minerals were undersaturated based on the PHREEQC modelling (Appendix 5). Therefore, their precipitation in the filters was unlikely. Also in the laboratory experiment by Wendling et al. (2017b) all the modelled Mn minerals were undersaturated. In contrast, Bäckström et al. (2003) reported that many manganese containing minerals were oversaturated in their field study. However, Bäckström et al. (2003) studied untreated stormwater, which means the results are not truly comparable. The earlier discussion of the lacking influent measurements is valid also for the Mn minerals. Based on the results provided in Section 3.8, both filter types acted similarly with respect to Mn.

3.9.11 Summary

In the current study, the observed Cu reduction was likely based on precipitation reactions. Pollutant removal via precipitation suggests that re-release from the filters due to e.g. changes in pH is unlikely. However, precipitation as a possible removal mechanism is ignored in many stormwater studies. Based on the results, precipitation of also Zn, P, Al and Fe may have occurred to some extent, but likely the removal of pollutants was due to combination of mechanisms. Removal of Pb was assumed quite permanent due to strong bounds with organic matter and minerals. It was concluded that the removal of many pollutants (Cd, Pb, Ni and Zn) was largely based on sorption reactions. This could explain

the slightly improved removal performance of the sand-biochar filter, since sand has low sorption capacity due to its low surface area (Genç-Fuhrman et al. 2007). However, sand can be considered inert only if it is made of pure quartz (SiO_2) (Norris et al. 2013), as discussed in Section 1.3. The sand material in both filters consisted of not just quartz (Section 2.1), indicating the sand itself can be reactive and is not necessarily just physical sieving media. Also Norris et al. (2013) concluded in their column experiment studying different gravel media for stormwater filtration that sorption was the major removal process for heavy metals. Wendling et al. (2017b) reported that removal of metals and phosphorus was based on a combination of sorption and precipitation reactions.

The results from laboratory studies are not entirely comparable with the present study as they typically use synthetic stormwater containing only a limited number of pollutants as an influent. In synthetic stormwater, pollutants are often in dissolved form. Hence, the importance of mechanical sieving in the pollutant retention is ignored. In real conditions, the influent stormwater contains a mix of several pollutants and suspended solids. For instance, Pb and TP, which are known to occur in particulate form in stormwater (Section 1.2), were removed efficiently in this study. Therefore, physical sieving was concluded to be an important removal mechanism and to at least contribute to the reduction of most pollutants along with sorption and precipitation.

As a summary, the utilized PHREEQC modelling revealed that precipitation reactions were possible for many mineral groups. However, saturation indices describe only what is thermodynamically possible and do not consider e.g. the dynamics of the reactions. For instance, *SI* could predict precipitation of a mineral which formation during the short retention time within the filters is unlikely. Also Appelo & Postma (2007) emphasized that the geochemical modelling results should be interpret critically because the mechanisms are complicated. PHREEQC modelling was limited for two samples per filter per event (Section 2.6). Since the measured concentrations changed during the events (Section 3.2; Appendices 1–3), it is inevitable that the timing of the samples had an influence on the modelling results.

Moreover, the modelled *SI*s do not directly yield information about other pollutant reduction mechanisms than precipitation. Drawing more reliable conclusions would require other analysis tools. For instance, laboratory analyses of pollutant division into particulate and dissolved phases both in the influent and effluent could be helpful. In addition, soil sampling could be utilized to determine, in which part of the filters the pollutants actually accumulate.

3.10 Uncertainties

The main uncertainties in this study were related to field measurements and geochemical modelling.

The influent stormwater was not sampled from the exact location of the filters due to practical reasons (Section 2.1). In other words, the sampled stormwater from the nearby bridge only mimicked the actual inflowing stormwater. The composition of the sampled water was not necessary precisely the same as in the water entering the filters, but was the best possible estimate. As there are no crossroads between the filters and the bridge, the traffic volume at the bridge is exactly the same as at the location of the filters. In addition, the bridge has the same surface material as the road at the location of the filters. Stormwater from bridges may contain elevated Zn concentrations due to galvanized safety fences

(Huber, Welker & Helmreich 2016). However, it can be assumed that the differences in stormwater properties were mostly small, and the sampled stormwater was representative of the actual filter inflow.

It would have been possible to collect the samples also from the exact location of the filters using a small flume or gutter installed at the road border, as in the studies by Bäckström et al. (2003) and Inha et al. (2013). This method is, however, vulnerable and requires constant maintenance (Inha et al. 2013), and was thus rejected. The downspout is made of steel, the detailed composition of which is unknown. It is possible that the downspout increased the concentrations of some metals in the stormwater discharging through the metal pipe. Borris et al. (2017) observed significant increases in metal concentrations when conveyed through 500 m long metal pipe. However, the pipe of the downspout is only ca. 1 m long. In addition, when the flow rate from the downspout is high (and when the influence on *EMC* is the highest), most of the water discharging through the pipe does not even touch it (Figure 11a in Section 2.1). Therefore, it is unlikely that the downspout affected the *EMC* values.

The catchment areas of the filters are not precisely known. The sizes of the areas were estimated based on the blueprints of the filters and visual observations. More detailed determination of the catchment areas would require detailed topographical information, e.g. by means of laser scanning. However, as the catchment areas are simple, the errors were likely to be small. In addition, the properties of the catchment areas are not absolutely identical. For instance, the catchment area of the sand-biochar filter had a small amount of recently built asphalt (Figure 6a in Section 2.1). Additionally, it was uncertain if the amount of stormwater entering the filters is exactly the same due to possible small differences in the structures. However, the existence of a reference filter (the sand filter) was seen as one of the strengths of this study, and despite the uncertainties, it clearly improved the study reliability.

The sample gathering and laboratory analyses had sources of error. For instance, the use of the same can in the collection of the consecutive water samples may lead to uncertainties due to traces of water from the previous sample. However, the can was flushed between the samples and, hence, this is unlikely to result in significant errors. pH is recommended to measure on-site as it can change during storage (Appelo & Postma 2007), but due to laborious field measurements, it was included in the laboratory analyzes. In addition, the laboratory analyses have limited accuracy. For instance, analyses by Metropolilab had uncertainties of 15–25% (Table 7 in Section 2.4). However, as each studied storm had numerous analyzed samples, these errors were not likely to be systematic.

In order to determine *EMC*s, the beginning and ending times of the events needed to be estimated. In addition, the end parts of the events required interpolation due to the gaps in the field data. However, the different methods used for the *EMC* calculation yielded almost identical results, indicating the method did not remarkably affect the results. This is reasonable, as the parts of the events with most uncertainties (beginnings and endings) had the lowest flow rates and thus the least influence on *EMC*s. Typically, studies only present the equation that *EMC*s are based on, but do not reveal the actual used method.

It was assumed that concentrations and flow rates changed linearly between the measurements, which can be estimated to be relatively accurate, if the interval between the measurements is short. On the contrary, if the interval is long, rapid changes in the

concentrations between the sampled points can be missed. Especially the concentrations of the untreated stormwater changed very rapidly (Section 3.2), underlining the need for frequent sampling. In this sense, the sampling of this study was mostly successful.

Heavy metals (Cd, Cu, Ni, Pd and Zn) were analyzed only for Events 2 and 3 and from fewer samples than the other parameters. Pollutographs of the metals (Appendices 2 and 3) show high temporal variance in the concentrations – especially during Event 3 – and it is uncertain what happened before, between and after the samples. For instance, Ni concentration of the sand filter effluent increased more than 5-fold in the last sample. It remains unknown if this was an error or if Ni concentrations started to rise only after the sampling. Therefore, more frequent and long-lasting sampling of the metals would be preferable. On the other hand, the amount and frequency of sampling in this study – also for metals – was high compared to many studies, and provided mostly reliable data.

The PHREEQC modelling was based on only two samples per event per filter, since the amount of additional analyzed parameters was limited (Sections 2.4 and 3.8). Given that all included parameters exhibited high temporal variability throughout the study, it is inevitable that the sample timing affected the modelling results. Larger amount of samples and thus larger amount of modelled saturation indices would have enabled investigation of the process dynamics, such as changes from undersaturation to oversaturation as the events proceeded. For these reasons, the geochemical modelling leaved uncertainties and provided only partial help for understanding the removal mechanisms.

The number of the studied events was small, and high variability was observed between the events. Therefore conclusions should not be drawn too far as noted also by Law et al. (2008). For instance, the results of this study do not reveal long-term effects of the filters or influence of different storm characteristics and seasonal variation. For instance, Bäckström et al. (2003) reported that heavy metal loadings were elevated during winter time and Sillanpää (2013) concluded that estimates based on just summer time observations led to biggest errors. Additionally, initial costs and need for maintenance should be taken account when selecting the most suitable filter materials (Monrabal-Martinez et al. 2017). However, these subjects were beyond the scope of this study.

4 Conclusions

Stormwater is regarded as an important diffuse pollution source for urban surface waters and groundwater, and different types of stormwater management structures have been developed. However, the knowledge on managing stormwater quality is only emerging. Especially, there seems to be a lack of full-scale studies conducted in realistic field conditions. This study provided information on the performance of roadside stormwater filters – especially on biochar amended filters, which were studied for the first time in full-scale. Even though conducted under real conditions, the study setting enabled comparison with a reference filter and the filters were investigated in high temporal accuracy.

The first objective of this study was to assess the impact of the filters on stormwater quality and quantity. Both the sand filter and the sand filter amended with biochar clearly changed the composition of stormwater – mostly positively. The clearest improvement in water quality by both filters was related to heavy metals and suspended solids, which were effectively removed from the stormwater. In addition, both filters expressed good total phosphorus retention capacity, but they were observed to release phosphate. Furthermore, both filters were able to efficiently delay flow peaks.

The second objective was to evaluate the benefits of biochar amendment. The clearest benefit was noticed in nitrogen removal, especially in the form of nitrate, which tended to leach out from the pure sand filter. This indicates that biochar amendment could be a usable option in areas with high nitrate loading, such as construction sites. In addition, biochar amendment expressed slightly better performance of heavy metal reduction, especially of lead, but the practical importance is questionable. Furthermore, the biochar amendment reduced phosphate leaching when compared with the pure sand filter. On the other hand, biochar was observed to release organic carbon, which should be considered in the design and placement of biochar amended sand filters. Finally, the biochar amendment seemed to improve the water holding capacity of the filter and thus to reduce water volumes and peak flows. Improved detention capacity could be useful for some locations, but the treatment performance should be studied also under freezing conditions.

The third objective was to describe the dynamics of the filters during rain events and the fourth objective was to develop reliable monitoring methods. The results of this study underline the rapid temporal changes in stormwater but also in the filter effluents. This indicates that high temporal accuracy is necessary and stormwater treatment systems should not be judged based on individual samples. This is important for both practical monitoring and scientific research of stormwater management systems. The results showed that analysis of multiple quality parameters is important, since the use of surrogate water quality parameters seemed reliable only for untreated stormwater. Additionally, the determination of the performance of stormwater filters is not straightforward, and different methods give varying or even conflicting results. Local legislation on stormwater threshold values and determination methods would simplify the assessment of different stormwater treatment systems.

Large variation between the studied storms revealed that stormwater treatment structures should be investigated during longer periods of time. A higher number of studied storms would provide better information about biochar amended filters and the effect of rain event characteristics and seasonal variability on filter performance. The study proved that accurate monitoring is possible even without expensive instrumentation. Therefore, filters could be

monitored by municipalities for instance once a year, resulting in several sampled storms over the years. Additionally, the optimal amount, placement and type of biochar amendment are recommended to be studied under controlled laboratory conditions.

The fifth objective was to deepen the knowledge on the operating principle of stormwater filters. The study showed that pollutants may be removed from stormwater via different mechanisms, which could influence the filter design. PHREEQC modelling was seen as a potential tool for this investigation. However, high temporal frequency should be applied also for the geochemical modelling input. Additional methods, such as determining the dissolved and particulate fractions of the pollutants, would enable drawing more reliable conclusions about the removal mechanisms. The results of this study could be used also for calibration and validation in other modelling studies considering stormwater filters.

The study was limited to three rain events and did not include all important pollutants present in stormwater, such as PAHs and microplastics. Further field studies are required to determine e.g. the long-term effects and need of maintenance of the studied filters. Despite these restrictions, this study provided new information especially on the biochar amended stormwater filters.

References

Alm, H., Banach, A. & Larm, T. 2010. Förekomst och rening av prioriterade ämnen, metaller samt vissa övriga ämnen i dagvatten. Svenskt Vatten Utveckling. Rapport Nr 2010–06. Available in Swedish: http://vav.griffel.net/filer/Rapport_2010-06.pdf

Appelo, C.A.J. & Postma, D. 2007. Geochemistry, groundwater and pollution. 2nd edition. A.A. Balkema publishers. Leiden, the Netherlands. ISBN 04 1536 428 0.

Arai, Y. & Sparks, D.L. 2001. ATR–FTIR spectroscopic investigation on phosphate adsorption mechanisms at the ferrihydrite–water interface. Journal of Colloid and Interface Science, 241(2), 317-326.

Ball, J.W. & Nordstrom, D.K. 1991. User's manual for WATEQ4F, with revised thermodynamic data base and text cases for calculating speciation of major, trace, and redox elements in natural waters. U.S. Geological Survey Open-File Report 91-183. Available: https://pubs.er.usgs.gov/publication/ofr91183

Barbosa, A. E., Fernandes, J. N. & David, L. M. 2012. Key issues for sustainable urban stormwater management. Water research, 46(20), 6787-6798.

Bigham, J.M., Schwertmann, U., Traina, S.J., Winland, R.L. & Wolf, M. 1996. Schwertmannite and the chemical modeling of iron in acid sulfate waters. Geochimica et Cosmochimica Acta, 60(12), 2111-2121.

Boclair, J.W. & Braterman, P.S. 1999. Layered double hydroxide stability. 1. Relative stabilities of layered double hydroxides and their simple counterparts. Chemistry of Materials, 11(2), 298-302.

Boller, M. 1997. Tracking heavy metals reveals sustainability deficits of urban drainage systems. Water Science and Technology, 35(9), 77-87.

Borris, M., Österlund, H., Marsalek, J. & Viklander, M. 2017. An exploratory study of the effects of stormwater pipeline materials on transported stormwater quality. Water Science and Technology, wst2017195.

Bäckström, M., Nilsson, U., Håkansson, K., Allard, B. & Karlsson, S. 2003. Speciation of heavy metals in road runoff and roadside total deposition. Water, Air, & Soil Pollution, 147(1), 343-366.

Chan, K.Y., Van Zwieten, L., Meszaros, I., Downie, A. & Joseph, S. 2008. Agronomic values of greenwaste biochar as a soil amendment. Soil Research, 45(8), 629-634.

City of Espoo. 2015. Espoon kaupungin työmaavesiopas. Available in Finnish: http://www.espoo.fi/download/noname/%7BA52F3656-63DF-4A62-AB03-ACFDDF8C4D52%7D/65952

Davis, A.P. & McCuen, R.H. 2005. Stormwater management for smart growth. Springer Science & Business Media.

Dixon, J.B. & Weed, S.B. 1989. Minerals in Soil Environments. 2nd Ed. Soil Science Society of America, Madison, WI, USA.

Dobbs, R.A., Wise, R.H. & Dean, R.B. 1972. The use of ultra-violet absorbance for monitoring the total organic carbon content of water and wastewater. Water Research, 6(10), 1173-1180.

Eaton, A.D., Clesceri, L.S., Rice, E.W. & Greenberg, A.B. 2005. Standard methods for the examination of water and wastewater. 21th ed. American Public Health Association

Ellis, J. B. & Mitchell, G. 2006. Urban diffuse pollution: key data information approaches for the Water Framework Directive. Water and Environment Journal, 20(1), 19-26.

EPA (Environmental Protection Agency) of Ireland. 2012. Guidance on the setting of trigger values for storm water discharges to off-site surface waters at EPA IPPC and waste licensed facilities. Available:
https://www.epa.ie/pubs/advice/licensee/Licensee%20Guidance%20on%20the%20setting%20of%20trigger%20values%20-%20Final%20.pdf

Erickson, A.J., Gulliver, J.S. & Weiss, P.T. 2011. Removing dissolved phosphorus from stormwater. 12nd International Conference on Urban Drainage, Porto Alegre/Brazil.

Eriksson, E., Baun, A., Scholes, L., Ledin, A., Ahlman, S., Revitt, M., Noutsopoulos, C. & Mikkelsen, P.S. 2007. Selected stormwater priority pollutants—a European perspective. Science of the total environment, 383(1), 41-51.

Finnish Meteorological Institute (FMI). 2017. Lämpötila- ja sadetilastoja vuodesta 1961. Available in Finnish: http://ilmatieteenlaitos.fi/tilastoja-vuodesta-1961

Galfi, H., Österlund, H., Marsalek, J., & Viklander, M. (2017). Mineral and Anthropogenic Indicator Inorganics in Urban Stormwater and Snowmelt Runoff: Sources and Mobility Patterns. Water, Air, & Soil Pollution, 228(7), 263.

Genç-Fuhrman, H., Mikkelsen, P.S. & Ledin, A. 2007. Simultaneous removal of As, Cd, Cr, Cu, Ni and Zn from stormwater: Experimental comparison of 11 different sorbents. Water research, 41(3), 591-602.

Good, J.F., O'Sullivan, A.D., Wicke, D. & Cochrane, T.A. 2014. pH Buffering in Stormwater Infiltration Systems—Sustainable Contaminant Removal with Waste Mussel Shells. Water, Air, & Soil Pollution, 225(3), 1885.

Green-Pedersen, H., Jensen, B.T. & Pind, N. 1997. Nickel adsorption on MnO_2, $Fe(OH)_3$, montmorillonite, humic acid and calcite: a comparative study. Environmental Technology, 18(8), 807-815.

Göbel, P., Dierkes, C. & Coldewey, W. G. 2007. Storm water runoff concentration matrix for urban areas. Journal of contaminant hydrology, 91(1), 26-42.

Hatt, B.E., Fletcher, T.D. & Deletic, A. 2009. Hydrologic and pollutant removal performance of stormwater biofiltration systems at the field scale. Journal of Hydrology, 365(3), 310-321.

Heinonen, P. 2016. Tampereen kaupungin yleisten alueiden huleveden hallintarakenteiden ylläpito (Storm water management structures maintenance on public lands in the city of Tampere). Hämeen ammattikorkeakoulu. Ylemmän ammattikorkeakoulututkinnon opinnäytetyö. Available in Finnish: http://www.theseus.fi/handle/10024/110594

Huber, M., Hilbig, H., Badenberg, S.C., Fassnacht, J., Drewes, J.E. & Helmreich, B. 2016. Heavy metal removal mechanisms of sorptive filter materials for road runoff treatment and remobilization under de-icing salt applications. Water research, 102, 453-463.

Huber, M., Welker, A. & Helmreich, B. 2016. Critical review of heavy metal pollution of traffic area runoff: Occurrence, influencing factors, and partitioning. Science of the Total Environment, 541, 895-919.

Inha, L., Kettunen, R. & Hell, K. 2013. Maanteiden hulevesien laatu. Liikennevirasto, väylätekniikkaosasto. Helsinki 2013. Liikenneviraston tutkimuksia ja selvityksiä 12/2013. 49 sivua ja 13 liitettä. ISSN-L 1798-6656, ISSN 1798-6664, ISBN 978-952-255-228-0. Available in Finnish: http://www.doria.fi/handle/10024/121259

Islam, M.N., Jo, Y.T. & Park, J.H. 2016. Leaching and redistribution of Cu and Pb due to simulated road runoff assessed by column leaching test, chemical analysis, and PHREEQC modeling. Environmental Earth Sciences, 75(12), 1-7.

Jormola, J., Vienonen, S. & Ristimäki, M. 2017. Vesihuoltoverkostojen tila ja riskien hallinta (VERTI): Rankkasateiden hallinta ja hulevedet Maanpäällisten hulevesien hallintakeinojen edistäminen - Työpaketti 6. Finnish Environment Institute SYKE. Available in Finnish: http://www.syke.fi/download/noname/%7BA47F0704-7558-4025-B2E9-F09ECABB0380%7D/125854

Kaczala, F., Marques, M., Vinrot, E. & Hogland, W. 2012. Stormwater run-off from an industrial log yard: characterization, contaminant correlation and first-flush phenomenon. Environmental technology, 33(14), 1615-1628.

Kuoppamäki, K., Hagner, M., Lehvävirta, S. & Setälä, H. 2016. Biochar amendment in the green roof substrate affects runoff quality and quantity. Ecological Engineering, 88, 1-9.

Land Use and Building Act 132/1999 (Maankäyttö- ja rakennuslaki 1999/132). Available in Finnish: http://www.finlex.fi/fi/laki/ajantasa/1999/19990132

Law, N., Fraley-McNeal, L., Cappiella, K. & Pitt, R. 2008. Monitoring to Demonstrate Environmental Results: Guidance to Develop Local Stormwater Monitoring Studies Using Six Example Study Designs. Center for Watershed Protection, Ellicott City, MD. Available: http://owl.cwp.org/mdocs-posts/monitoring-guidance-for-ms4s-six-example-study-designs/

LeFevre, G.H., Paus, K. H., Natarajan, P., Gulliver, J. S., Novak, P.J. & Hozalski, R.M. 2014. Review of dissolved pollutants in urban storm water and their removal and fate in bioretention cells. Journal of Environmental Engineering, 141(1), 04014050.

Lehikoinen, E. 2015. Kadun vastavalmistuneiden huleveden biosuodatusalueiden toimivuus Vantaalla (The performance of the post-construction bioretention systems in Vantaa). Master's thesis. Aalto University, School of Engineering. Available in Finnish: https://aaltodoc.aalto.fi/handle/123456789/16663

Leinonen, M. 2017. Huleveden hallinta liikennöidyillä alueilla tienvarren suodatusrakenteiden avulla (Stormwater management in traffic areas with roadside filter structures). Master's thesis. Aalto University, School of Engineering. Available in Finnish: http://www.vtt.fi/sites/stormfilter/Documents/D5.1_WP5_AaltoMaster_thesis_Leinonen.pdf

Li, L. & Davis, A.P. 2014. Urban stormwater runoff nitrogen composition and fate in bioretention systems. Environmental science & technology, 48(6), 3403-3410.

Lidman, F., Kohler, S. J., Mörth, C. M. & Laudon, H. 2014. Metal Transport in the Boreal Landscape – The Role of Wetlands and the Affinity for Organic Matter. Environmental science & technology, 48(7), 3783-3790.

Magnusson, K., Eliasson, K., Fråne, A., Haikonen, K., Hultén, J., Olshammar, M., Stadmark, J. & Voisin, A. 2016. Swedish sources and pathways for microplastics to the marine environment. A review of existing data. IVL, C, 183.

Manyà, J.J. 2012. Pyrolysis for biochar purposes: a review to establish current knowledge gaps and research needs. Environmental science & technology, 46(15), 7939-7954.

Mattila, T., Grönroos, J., Judl, J. & Korhonen, M. R. 2012. Is biochar or straw-bale construction a better carbon storage from a life cycle perspective?. Process Safety and Environmental Protection, 90(6), 452-458.

McElmurry, S.P., Long, D.T. & Voice, T.C. 2013. Stormwater dissolved organic matter: influence of land cover and environmental factors. Environmental science & technology, 48(1), 45-53.

Mertens, J. & Smolders, E. 2013. Zinc. Section 17 in book: B.J. Alloway (ed.). Heavy Metals in Soils: Trace Metals and Metalloids in Soils and their Bioavailability, Environmental Pollution 22.

Mohanty, S.K., Cantrell, K. B., Nelson, K.L. & Boehm, A.B. 2014. Efficacy of biochar to remove Escherichia coli from stormwater under steady and intermittent flow. Water research, 61, 288-296.

Monrabal-Martinez, C., Ilyas, A. & Muthanna, T.M. 2017. Pilot Scale Testing of Adsorbent Amended Filters under High Hydraulic Loads for Highway Runoff in Cold Climates. Water, 9(3), 230.

Niemi, T. 2017. Improved Precipitation Information for Hydrological Problem Solving-Focus on Open Data and Simulation.

Norris, M.J., Pulford, I.D., Haynes, H., Dorea, C.C. & Phoenix, V.R. 2013. Treatment of heavy metals by iron oxide coated and natural gravel media in sustainable urban drainage systems. Water Science and Technology, 68(3), 674-680.

Oorts, K. 2013. Copper. Section 13 in book: B.J. Alloway (ed.). Heavy Metals in Soils: Trace Metals and Metalloids in Soils and their Bioavailability, Environmental Pollution 22, DOI 10.1007/978-94-007-4470-7_13.

Parkhurst, D.L. & Appelo, C.A.J. 2013. Description of input and examples for PHREEQC version 3—A computer program for speciation, batch-reaction, one-dimensional transport, and inverse geochemical calculations: U.S. Geological Survey Techniques and Methods, book 6, chap. A43, 497 p. Available: https://pubs.usgs.gov/tm/06/a43/

Paus, K.H., Morgan, J., Gulliver, J.S., Leiknes, T. & Hozalski, R.M. 2013. Assessment of the hydraulic and toxic metal removal capacities of bioretention cells after 2 to 8 years of service. Water, Air, & Soil Pollution, 225(1), 1803.

Pennington, S.L. & Webster-Brown, J.G. 2008. Stormwater runoff quality from copper roofing, auckland, new zealand. New Zealand Journal of Marine and Freshwater Research, 42(1), 99-108.

Pirinen, P., Simola, H., Aalto, J. Kaukoranta, J. Karlsson, P. & Ruuhela, R. Finnish Meteorological Institute. 2012. Tilastoja Suomen ilmastosta 1981-2010. https://helda.helsinki.fi/bitstream/handle/10138/35880/Tilastoja_Suomen_ilmastosta_1981_2010.pdf?sequence=4

Pitt, R. 1996. Groundwater contamination from stormwater infiltration. CRC Press.

Pitt, R., Clark, S. & Field, R. 1999. Groundwater contamination potential from stormwater infiltration practices. Urban water, 1(3), 217-236.

Prestes, E.C., Anjos, V.E.D., Sodré, F.F. & Grassi, M.T. 2006. Copper, lead and cadmium loads and behavior in urban stormwater runoff in Curitiba, Brazil. Journal of the Brazilian Chemical Society, 17(1), 53-60.

Reddy, K.R., Xie, T. & Dastgheibi, S. 2014.
a) Evaluation of biochar as a potential filter media for the removal of mixed contaminants from urban storm water runoff. Journal of Environmental Engineering, 140(12), 04014043.
b) Removal of heavy metals from urban stormwater runoff using different filter materials. Journal of Environmental Chemical Engineering, 2(1), 282-292.

SFS-EN ISO 9963-1. 1996. Water quality. Determination of alkalinity Part 1: Determination of total and composite alkalinity. Helsinki: Finnish Standards Association SFS. 17 p.

Sillanpää, N. 2013. Effects of suburban development on runoff generation and water quality. Doctoral dissertation. Aalto University School of Engineering. Available: https://aaltodoc.aalto.fi/handle/123456789/11162

Sillanpää, N. & Koivusalo, H. 2015. Stormwater quality during residential construction activities: influential variables. Hydrological Processes, 29(19), 4238-4251.

Siriwardene, N.R., Deletic, A. & Fletcher, T.D. 2007. Clogging of stormwater gravel infiltration systems and filters: Insights from a laboratory study. Water research, 41(7), 1433-1440.

SKL (Suomen Kuntaliitto; The Association of Finnish Local and Regional Authorities). 2012. Hulevesiopas. Available in Finnish: shop.kunnat.net/download.php?filename=uploads/hulevesiopas-2012.pdf

Solpuker, U., Sheets, J., Kim, Y. & Schwartz, F.W. 2014. Leaching potential of pervious concrete and immobilization of Cu, Pb and Zn using pervious concrete. Journal of contaminant hydrology, 161, 35-48.

Steinnes, E. 2013. Lead. Section 14 in book: B.J. Alloway (ed.). Heavy Metals in Soils: Trace Metals and Metalloids in Soils and their Bioavailability, Environmental Pollution 22.

Stockholm Vatten AB. 2001. Klassificering av dagvatten och recipienter samt riktlinjer för reningskrav- del 2, Dagvattenklassificering. Available in Swedish: http://www.stockholmvattenochavfall.se/globalassets/pdf1/rapporter/dagvatten/dagvattenklassificeringdel2.pdf

Suihko, M. 2016. Biofiltration for stormwater management in Finnish climate. Master's thesis. Aalto University, School of Engineering. Available: https://aaltodoc.aalto.fi/handle/123456789/23953

Taebi, A. & Droste, R.L. 2004. Pollution loads in urban runoff and sanitary wastewater. Science of the total Environment, 327(1), 175-184.

Taka, M. 2017. Key drivers of stream water quality along an urban-rural transition-a watershed-scale perspective. University of Helsinki, Department of Geosciences and Geography.

Tian, J., Yi, S., Imhoff, P.T., Chiu, P., Guo, M., Maresca, J.A., Beneski, V. & Cooksey, S.H. 2014. Biochar-amended media for enhanced nutrient removal in stormwater facilities. In World Environmental and Water Resources Congress 2014 (pp. 197-208).

Tiberg, C., Sjöstedt, C., Persson, I. & Gustafsson, J. P. 2013. Phosphate effects on copper (II) and lead (II) sorption to ferrihydrite. Geochimica et Cosmochimica Acta, 120, 140-157.

Tiefenthaler, L.L., Schiff, K.C., Bay, S.M. & Greenstein, D.J. 2002. Effect of antecedent dry periods on the accumulation of potential pollutants on parking lot surfaces using simulated rainfall. Southern California Coastal Water Research Project annual report, 2003, 216-223.

Trafikverket. 2011. Vägdagvatten – råd och rekommendationer för val av miljöåtgärd. 2011:112. ISBN: 978-91-7467-179-7. Available in Swedish: https://trafikverket.ineko.se/se/v%C3%A4gdagvatten-r%C3%A5d-och-rekommendationer-f%C3%B6r-val-av-milj%C3%B6%C3%A5tg%C3%A4rd

Treese, D.P., Clark, S.E. & Baker, K.H. 2012. Nutrient release from disturbance of infiltration system soils during construction. Advances in Civil Engineering, 2012.

Tuomela, C. 2017. Modelling Source Area Contributions of Stormwater Pollutants for Stormwater Quality Management. Master's thesis. Aalto University, School of Engineering. Available: https://aaltodoc.aalto.fi/handle/123456789/28476

Ulvi, T. 2016. Hulevesiä koskeva lainsäädäntö. Finnish Environment Institute (SYKE). Available in Finnish: http://www.ymparisto.fi/download/noname/%7B12D4C74F-BF3B-4608-B03E-44FECE09EE28%7D/116211

Valtanen, M. 2015. Effects of urbanization on seasonal runoff generation and pollutant transport under cold climate. University of Helsinki.

Valtanen, M., Sillanpää, N. & Setälä, H. 2014. The effects of urbanization on runoff pollutant concentrations, loadings and their seasonal patterns under cold climate. Water, Air, & Soil Pollution, 225(6), 1977.

Valtanen, M., Sillanpää, N. & Setälä, H. 2017. A large-scale lysimeter study of stormwater biofiltration under cold climatic conditions. Ecological Engineering, 100, 89-98.

Valtanen, M., Sillanpää, N., Hätinen, N. & Setälä, H. 2010. Hulevesien imeyttäminen ja suodattaminen: haitta-aineet ja menetelmät. Helsingin Yliopisto. Ympäristötieteiden laitos

VTT Expert Services Oy. 2017. Kiviainestutkimus. Tutkimusselostus Nro. VTT-S-03076-17

Walker, W.J., McNutt, R.P. & Maslanka, C.K. 1999. The potential contribution of urban runoff to surface sediments of the Passaic River: sources and chemical characteristics. Chemosphere, 38(2), 363-377.

Wendling, L., Koimula, K., Kuosa, H., Korkealaakso, J., Iiti, H. & Holt, E. 2017.
a) Storm-Filter Material Testing Summary Report. Localized performance of bio- and mineral-based filtration material components. VTT Research Report VTT-R-01757-17. VTT Technical Research Centre of Finland, Espoo. 55 pp. Available: http://www.vtt.fi/sites/stormfilter/Documents/VTT_R_01757_17_1708.pdf
b) Storm-Filter Material Testing Summary Report. Performance of stormwater filtration systems. VTT Research Report VTT-R-05545-17. VTT Technical Research Centre of Finland, Espoo. 50 pp. Available: http://www.vtt.fi/sites/stormfilter/Documents/VTT_R_05545_17.pdf

Wendling, L.A., Douglas, G.B., Coleman, S. & Yuan, Z. 2013. Nutrient and dissolved organic carbon removal from natural waters using industrial by-products. Science of the Total Environment, 442, 63-72.

Westerlund, C., Viklander, M. & Bäckström, M. 2003. Seasonal variations in road runoff quality in Luleå, Sweden. Water science and technology, 48(9), 93-101.

Wu, P. & Zhou, Y.S. 2009. Simultaneous removal of coexistent heavy metals from simulated urban stormwater using four sorbents: a porous iron sorbent and its mixtures with zeolite and crystal gravel. Journal of hazardous materials, 168(2), 674-680.

Appendices

Appendix 1. Event 1 dynamic figures. 5 pages.

Appendix 2. Event 2 dynamic figures. 6 pages.

Appendix 3. Event 3 dynamic figures. 6 pages.

Appendix 4. PHREEQC modelling input values. 1 page.

Appendix 5. PHREEQC modelling results. 4 pages.

Appendix 6. Spearman correlation matrices. 3 pages.

Appendix 1. Event 1 dynamic figures

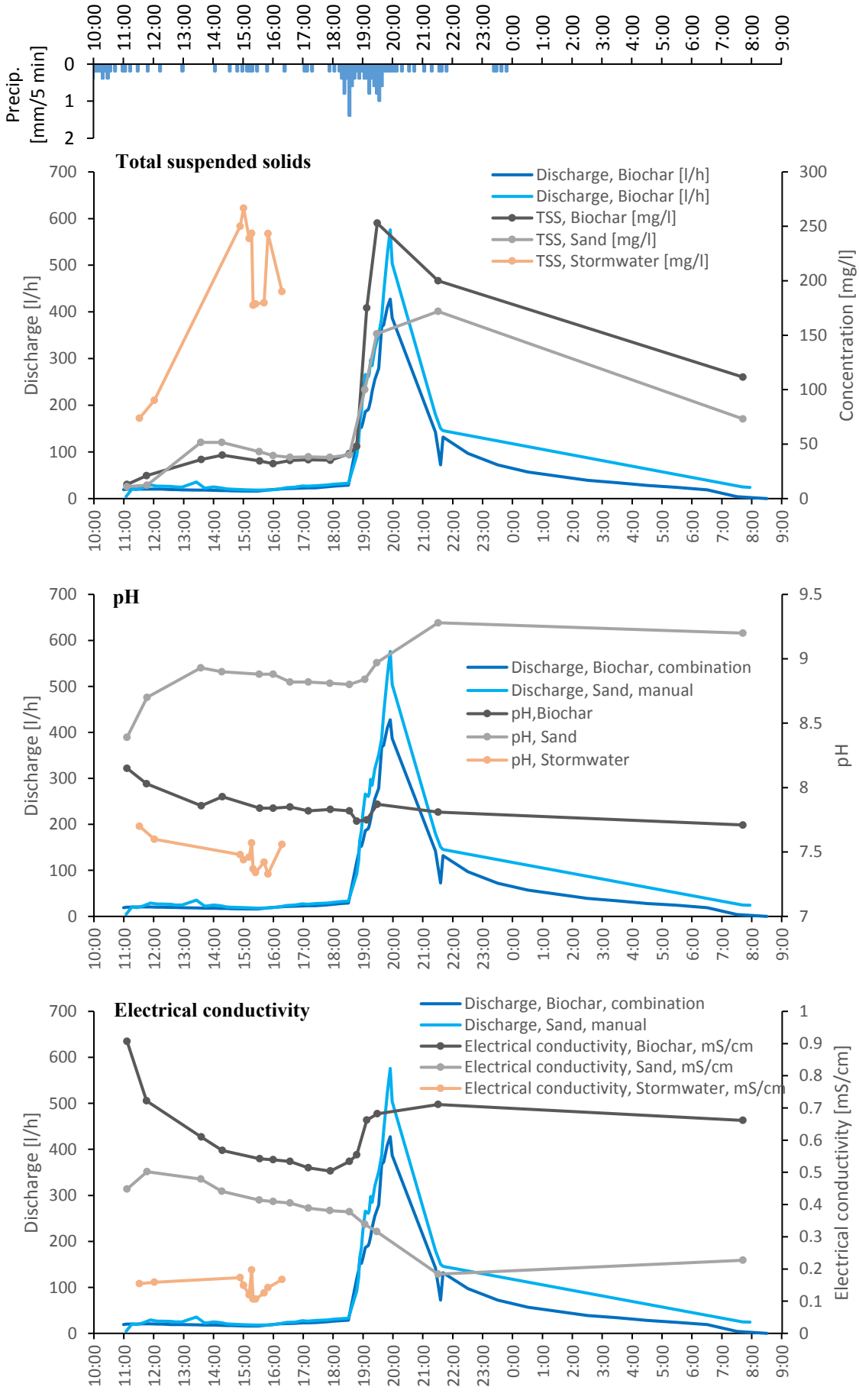

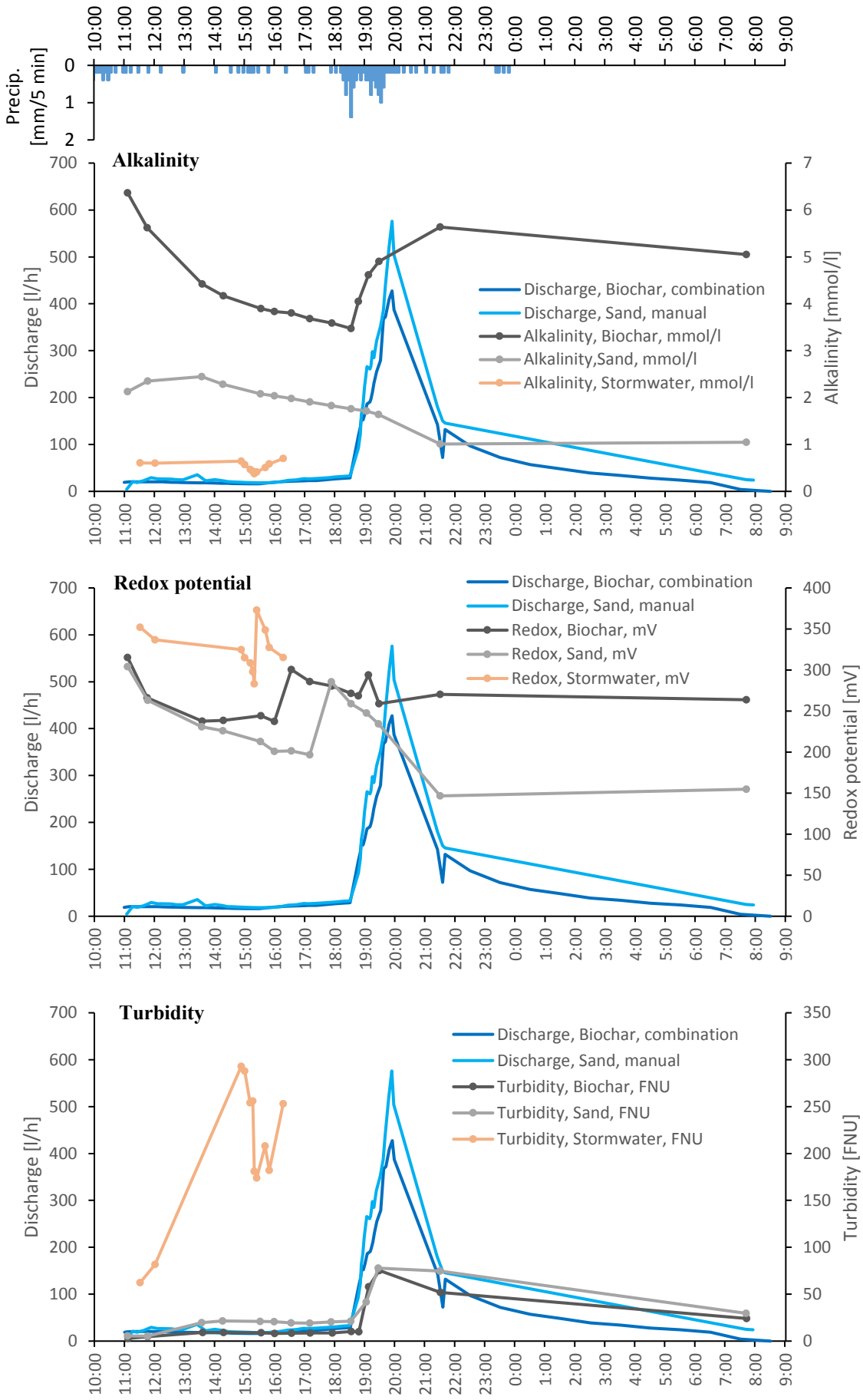
Precip. [mm/5 min]
Alkalinity
Discharge [l/h]
Alkalinity [mmol/l]
Discharge, Biochar, combination
Discharge, Sand, manual
Alkalinity, Biochar, mmol/l
Alkalinity,Sand, mmol/l
Alkalinity, Stormwater, mmol/l
Redox potential
Redox potential [mV]
Redox, Biochar, mV
Redox, Sand, mV
Redox, Stormwater, mV
Turbidity
Turbidity [FNU]
Turbidity, Biochar, FNU
Turbidity, Sand, FNU
Turbidity, Stormwater, FNU

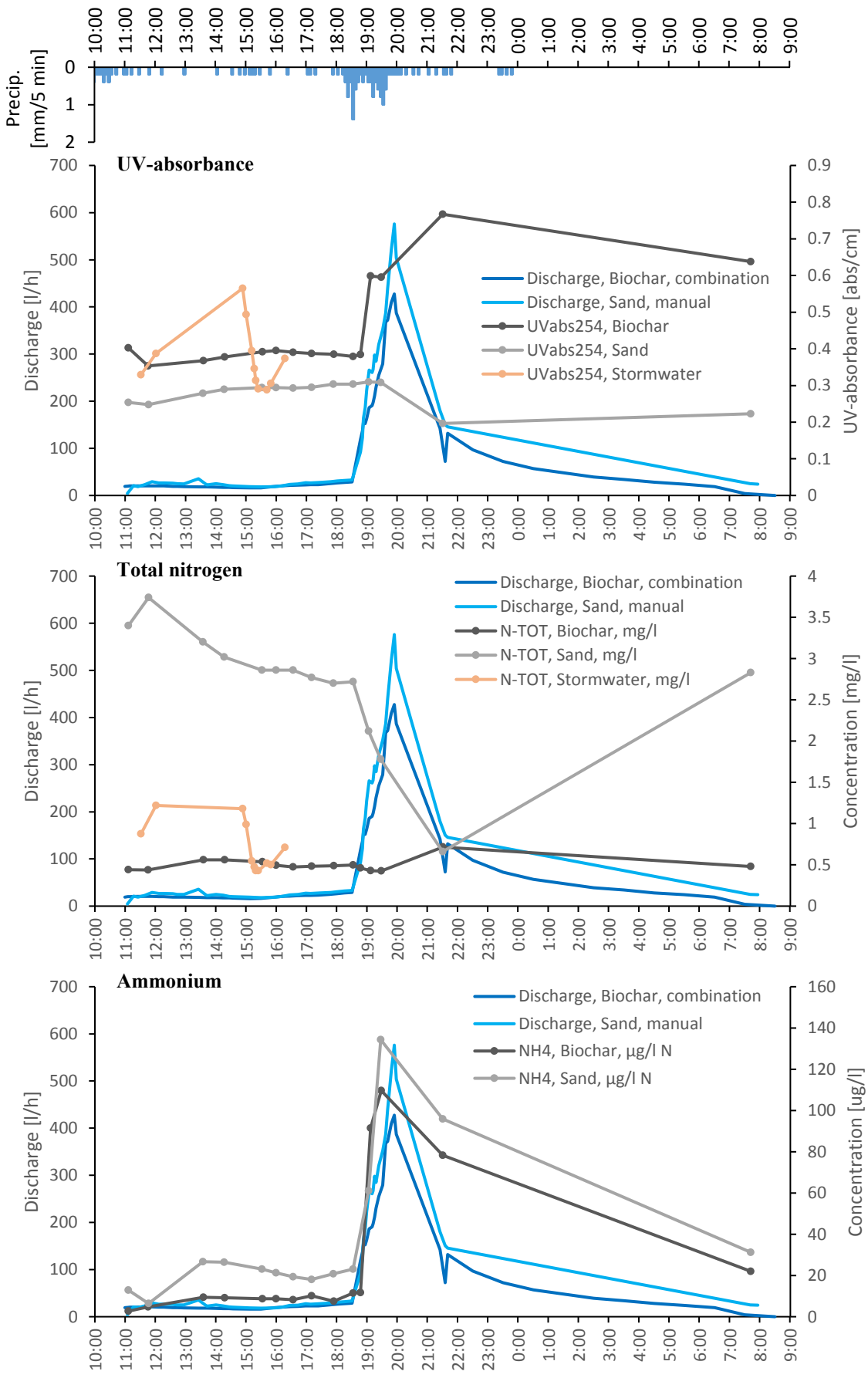
Precip. [mm/5 min]
UV-absorbance
Discharge [l/h]
UV-absorbance [abs/cm]
Discharge, Biochar, combination
Discharge, Sand, manual
UVabs254, Biochar
UVabs254, Sand
UVabs254, Stormwater
Total nitrogen
Concentration [mg/l]
N-TOT, Biochar, mg/l
N-TOT, Sand, mg/l
N-TOT, Stormwater, mg/l
Ammonium
Concentration [ug/l]
NH4, Biochar, µg/l N
NH4, Sand, µg/l N

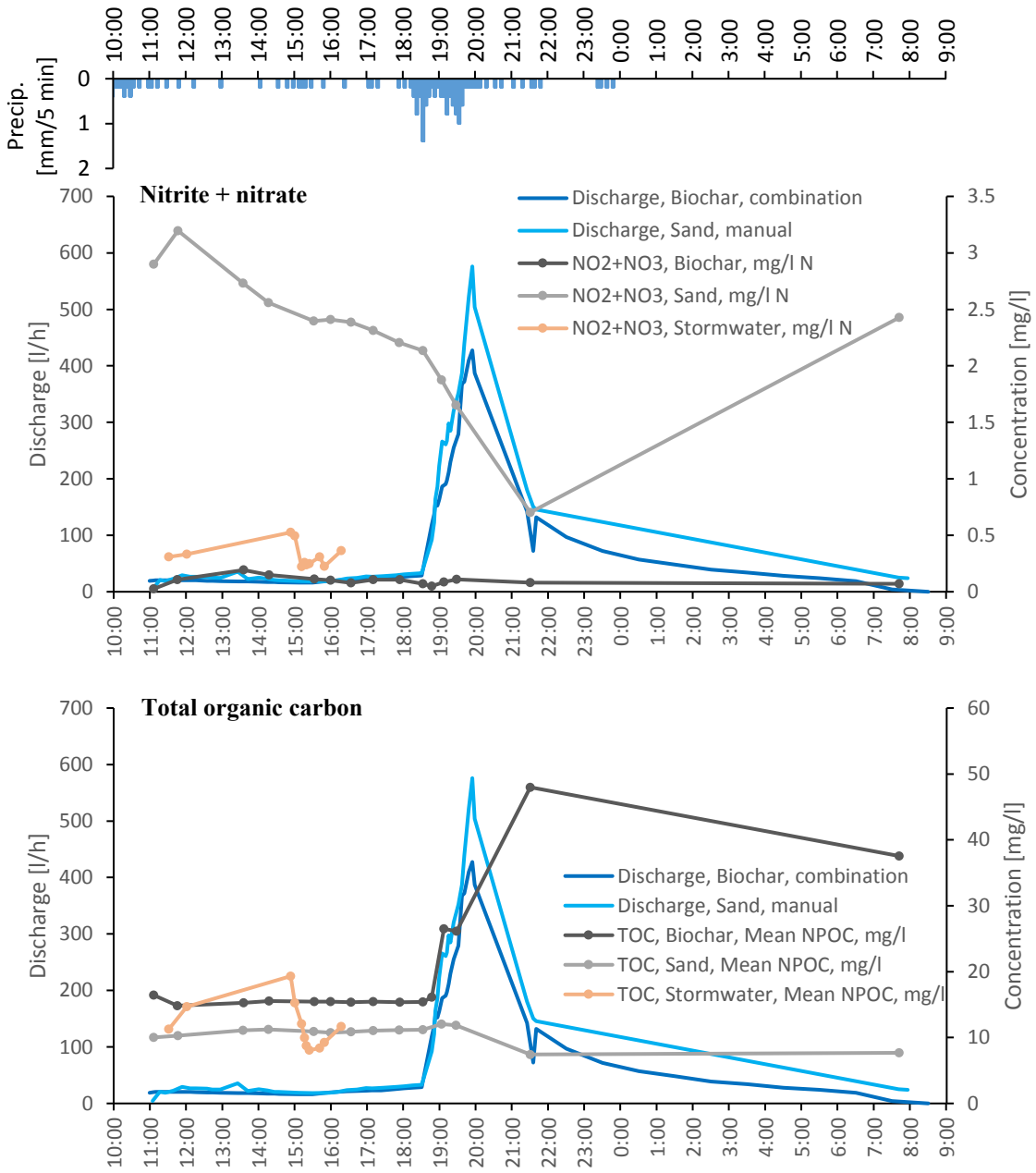
Precip. [mm/5 min]
Nitrite + nitrate
Discharge, Biochar, combination
Discharge, Sand, manual
NO2+NO3, Biochar, mg/l N
NO2+NO3, Sand, mg/l N
NO2+NO3, Stormwater, mg/l N
Discharge [l/h]
Concentration [mg/l]
Total organic carbon
Discharge, Biochar, combination
Discharge, Sand, manual
TOC, Biochar, Mean NPOC, mg/l
TOC, Sand, Mean NPOC, mg/l
TOC, Stormwater, Mean NPOC, mg/l
Discharge [l/h]
Concentration [mg/l]

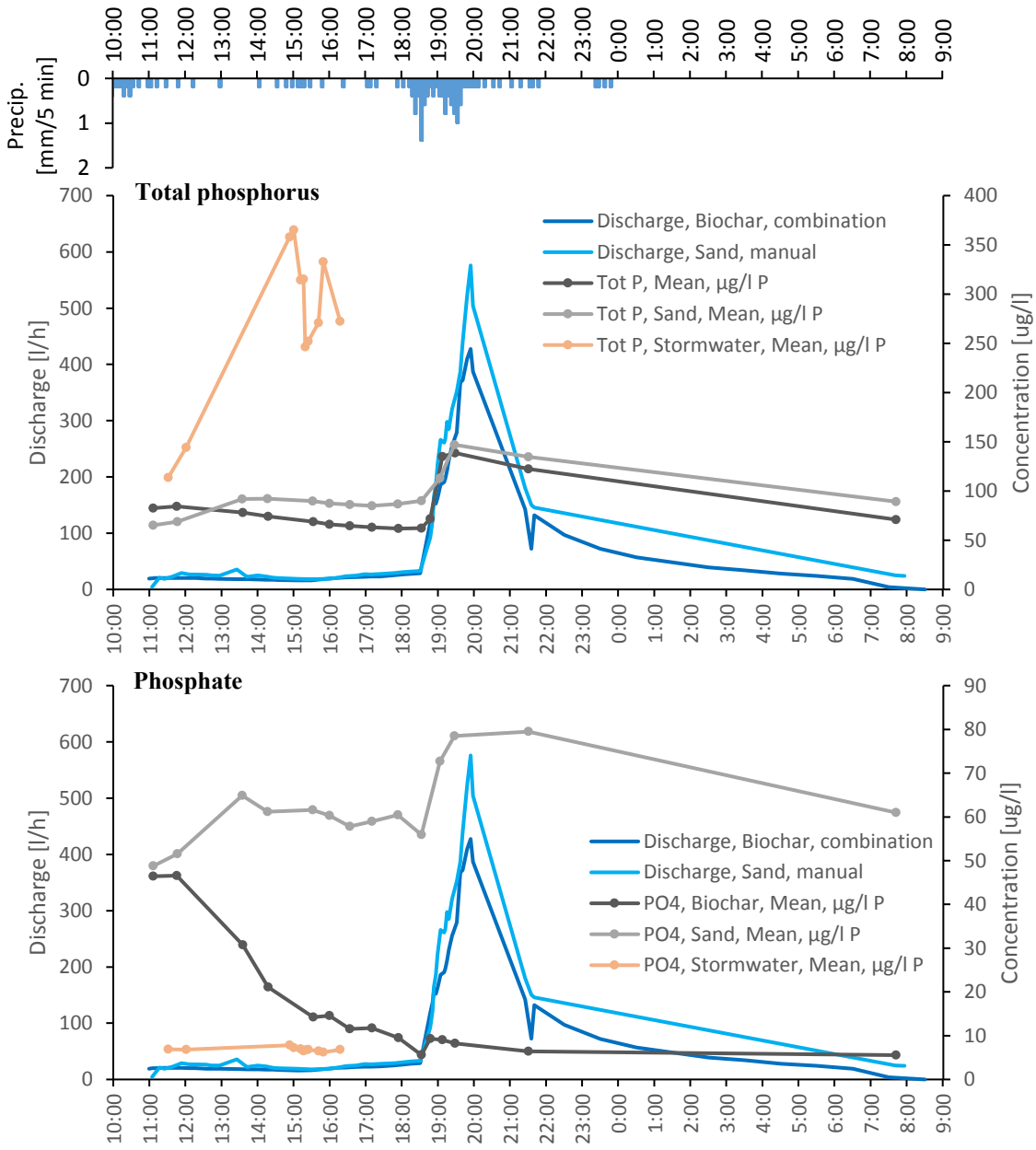
Precip. [mm/5 min]
Total phosphorus
Discharge [l/h]
Concentration [ug/l]
Discharge, Biochar, combination
Discharge, Sand, manual
Tot P, Mean, µg/l P
Tot P, Sand, Mean, µg/l P
Tot P, Stormwater, Mean, µg/l P
Phosphate
PO4, Biochar, Mean, µg/l P
PO4, Sand, Mean, µg/l P
PO4, Stormwater, Mean, µg/l P

Appendix 2. Event 2 dynamic figures

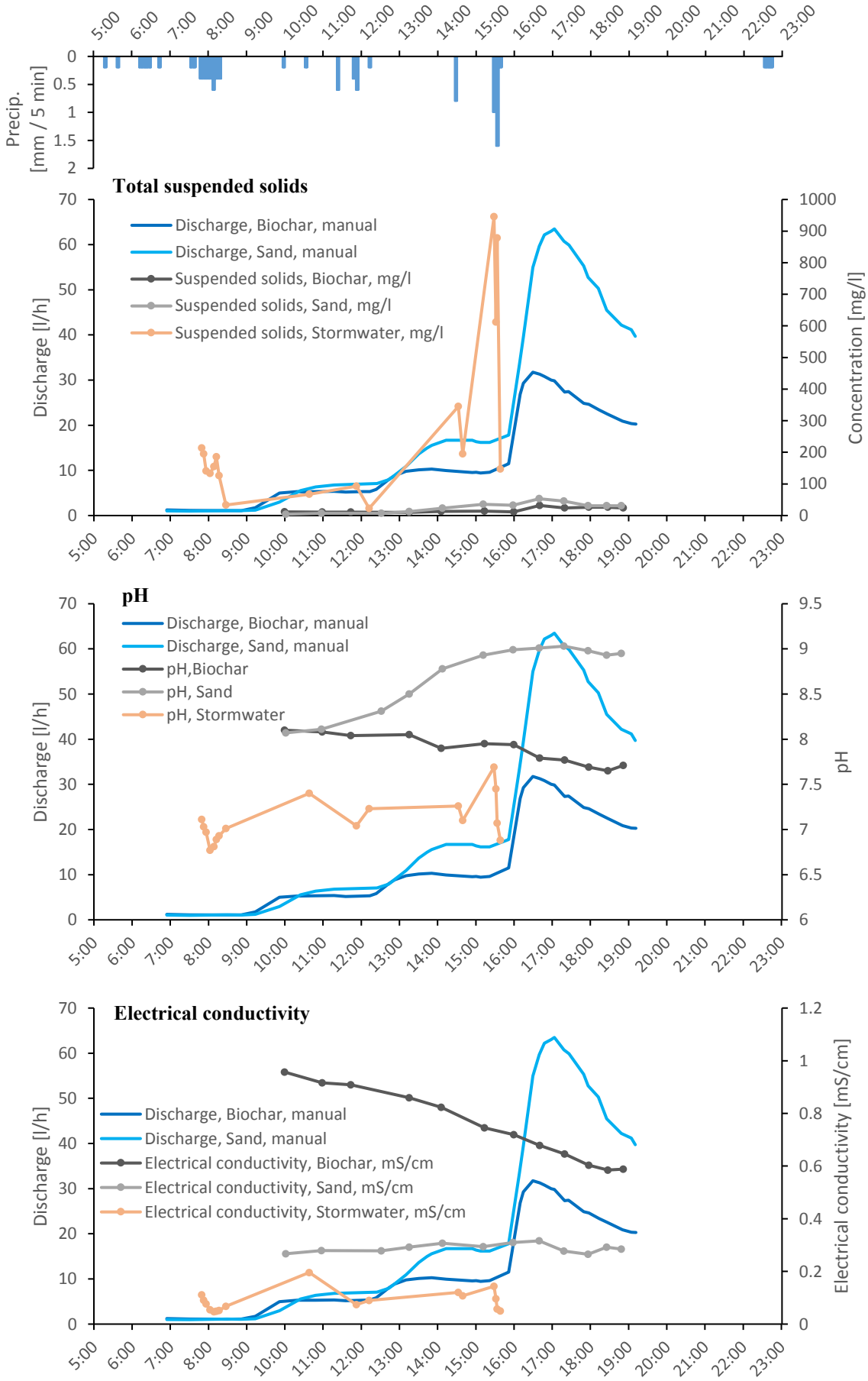

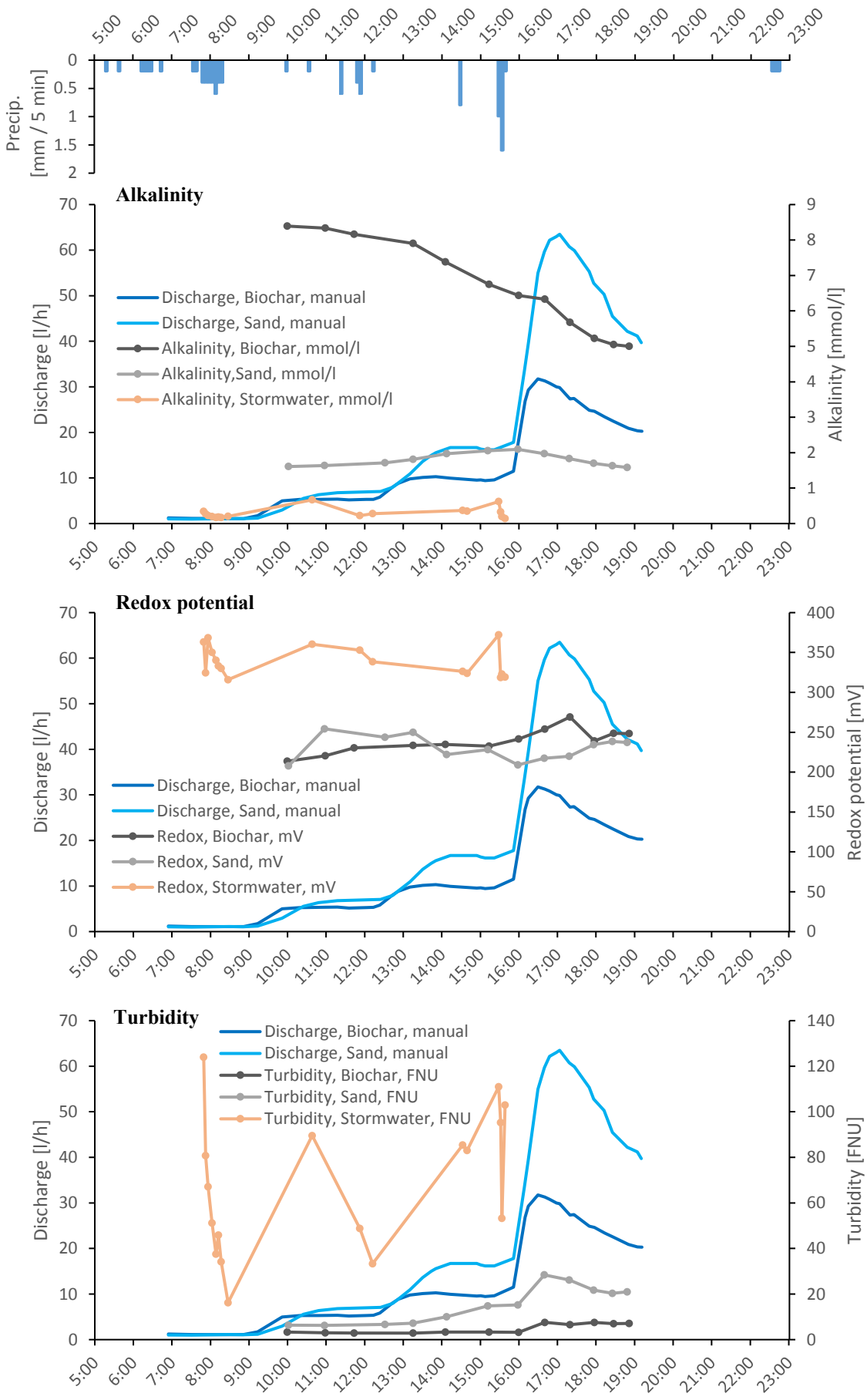
Precip. [mm / 5 min]
Alkalinity
Discharge [l/h]
Alkalinity [mmol/l]
Discharge, Biochar, manual
Discharge, Sand, manual
Alkalinity, Biochar, mmol/l
Alkalinity,Sand, mmol/l
Alkalinity, Stormwater, mmol/l
Redox potential
Redox potential [mV]
Redox, Biochar, mV
Redox, Sand, mV
Redox, Stormwater, mV
Turbidity
Turbidity [FNU]
Turbidity, Biochar, FNU
Turbidity, Sand, FNU
Turbidity, Stormwater, FNU

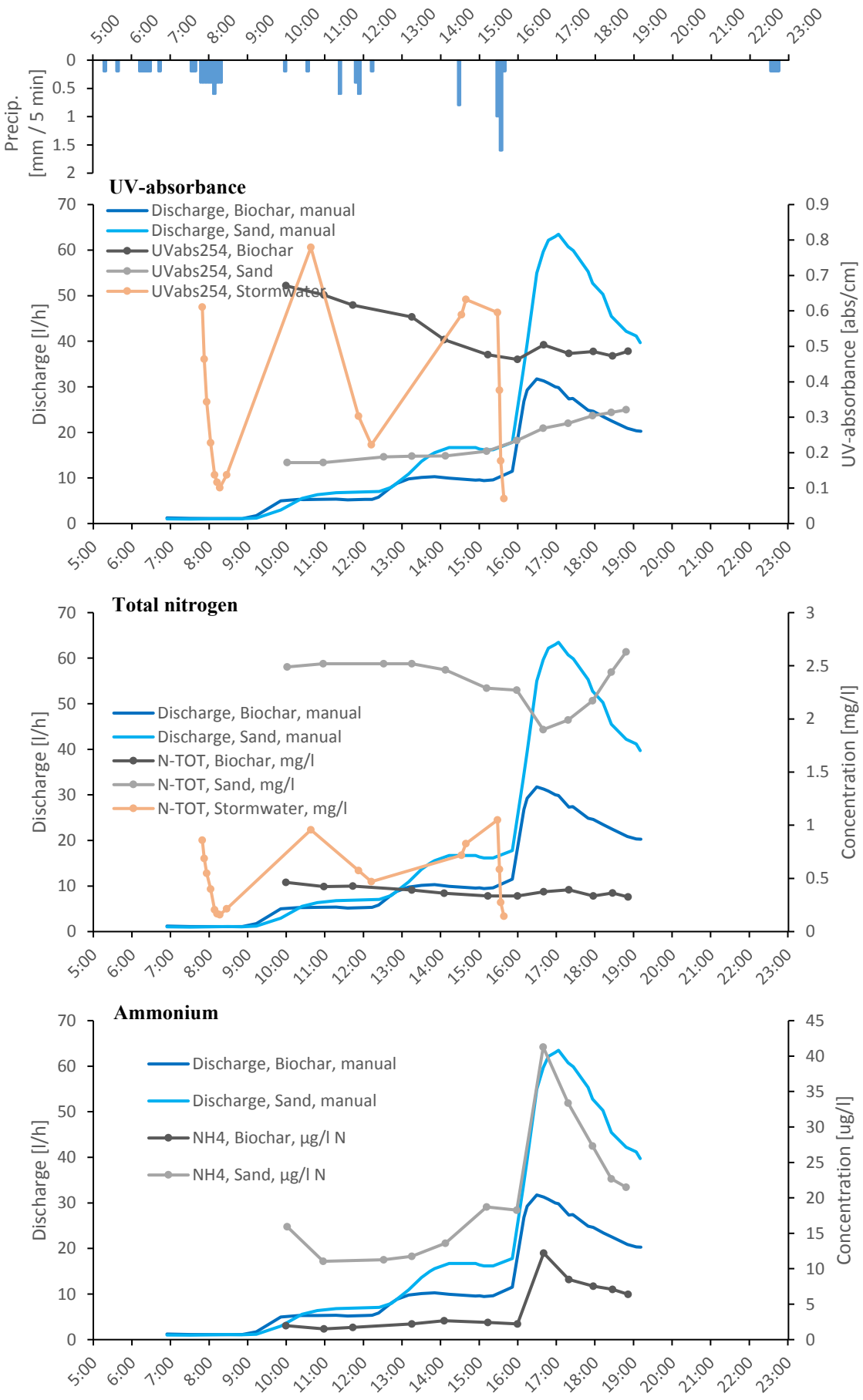
Precip. [mm / 5 min]
UV-absorbance
Discharge, Biochar, manual
Discharge, Sand, manual
UVabs254, Biochar
UVabs254, Sand
UVabs254, Stormwater
Discharge [l/h]
UV-absorbance [abs/cm]
Total nitrogen
N-TOT, Biochar, mg/l
N-TOT, Sand, mg/l
N-TOT, Stormwater, mg/l
Concentration [mg/l]
Ammonium
NH4, Biochar, µg/l N
NH4, Sand, µg/l N
Concentration [ug/l]

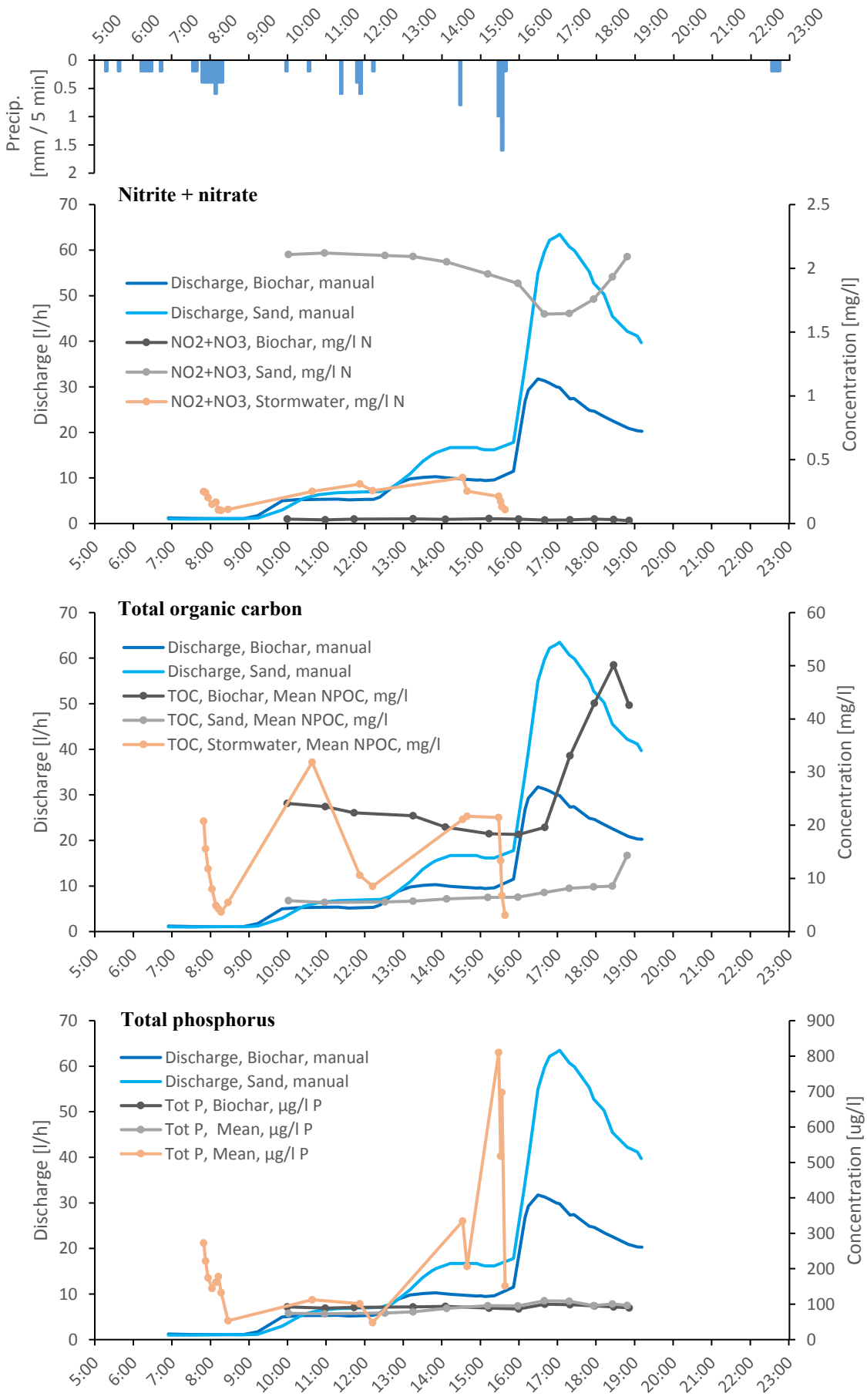
Precip. [mm / 5 min]
Nitrite + nitrate
Discharge [l/h]
Concentration [mg/l]
Discharge, Biochar, manual
Discharge, Sand, manual
NO2+NO3, Biochar, mg/l N
NO2+NO3, Sand, mg/l N
NO2+NO3, Stormwater, mg/l N
Total organic carbon
TOC, Biochar, Mean NPOC, mg/l
TOC, Sand, Mean NPOC, mg/l
TOC, Stormwater, Mean NPOC, mg/l
Total phosphorus
Tot P, Biochar, µg/l P
Tot P, Mean, µg/l P
Concentration [ug/l]

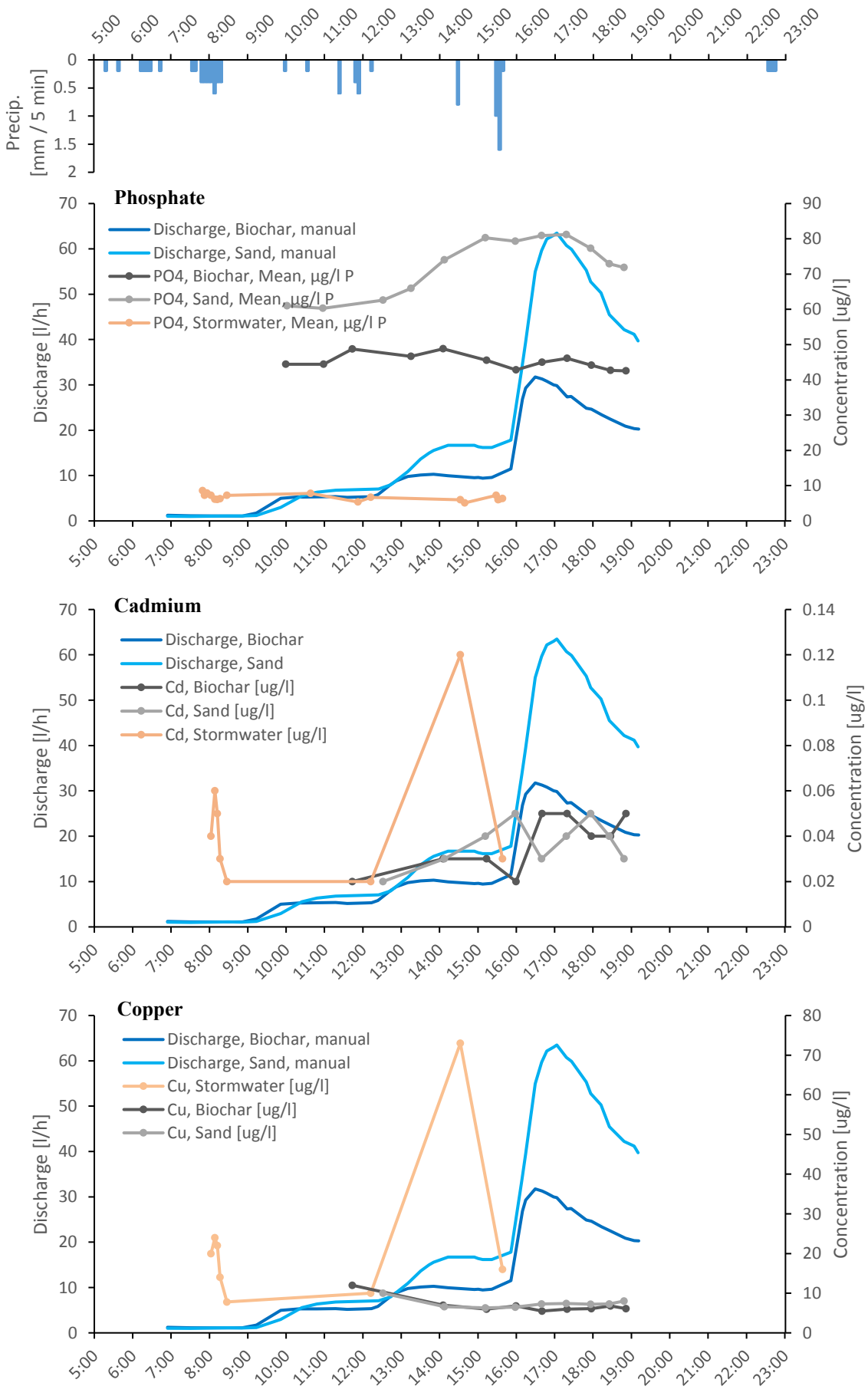
Precip. [mm / 5 min]
Phosphate
Discharge, Biochar, manual
Discharge, Sand, manual
PO4, Biochar, Mean, µg/l P
PO4, Sand, Mean, µg/l P
PO4, Stormwater, Mean, µg/l P
Discharge [l/h]
Concentration [ug/l]
Cadmium
Discharge, Biochar
Discharge, Sand
Cd, Biochar [ug/l]
Cd, Sand [ug/l]
Cd, Stormwater [ug/l]
Copper
Discharge, Biochar, manual
Discharge, Sand, manual
Cu, Stormwater [ug/l]
Cu, Biochar [ug/l]
Cu, Sand [ug/l]

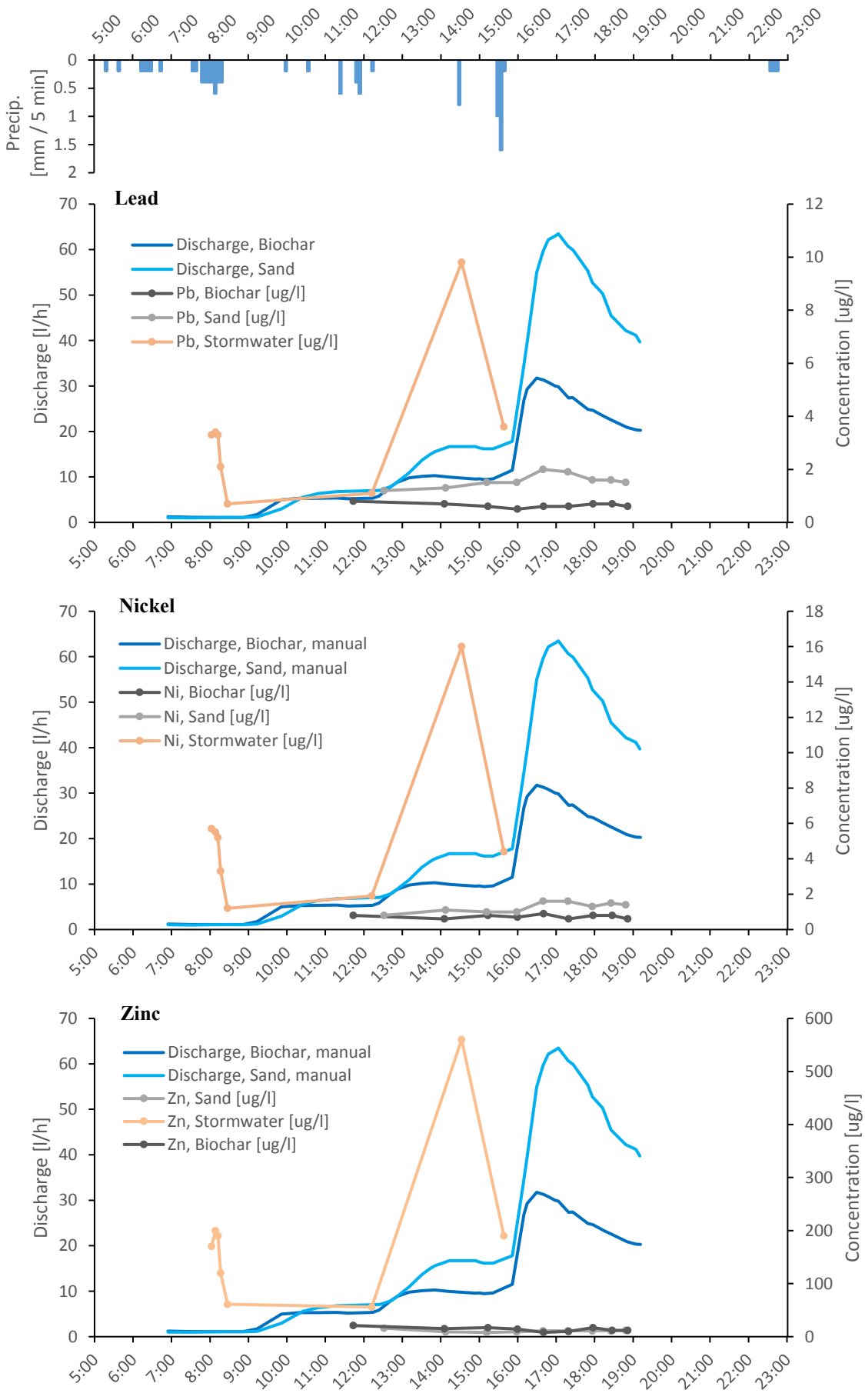
Precip. [mm / 5 min]
Lead
Discharge, Biochar
Discharge, Sand
Pb, Biochar [ug/l]
Pb, Sand [ug/l]
Pb, Stormwater [ug/l]
Discharge [l/h]
Concentration [ug/l]
Nickel
Discharge, Biochar, manual
Discharge, Sand, manual
Ni, Biochar [ug/l]
Ni, Sand [ug/l]
Ni, Stormwater [ug/l]
Zinc
Discharge, Biochar, manual
Discharge, Sand, manual
Zn, Sand [ug/l]
Zn, Stormwater [ug/l]
Zn, Biochar [ug/l]

Appendix 3. Event 3 dynamic figures

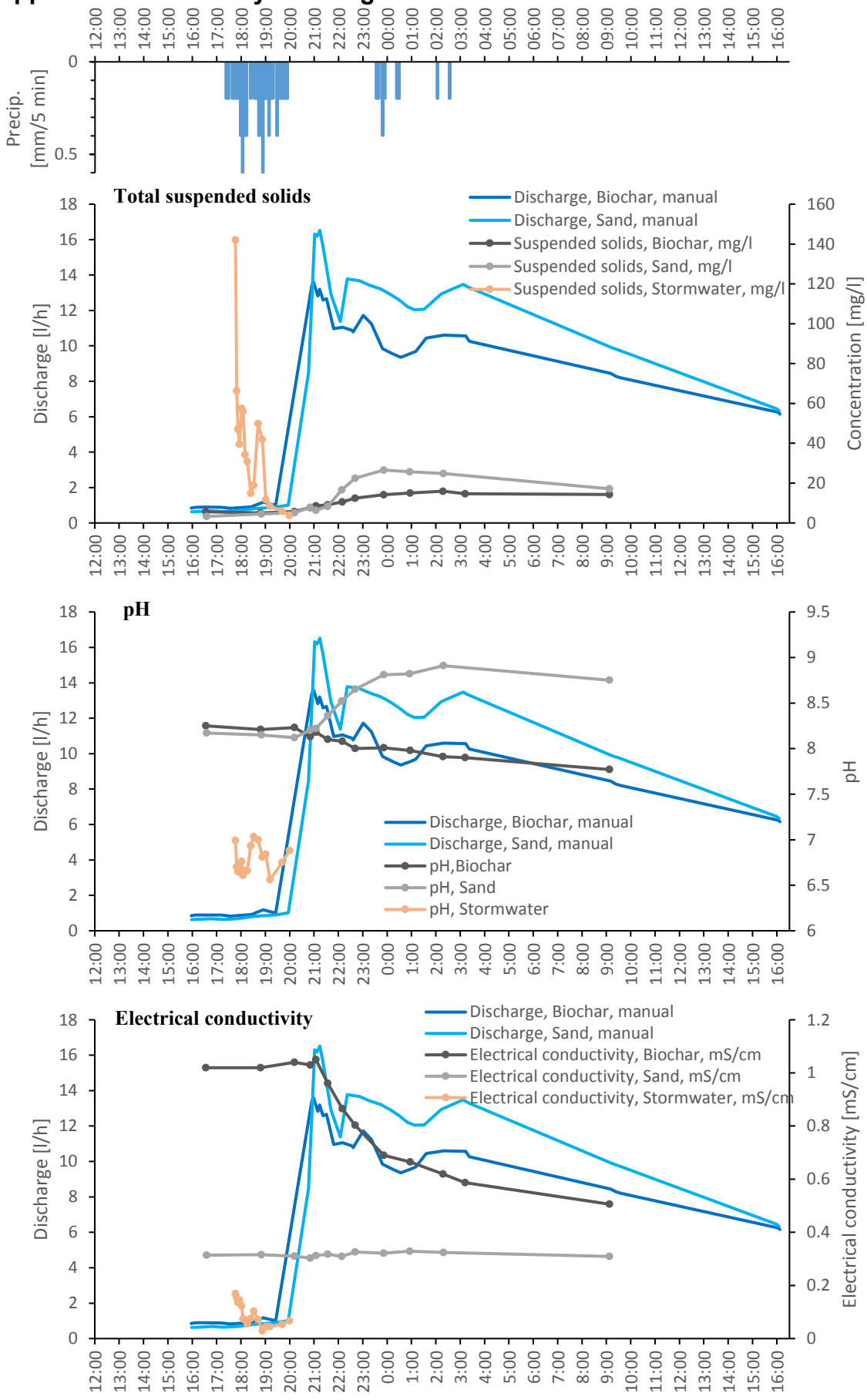

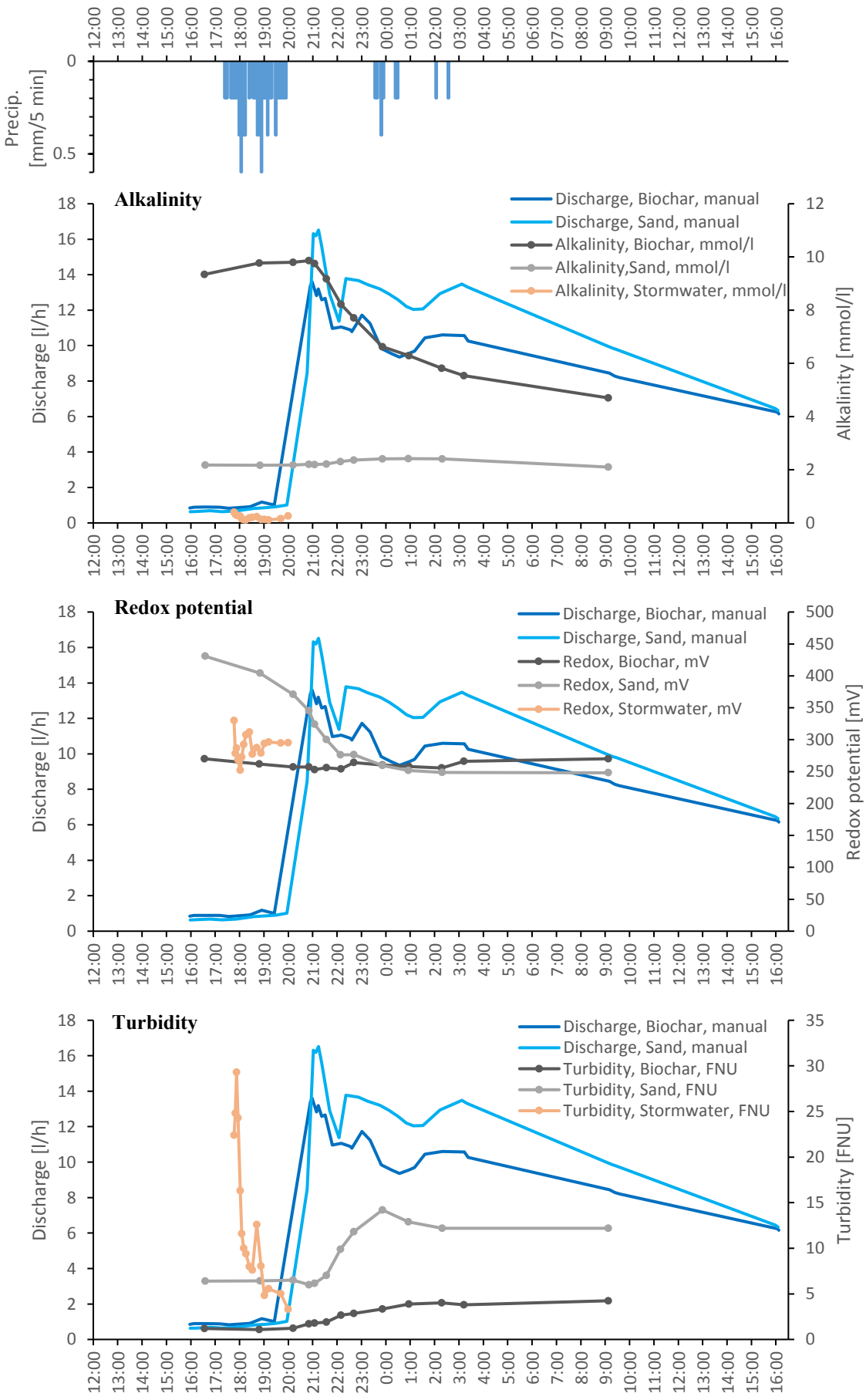
Precip. [mm/5 min]
Alkalinity
Discharge, Biochar, manual
Discharge, Sand, manual
Alkalinity, Biochar, mmol/l
Alkalinity,Sand, mmol/l
Alkalinity, Stormwater, mmol/l
Discharge [l/h]
Alkalinity [mmol/l]
Redox potential
Redox, Biochar, mV
Redox, Sand, mV
Redox, Stormwater, mV
Redox potential [mV]
Turbidity
Turbidity, Biochar, FNU
Turbidity, Sand, FNU
Turbidity, Stormwater, FNU
Turbidity [FNU]

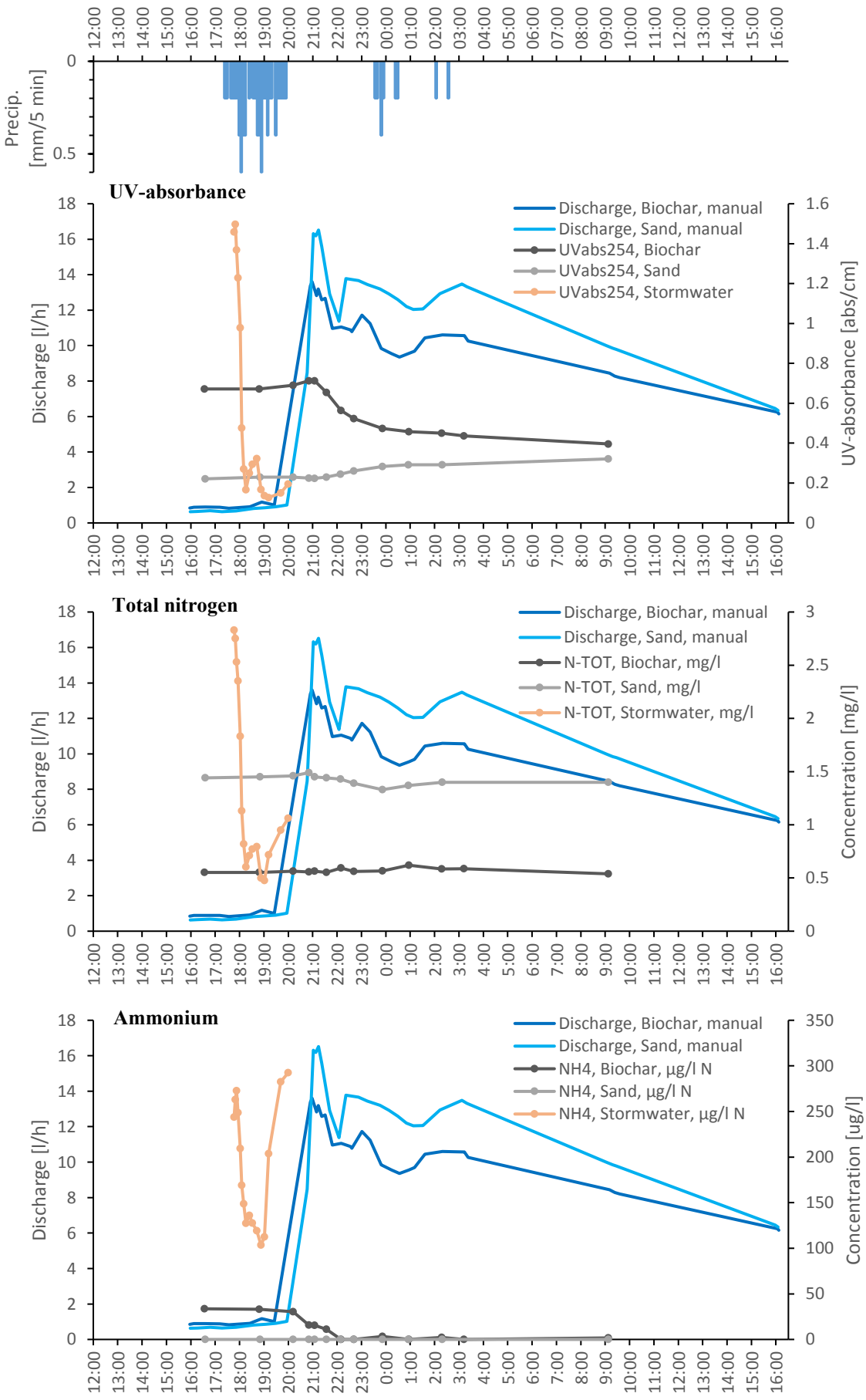
Precip. [mm/5 min]
UV-absorbance
Discharge, Biochar, manual
Discharge, Sand, manual
UVabs254, Biochar
UVabs254, Sand
UVabs254, Stormwater
Discharge [l/h]
UV-absorbance [abs/cm]
Total nitrogen
N-TOT, Biochar, mg/l
N-TOT, Sand, mg/l
N-TOT, Stormwater, mg/l
Concentration [mg/l]
Ammonium
NH4, Biochar, µg/l N
NH4, Sand, µg/l N
NH4, Stormwater, µg/l N
Concentration [ug/l]

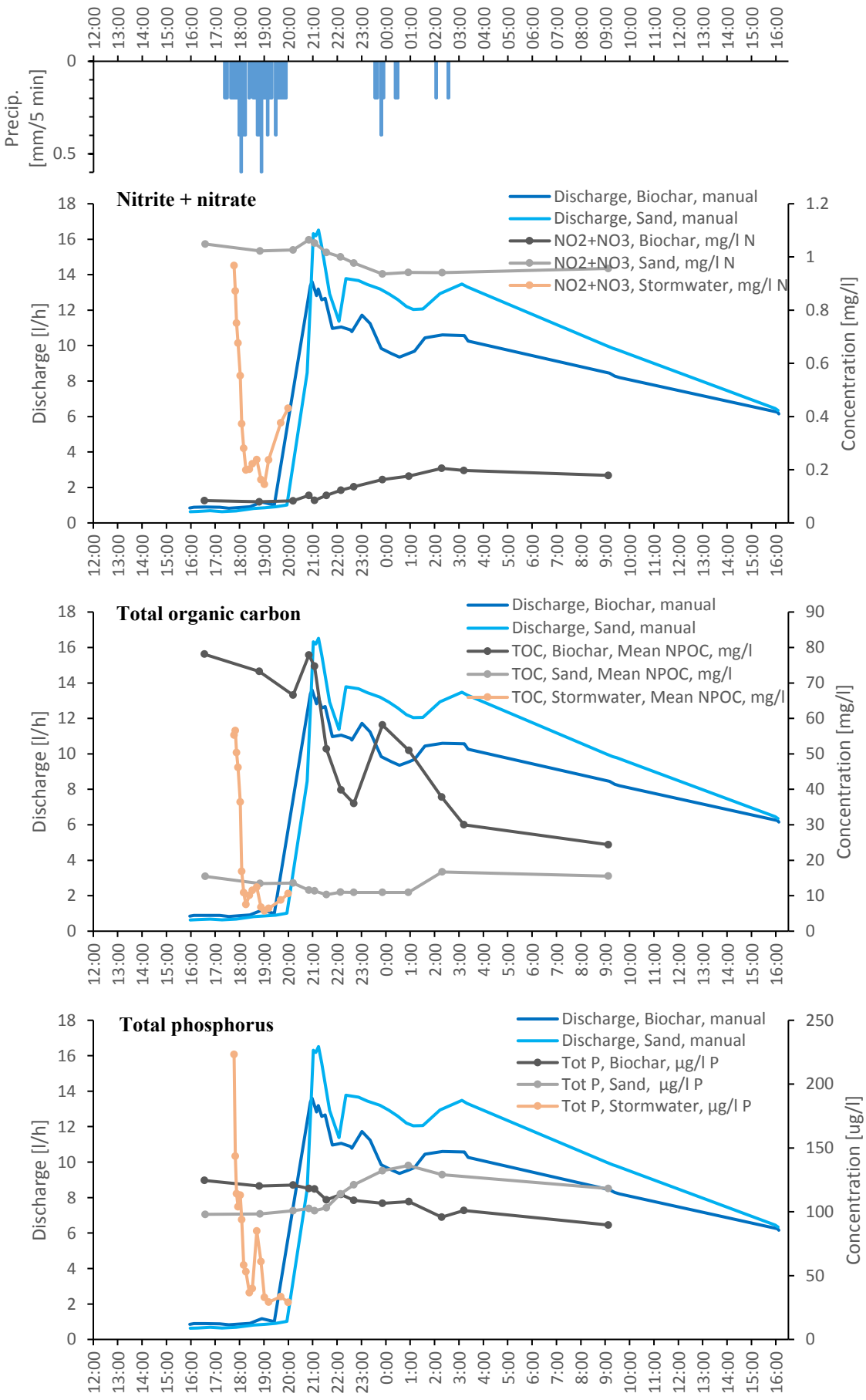
Precip. [mm/5 min]
Nitrite + nitrate
Discharge, Biochar, manual
Discharge, Sand, manual
NO2+NO3, Biochar, mg/l N
NO2+NO3, Sand, mg/l N
NO2+NO3, Stormwater, mg/l N
Discharge [l/h]
Concentration [mg/l]
Total organic carbon
TOC, Biochar, Mean NPOC, mg/l
TOC, Sand, Mean NPOC, mg/l
TOC, Stormwater, Mean NPOC, mg/l
Concentration [mg/l]
Total phosphorus
Tot P, Biochar, µg/l P
Tot P, Sand, µg/l P
Tot P, Stormwater, µg/l P
Concentration [ug/l]

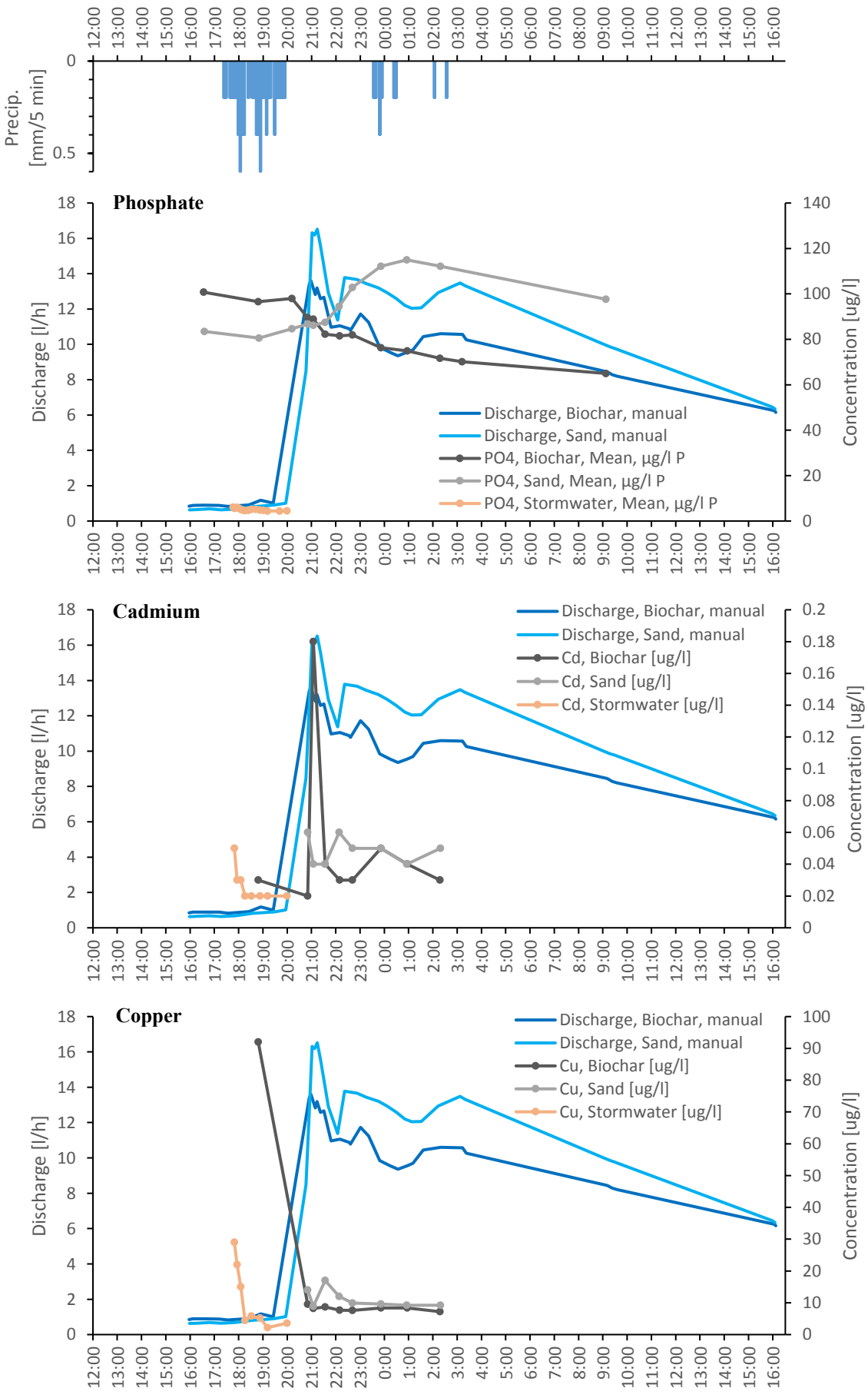
Precip. [mm/5 min]
Phosphate
Discharge [l/h]
Concentration [ug/l]
Discharge, Biochar, manual
Discharge, Sand, manual
PO4, Biochar, Mean, µg/l P
PO4, Sand, Mean, µg/l P
PO4, Stormwater, Mean, µg/l P
Cadmium
Discharge, Biochar, manual
Discharge, Sand, manual
Cd, Biochar [ug/l]
Cd, Sand [ug/l]
Cd, Stormwater [ug/l]
Copper
Discharge, Biochar, manual
Discharge, Sand, manual
Cu, Biochar [ug/l]
Cu, Sand [ug/l]
Cu, Stormwater [ug/l]

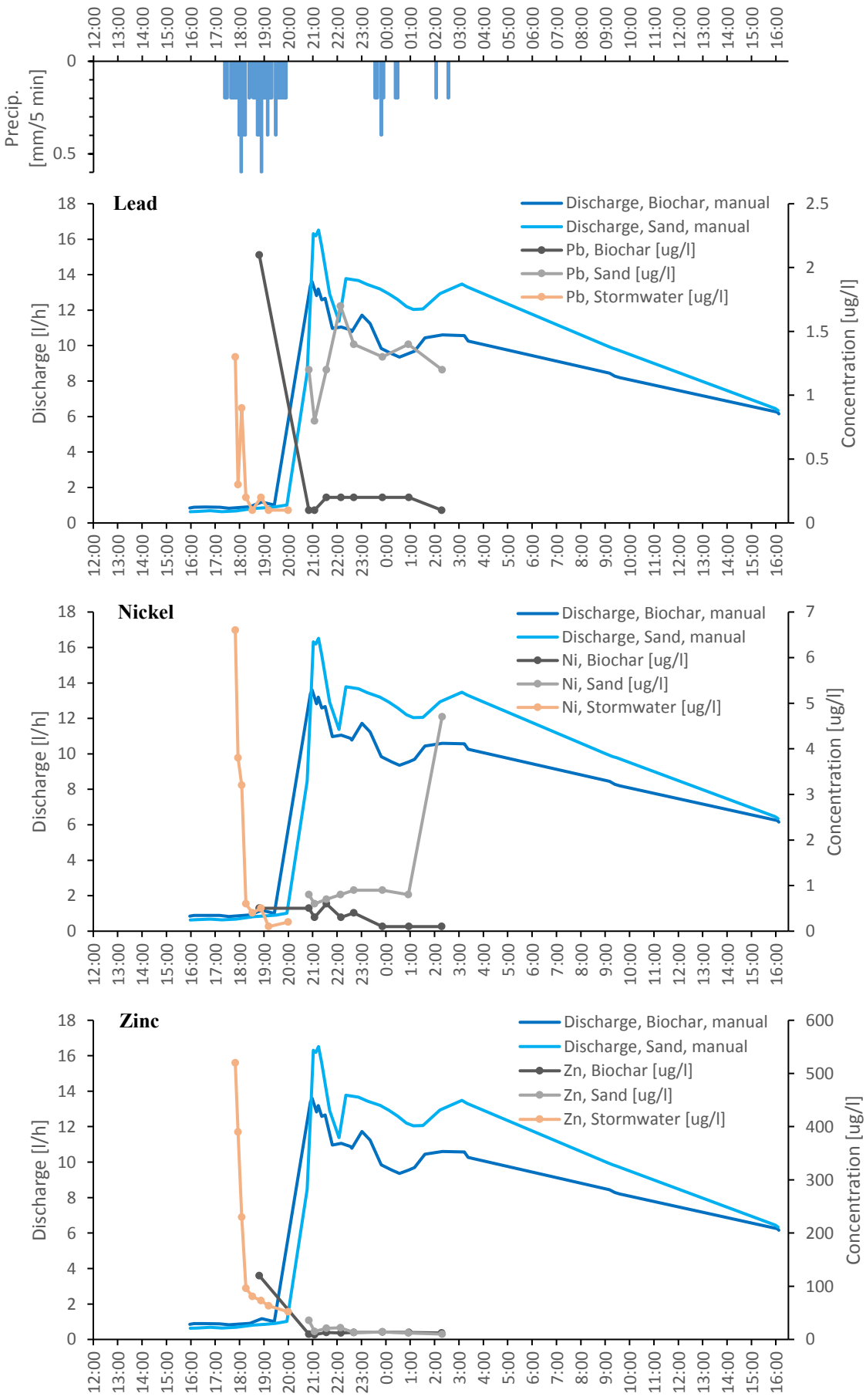
Precip. [mm/5 min]
Lead
Discharge, Biochar, manual
Discharge, Sand, manual
Pb, Biochar [ug/l]
Pb, Sand [ug/l]
Pb, Stormwater [ug/l]
Discharge [l/h]
Concentration [ug/l]
Nickel
Ni, Biochar [ug/l]
Ni, Sand [ug/l]
Ni, Stormwater [ug/l]
Zinc
Zn, Biochar [ug/l]
Zn, Sand [ug/l]
Zn, Stormwater [ug/l]

Appendix 4. PHREEQC modelling input values

Table 1. Input values for PHREEQC modelling. All variables in mg/l except temperature (°C) and pH.

	Event 2				Event 3			
	Biochar		Sand		Biochar		Sand	
Time	**16:40**	**18:51**	**16:39**	**18:48**	**20:50**	**22:41**	**20:50**	**22:41**
Temperature	13.5	13.5	14	14	17.5	17.5	17	17
pH	7.79	7.71	9.01	8.95	8.13	8	8.2	8.65
Alkalinity as HCO_3	386.06	305.05	120.12	96.55	601.46	470.31	134.66	144.35
Al	1.1	1.4	5.2	4.1	0.46	0.92	2.6	4.4
Ca	21	18	2.8	2.4	22	18	3	3.3
Cd	0.00005	0.00005	0.00003	0.00003	0.00002	0.00003	0.00006	0.00005
Cu	0.0055	0.0061	0.0073	0.008	0.0095	0.0076	0.014	0.0099
Cl	18	15	10	16	24	17	9.9	11
Fe	0.23	0.3	1.5	1.1	0.11	0.15	0.54	0.88
K	37	33	2	1.8	61	52	1.9	1.9
Mg	4.7	3.9	1.5	1.2	6.1	4.9	0.93	1.3
Mn	0.05	0.054	0.025	0.018	0.009	0.007	0.008	0.014
Na	120	91	59	55	170	130	61	66
N(-3) (NH_4)	0.01221	0.0064	0.04128	0.02151	0.01574	0	0	0
N(5) (NO_3)	0.027	0.022	1.64	2.09	0.1	0.14	1.06	0.98
Ni	0.0009	0.0006	0.0016	0.0014	0.0005	0.0004	0.0008	0.0009
S(6) (SO_4)	7.2	6.5	7.8	7.7	9.2	8.6	8.8	7.8
Si	7.6	7.6	14	12	7.8	8.2	9.5	13
P	0.09983	0.08967	0.1094	0.09652	0.1183	0.109	0.1026	0.1211
Pb	0.0006	0.0006	0.002	0.0015	0.0001	0.0002	0.0012	0.0014
Zn	0.008	0.012	0.011	0.012	0.01	0.013	0.036	0.013

Appendix 5. PHREEQC modelling results

Table 2. Modelled saturation indices of cadmium-containing mineral phases. Values exceeding -0.5 indicating approximate equilibrium or supersaturation are shown in bold text.

		Event 2				Event 3			
		Biochar		Sand		Biochar		Sand	
Mineral	**Formula**	**16:40**	**18:51**	**16:39**	**18:48**	**20:50**	**22:41**	**20:50**	**22:41**
$Cd(OH)_2$	$Cd(OH)_2$	-7.7	-7.8	-5.4	-5.5	-7.4	-7.5	-6.7	-5.9
$Cd_3(PO_4)_2$	$Cd_3(PO_4)_2$	-17.1	-17.2	-14.6	-14.8	-17.5	-17.2	-15.3	-14.6
$CdSiO_3$	$CdSiO_3$	-7.1	-7.3	-4.6	-4.8	-6.7	-6.7	-5.9	-5.0
$CdSO_4$	$CdSO_4$	-14.2	-14.2	-14.2	-14.2	-14.5	-14.3	-13.8	-13.9
Otavite	$CdCO_3$	-2.4	-2.6	-2.1	-2.2	-2.3	-2.3	-2.3	-2.0

Table 3. Modelled saturation indices of copper-containing mineral phases. Values exceeding -0.5 indicating approximate equilibrium or supersaturation are shown in bold text.

		Event 2				Event 3			
		Biochar		Sand		Biochar		Sand	
Mineral	**Formula**	**16:40**	**18:51**	**16:39**	**18:48**	**20:50**	**22:41**	**20:50**	**22:41**
Antlerite	$Cu_3(OH)_4SO_4$	-9.2	-8.9	-10.3	-10.1	-8.9	-9.0	-7.9	-9.2
Atacamite	$Cu_2(OH)_3Cl$	-6.3	-6.2	-7.0	-6.6	-5.8	-6.0	-5.5	-6.2
Azurite	$Cu_3(OH)_2(CO_3)_2$	-5.7	-5.6	-8.5	-8.4	-4.9	-5.1	-5.4	-6.8
Brochantite	$Cu_4(OH)_6SO_4$	-9.9	-9.5	-10.6	-10.3	-9.4	-9.5	-8.0	-9.4
Chalcanthite	$CuSO_4{:}5H_2O$	-10.9	-10.7	-12.8	-12.6	-11.2	-11.1	-10.9	-12.0
$Cu(OH)_2$	$Cu(OH)_2$	-2.8	-2.7	-2.3	-2.3	-2.3	-2.4	-2.0	-2.1
$Cu_2(OH)_3NO_3$	$Cu_2(OH)_3NO_3$	-10.6	-10.5	-9.2	-9.0	-9.7	-9.6	-8.0	-8.7
Cu_2SO_4	Cu_2SO_4	-23.6	-23.2	-27.6	-27.3	-24.3	-24.0	-23.8	-25.9
$Cu_3(PO_4)_2$	$Cu_3(PO4)_2$	-11.8	-11.4	-15.1	-14.8	-12.1	-11.9	-11.1	-13.1
$Cu_3(PO_4)_2{:}3H_2O$	$Cu_3(PO_4)_2{:}3H_2O$	-13.5	-13.1	-16.8	-16.5	-13.8	-13.6	-12.9	-14.9
$CuCO_3$	$CuCO_3$	-4.5	-4.5	-6.1	-6.1	-4.3	-4.4	-4.8	-5.4
Cu metal	Cu	-5.3	-5.1	-7.4	-7.2	-5.9	-5.7	-5.6	-6.6
$CuOCuSO_4$	$CuOCuSO_4$	-19.8	-19.6	-21.3	-21.1	-19.5	-19.4	-18.8	-20.0
Cuprite	Cu_2O	-3.8	-3.6	-5.5	-5.3	-4.0	-3.9	-3.4	-4.5
CupricFerrite	$CuFe_2O_4$	**14.7**	**14.9**	**16.7**	**16.5**	**14.5**	**14.6**	**16.3**	**16.5**
CuprousFerrite	$CuFeO_2$	**13.7**	**13.9**	**13.7**	**13.7**	**13.3**	**13.4**	**14.3**	**13.9**
$CuSO_4$	$CuSO_4$	-17.1	-16.9	-19.0	-18.8	-17.2	-17.1	-16.9	-18.0
Dioptase	$CuSiO_3{:}H2O$	-4.0	-3.9	-3.4	-3.4	-3.6	-3.7	-3.2	-3.2
Langite	$Cu_4(OH)_6SO_4{:}H_2O$	-12.5	-12.2	-13.2	-12.9	-11.6	-11.7	-10.2	-11.7
Malachite	$Cu_2(OH)_2CO_3$	-3.1	-3.0	-4.3	-4.2	-2.5	-2.7	-2.6	-3.3
Melanothallite	$CuCl_2$	-20.0	-19.9	-22.5	-21.9	-20.0	-20.2	-20.6	-21.5
Nantokite	CuCl	-6.9	-6.7	-9.1	-8.8	-7.2	-7.2	-7.4	-8.3
Tenorite	CuO	-1.7	-1.7	-1.3	-1.3	-1.3	-1.4	-1.0	-1.1
Tsumebite	$Pb_2CuPO_4(OH)_3{:}3H_2O$	-8.3	-8.1	-5.2	-5.3	-10.1	-9.3	-5.9	-5.8

Table 4. Modelled saturation indices of lead-containing mineral phases. Values exceeding -0.5 indicating approximate equilibrium or supersaturation are shown in bold text.

		Event 2				Event 3			
		Biochar		Sand		Biochar		Sand	
Mineral	**Formula**	**16:40**	**18:51**	**16:39**	**18:48**	**20:50**	**22:41**	**20:50**	**22:41**
Anglesite	$PbSO_4$	-7.4	-7.2	-7.2	-7.2	-8.7	-8.1	-6.8	-7.2

Cerussite	$PbCO_3$	-2.5	-2.5	-2.1	-2.2	-3.4	-3.1	-2.3	-2.2
Pb(OH)2	$Pb(OH)_2$	-3.9	-3.9	-1.4	-1.5	-4.4	-4.1	-2.6	-2.0
Tsumebite	$Pb_2CuPO_4(OH)_3{:}3H_2O$	-8.3	-8.1	-5.2	-5.3	-10.1	-9.3	-5.9	-5.8

Table 5. Modelled saturation indices of nickel-containing mineral phases. Values exceeding -0.5 indicating approximate equilibrium or supersaturation are shown in bold text.

		Event 2				**Event 3**			
		Biochar		**Sand**		**Biochar**		**Sand**	
Mineral	**Formula**	**16:40**	**18:51**	**16:39**	**18:48**	**20:50**	**22:41**	**20:50**	**22:41**
Bunsenite	NiO	-7.4	-7.5	-5.1	-5.1	-7.3	-7.4	-6.3	-5.8
Morenosite	$NiSO_4{:}7H_2O$	-11.7	-11.7	-11.8	-11.7	-12.5	-12.3	-11.5	-11.9
$Ni(OH)_2$	$Ni(OH)_2$	-4.1	-4.3	-1.9	-2.0	-4.6	-4.7	-3.6	-3.0
Ni_2SiO_4	Ni_2SiO_4	-7.5	-7.8	-2.8	-2.9	-7.5	-7.7	-5.4	-4.2
$Ni_3(PO_4)_2$	$Ni_3(PO_4)_2$	-19.0	-19.2	-16.8	-16.8	-20.7	-20.5	-17.7	-17.7
$Ni_4(OH)_6SO_4$	$Ni_4(OH)_6SO_4$	-28.8	-29.2	-22.2	-22.2	-30.1	-30.2	-26.0	-24.8
$NiCO_3$	$NiCO_3$	-8.2	-8.3	-7.9	-8.0	-8.3	-8.4	-8.1	-8.1
Retgersite	$NiSO_4{:}6H_2O$	-12.0	-12.1	-12.1	-12.1	-12.8	-12.7	-11.9	-12.3

Table 6. Modelled saturation indices of zinc-containing mineral phases. Values exceeding -0.5 indicating approximate equilibrium or supersaturation are shown in bold text.

		Event 2				**Event 3**			
		Biochar		**Sand**		**Biochar**		**Sand**	
Mineral	**Formula**	**16:40**	**18:51**	**16:39**	**18:48**	**20:50**	**22:41**	**20:50**	**22:41**
Smithsonite	$ZnCO_3$	-2.7	-2.6	-2.8	-2.8	-2.7	-2.5	-2.0	-2.5
Willemite	Zn_2SiO_4	-4.0	-3.7	**0.0**	**0.0**	-3.5	-3.1	**-0.5**	**-0.4**
$Zn(OH)_2$	$Zn(OH)_2$	-3.6	-3.4	-1.7	-1.6	-3.5	-3.3	-2.0	-2.0
$ZnSiO_3$	$ZnSiO_3$	**0.9**	**1.0**	**3.0**	**3.0**	**1.2**	**1.4**	**2.7**	**2.8**

Table 7 Modelled saturation indices of phosphorus-containing mineral phases. Values exceeding -0.5 indicating approximate equilibrium or supersaturation are shown in bold text. Note that these are included in the other tables as well.

		Event 2				**Event 3**			
		Biochar		**Sand**		**Biochar**		**Sand**	
Mineral name	**Formula**	**16:40**	**18:51**	**16:39**	**18:48**	**20:50**	**22:41**	**20:50**	**22:41**
$Cd_3(PO_4)_2$	$Cd_3(PO_4)_2$	-17.1	-17.2	-14.6	-14.8	-17.5	-17.2	-15.3	-14.6
$Cu_3(PO_4)_2$	$Cu_3(PO_4)_2$	-11.8	-11.4	-15.1	-14.8	-12.1	-11.9	-11.1	-13.1
$Cu_3(PO_4)_2{:}3H_2O$	$Cu_3(PO_4)_2{:}3H_2O$	-13.5	-13.1	-16.8	-16.5	-13.8	-13.6	-12.9	-14.9
Hydroxyapatite	$Ca_5(PO_4)_3OH$	-1.2	-1.9	**0.2**	**-0.4**	**0.6**	**-0.2**	-2.6	**-0.4**
$Ni_3(PO_4)_2$	$Ni_3(PO_4)_2$	-19.0	-19.2	-16.8	-16.8	-20.7	-20.5	-17.7	-17.7
Struvite	$MgNH_4PO_4{:}6H_2O$	-33.7	-34.1	-32.2	-32.7	-33.0	-1000	-1000	-1000
Tsumebite	$Pb_2CuPO_4(OH)_3{:}3H_2O$	-8.3	-8.1	-5.2	-5.3	-10.1	-9.3	-5.9	-5.8
Vivianite	$Fe_3(PO_4)_2{:}8H_2O$	-4.1	-3.4	-9.9	-9.9	-7.8	-6.6	-6.0	-8.5

Table 8. Modelled saturation indices of aluminum-containing mineral phases. Values exceeding -0.5 indicating approximate equilibrium or supersaturation are shown in bold text.

		Event 2				**Event 3**			
		Biochar		**Sand**		**Biochar**		**Sand**	
Mineral name	**Formula**	**16:40**	**18:51**	**16:39**	**18:48**	**20:50**	**22:41**	**20:50**	**22:41**
$Al(OH)_3$(amorph.)	$Al(OH)_3$ (am)	**0.1**	**0.3**	**-0.4**	**-0.5**	-0.8	**-0.3**	**-0.1**	**-0.3**

Albite	$NaAlSi_3O_8$	**1.3**	**1.3**	**2.3**	**2.0**	**0.8**	**1.1**	**1.4**	**2.1**
Alunite	$KAl_3(SO_4)_2(OH)_6$	**1.4**	**2.1**	-5.1	-5.1	-2.8	-1.2	-2.0	-4.2
Anorthite	$CaAl_2Si_2O_8$	**0.6**	**0.8**	**1.6**	**1.2**	**-0.3**	**0.3**	**0.7**	**1.4**
Basaluminite	$Al_4SO_4(OH)_{10}:5H_2O$	**4.2**	**5.0**	**-0.5**	**-0.5**	-1.1	**0.9**	**1.9**	**0.0**
Ca-Montmorillonite	$Ca_{0.165}Al_{2.33}Si_{3.67}O_{10}(OH)_2$	**7.2**	**7.6**	**7.0**	**6.6**	**5.0**	**6.0**	**6.9**	**7.0**
Gibbsite	$Al(OH)_3$	**2.9**	**3.1**	**2.4**	**2.3**	**2.0**	**2.4**	**2.7**	**2.5**
HydrotalciteMgAl (Meixnerite*)	$Mg_6Al_2(OH)_{16}(OH)_2$	**41.6**	**40.7**	**52.5**	**51.2**	**43.8**	**42.7**	**41.9**	**47.7**
Illite	$K_{0.6}Mg_{0.25}Al_{2.3}Si_{3.5}O_{10}(OH)_2$	**7.0**	**7.3**	**7.0**	**6.6**	**5.3**	**6.2**	**6.3**	**6.8**
Jurbanite	$AlSO_4OH$	-5.0	-4.7	-7.9	-7.8	-6.7	-6.1	-6.0	-7.2
Kaolinite	$Al_2Si_2O_5(OH)_4$	**7.8**	**8.1**	**7.1**	**6.9**	**5.8**	**6.7**	**7.5**	**7.3**
K-feldspar	$KAlSi_3O_8$	**3.3**	**3.3**	**3.3**	**3.0**	**2.8**	**3.1**	**2.4**	**3.0**
K-mica	$KAl_3Si_3O_{10}(OH)_2$	**14.6**	**15.1**	**13.6**	**13.2**	**12.3**	**13.5**	**13.4**	**13.5**

* Boclair & Braterman 1999

Table 9. Modelled saturation indices of iron-containing mineral phases. Values exceeding -0.5 indicating approximate equilibrium or supersaturation are shown in bold text.

		Event 2				**Event 3**			
		Biochar		**Sand**		**Biochar**		**Sand**	
Mineral	**Formula**	**16:40**	**18:51**	**16:39**	**18:48**	**20:50**	**22:41**	**20:50**	**22:41**
Cupric ferrite	$CuFe_2O_4$	**14.7**	**14.9**	**16.7**	**16.5**	**14.5**	**14.6**	**16.3**	**16.5**
Cuprous ferrite	$CuFeO_2$	**13.7**	**13.9**	**13.7**	**13.7**	**13.3**	**13.4**	**14.3**	**13.9**
$Fe(OH)_3$(amorph.)	$Fe(OH)_3$ (am)	**2.8**	**2.8**	**3.6**	**3.5**	**2.3**	**2.5**	**3.1**	**3.2**
Goethite	FeOOH	**8.3**	**8.3**	**9.1**	**9.0**	**8.0**	**8.1**	**8.7**	**8.8**
Hematite	Fe_2O_3	**18.5**	**18.6**	**20.1**	**19.9**	**17.9**	**18.2**	**19.3**	**19.7**
Hydrotalcite MgFe	$Mg_6Fe_2(OH)_{16}(OH)_2$	**33.6**	**32.4**	**47.2**	**45.7**	**37.2**	**35.5**	**35.3**	**41.8**
Jarosite-K	$KFe_3(SO_4)_2(OH)_6$	-2.8	-2.5	-5.1	-5.3	-4.8	-4.1	-4.1	-5.1
Jarosite-Na	$NaFe_3(SO_4)_2(OH)_6$	-6.0	-5.8	-7.3	-7.5	-8.0	-7.4	-6.3	-7.2
Melanterite	$FeSO_4:7H_2O$	-8.3	-8.1	-11.1	-11.0	-9.9	-9.4	-9.3	-10.5
Schwertmannite	$Fe_8O_8(OH)6SO_4$	**23.6**	**24.2**	**27.6**	**26.8**	**19.4**	**20.7**	**25.2**	**25.6**
Siderite	$FeCO_3$	**-0.5**	**-0.4**	-2.9	-3.0	-1.4	-1.2	-1.6	-2.3
Vivianite	$Fe_3(PO_4)_2:8H_2O$	-4.1	-3.4	-9.9	-9.9	-7.8	-6.6	-6.0	-8.5

Table 10. Modelled saturation indices of magnesium-containing mineral phases. Values exceeding -0.5 indicating approximate equilibrium or supersaturation are shown in bold text.

		Event 2				**Event 3**			
		Biochar		**Sand**		**Biochar**		**Sand**	
Mineral	**Formula**	**16:40**	**18:51**	**16:39**	**18:48**	**20:50**	**22:41**	**20:50**	**22:41**
Brucite	$Mg(OH)_2$	-4.6	-4.8	-2.6	-2.8	-3.9	-4.2	-4.4	-3.4
Chlorite	$Mg_5Al_2Si_3O_{10}(OH)_8$	-1.7	-2.5	**8.0**	**6.7**	**1.3**	**0.6**	**0.0**	**5.2**
Chrysotile	$Mg_3Si_2O_5(OH)_4$	-5.8	-6.4	**0.8**	**0.0**	-3.0	-3.9	-4.6	-1.2
Dolomite	$CaMg(CO_3)_2$	**-0.4**	-0.8	-0.7	-1.1	**0.9**	**0.3**	-1.8	-0.9
HydrotalciteMgAl (Meixnerite *)	$Mg_6Al_2(OH)_{16}(OH)_2$	**41.6**	**40.7**	**52.5**	**51.2**	**43.8**	**42.7**	**41.9**	**47.7**
HydrotalciteMgFe	$Mg_6Fe_2(OH)_{16}(OH)_2$	**33.6**	**32.4**	**47.2**	**45.7**	**37.2**	**35.5**	**35.3**	**41.8**
Sepiolite	$Mg_2Si_3O_{7.5}OH:3H_2O$	-3.4	-3.8	**1.3**	**0.7**	-1.8	-2.4	-2.7	**-0.2**
Struvite	$MgNH_4PO_4:6H_2O$	-33.7	-34.1	-32.2	-32.7	-33.0	-1000	-1000	-1000
Talc	$Mg_3Si_4O_{10}(OH)_2$	-2.0	-2.6	**5.0**	**4.1**	**0.8**	**-0.1**	-0.6	**3.0**

* Boclair & Braterman 1999

Table 11. Modelled saturation indices of manganese-containing mineral phases. Values exceeding -0.5 indicating approximate equilibrium or supersaturation are shown in bold text.

		Event 2				Event 3			
		Biochar		Sand		Biochar		Sand	
Mineral	**Formula**	**16:40**	**18:51**	**16:39**	**18:48**	**20:50**	**22:41**	**20:50**	**22:41**
Hausmannite	Mn_3O_4	-13.2	-13.5	-4.7	-5.3	-12.6	-13.5	-11.0	-7.3
Manganite	MnOOH	-4.5	-4.6	-1.3	-1.5	-4.5	-4.9	-3.9	-2.5
Pyrochroite	$Mn(OH)_2$	-6.1	-6.2	-4.1	-4.3	-6.5	-6.7	-6.0	-5.0
Pyrolusite	MnO_2:H_2O	-10.6	-10.8	-6.1	-6.4	-9.7	-10.1	-9.1	-7.2
Rhodochrosite	$MnCO_3$	**-0.3**	**-0.4**	**-0.3**	**-0.5**	-0.8	-1.0	-1.1	-0.6

Table 12. Modelled saturation indices of other mineral phases. Values exceeding -0.5 indicating approximate equilibrium or supersaturation are shown in bold text.

		Event 2				Event 3			
		Biochar		Sand		Biochar		Sand	
Mineral name	**Formula**	**16:40**	**18:51**	**16:39**	**18:48**	**20:50**	**22:41**	**20:50**	**22:41**
Anhydrite	$CaSO_4$	-3.6	-3.7	-4.3	-4.4	-3.5	-3.6	-4.2	-4.2
Aragonite	$CaCO_3$	**-0.1**	**-0.3**	**-0.5**	-0.7	**0.5**	**0.2**	-0.9	-0.5
Calcite	$CaCO_3$	**0.1**	**-0.2**	**-0.3**	**-0.5**	**0.6**	**0.3**	-0.9	**-0.4**
Chalcedony	SiO_2	**0.1**	**0.1**	**0.3**	**0.3**	**0.1**	**0.1**	**0.2**	**0.3**
Gypsum	$CaSO_4$:$2H_2O$	-3.2	-3.3	-3.9	-3.9	-3.1	-3.2	-3.8	-3.8
Halite	NaCl	-7.2	-7.4	-7.7	-7.6	-7.0	-7.2	-7.7	-7.7
Hydroxyapatite	$Ca_5(PO_4)_3OH$	-1.2	-1.9	**0.2**	**-0.4**	**0.6**	**-0.2**	-2.6	**-0.4**
Quartz	SiO_2	**0.6**	**0.6**	**0.8**	**0.7**	**0.5**	**0.6**	**0.2**	**0.7**
SiO_2 (amorph.)	SiO_2 (am)	-0.8	-0.8	**-0.5**	-0.6	-0.8	-0.8	-0.7	-0.6
Sylvite	KCl	-7.2	-7.4	-8.7	-8.6	-6.9	-7.1	-8.8	-8.7

Appendix 6. Spearman correlation matrices

Table 1. Correlation between the analyzed parameters in the untreated stormwater. Spearman correlation coefficients above the diagonal and significance (2-tailed) below the diagonal. Spearman correlations above 0.8 and below -0.8 are shown in bold. $NO_{2,3}$ stands for NO2+NO3 (nitrite and nitrate).

		TSS	pH	EC	ALK	REDOX	TURB	UV	NH_4	TN	$NO_{2,3}$	TOC	DOC	PO_4	TP	Cd	Cu	Pb	Ni	Zn
	N	***44***	***44***	***44***	***44***	***44***	***44***	***44***	***16***	***44***	***44***	***44***	***44***	***44***	***44***	***16***	***16***	***16***	***16***	***16***
TSS	***44***	-	.648**	.412**	.569**	.456**	**.863****	.341*	-0.024	-0.161	-0.069	0.195	0.178	.579**	**.979****	**.891****	**.830****	**.922****	**.876****	.739**
pH	***44***	0.000	-	.597**	**.814****	.510**	.769**	0.257	-0.284	-0.072	0.024	0.152	0.112	.629**	.643**	0.026	0.133	0.304	0.124	-0.206
EC	***44***	0.005	0.000	-	**.895****	0.135	.584**	**.814****	0.450	.567**	.649**	.734**	.706**	.470**	.498**	0.119	0.349	-0.021	0.256	0.331
ALK	***44***	0.000	0.000	0.000	-	.366*	.747**	.652**	.576*	.340*	.458**	.549**	.518**	.614**	.630**	0.314	.511*	0.21	0.424	0.235
REDOX	***44***	0.002	0.000	0.384	0.015	-	.489**	-0.049	-0.018	-0.280	-0.230	-0.118	-0.153	.628**	.413**	0.347	0.25	.638**	0.409	-0.09
TURB	***44***	0.000	0.000	0.000	0.000	0.001	-	.351*	0.209	-0.148	0.057	0.180	0.151	.739**	**.872****	.764**	.787**	**.969****	**.871****	.572*
UV	***44***	0.024	0.092	0.000	0.000	0.750	0.020	-	0.368	.750**	.687**	**.969****	**.956****	0.278	.405**	0.172	0.33	-0.127	0.237	0.39
NH_4	***16***	0.931	0.286	0.080	0.019	0.948	0.438	0.161	-	.771**	**.826****	.500*	0.494	0.150	0.165	0.44	0.143	0.086	0.095	0.071
TN	***44***	0.296	0.644	0.000	0.024	0.065	0.337	0.000	0.000	-	**.810****	**.851****	**.849****	-0.137	-0.084	-0.098	-0.021	-0.496	-0.144	0.203
$NO_{2,3}$	***44***	0.657	0.878	0.000	0.002	0.133	0.716	0.000	0.000	0.000	-	.720**	.710**	-0.075	0.018	-0.012	0.084	-0.332	-0.038	0.213
TOC	***44***	0.204	0.324	0.000	0.000	0.447	0.243	0.000	0.049	0.000	0.000	-	**.994****	0.145	0.253	0.071	0.209	-0.25	0.109	0.315
DOC	***44***	0.248	0.468	0.000	0.000	0.320	0.328	0.000	0.052	0.000	0.000	0.000	-	0.100	0.236	0.071	0.209	-0.25	0.109	0.315
PO_4	***44***	0.000	0.000	0.001	0.000	0.000	0.000	0.068	0.579	0.375	0.629	0.347	0.518	-	.600**	0.313	0.467	.641**	.526*	0.093
TP	***44***	0.000	0.000	0.001	0.000	0.005	0.000	0.006	0.542	0.587	0.905	0.098	0.123	0.000	-	**.920****	**.886****	**.917****	**.918****	.789**
Cd	***16***	0	0.925	0.66	0.236	0.188	0.001	0.524	0.275	0.719	0.964	0.793	0.793	0.238	0	-	**.932****	**.833****	**.931****	**.857****
Cu	***16***	0	0.624	0.185	0.043	0.35	0	0.212	0.736	0.94	0.757	0.437	0.437	0.069	0	0	-	**.820****	**.960****	**.864****
Pb	***16***	0	0.252	0.939	0.436	0.008	0	0.639	0.84	0.051	0.209	0.351	0.351	0.007	0	0	0	-	**.894****	.622*
Ni	***16***	0	0.648	0.339	0.102	0.116	0	0.377	0.823	0.594	0.888	0.688	0.688	0.036	0	0	0	0	-	**.811****
Zn	***16***	0.001	0.445	0.21	0.38	0.741	0.02	0.135	0.867	0.451	0.427	0.235	0.235	0.733	0	0	0	0.01	0	-

* Correlation is significant at the 0.05 level (2-tailed).

** Correlation is significant at the 0.01 level (2-tailed).

Table 2. Correlation between the analyzed parameters in the sand-biochar filter effluent. Spearman correlation coefficients above the diagonal and significance (2-tailed) below the diagonal. Spearman correlations above 0.8 and below -0.8 are shown in bold. $NO_{2,3}$ stands for NO_2+NO_3 (nitrite and nitrate).

		TSS	pH	EC	ALK	REDOX	TURB	UV	NH_4	TN	$NO_{2,3}$	TOC	DOC	PO_4	TP	Cd	Cu	Pb	Ni	Zn	Q
	N	***40***	***40***	***40***	***40***	***40***	***40***	***40***	***40***	***40***	***40***	***40***	***26***	***40***	***40***	***18***	***18***	***18***	***18***	***18***	***40***
TSS	***40***	-	**-.807****	-.775**	**-.887****	.316*	**.987****	-.524**	.315*	-0.11	0.11	-.499**	-.400*	**-.884****	**.806****	.471*	-.769**	0.253	0.355	-0.204	-.403**
pH	***40***	0	-	**.808****	.778**	-0.187	**-.823****	.418**	-0.129	.354*	0.139	0.299	.418*	.727**	-.712**	-0.273	**.819****	-0.377	-.482*	0.118	.364*
EC	***40***	0	0	-	**.946****	-0.289	-.777**	.776**	0.041	0.091	-0.211	.548**	0.375	.667**	-.537**	-0.347	.663**	-0.222	-0.212	0.111	.629**
ALK	***40***	0	0	0	-	-.338*	**-.882****	.767**	-0.124	0.129	-0.177	.653**	.445*	**.810****	-.669**	-0.395	.707**	-0.25	-0.263	0.124	.645**
REDOX	***40***	0.047	0.248	0.071	0.033	-	0.235	-0.192	.322*	0.287	0.216	0.003	0.312	-0.145	.418**	0.235	0.292	-0.4	-.608**	-0.312	0.035
TURB	***40***	0	0	0	0	0.144	-	-.496**	.313*	-0.156	0.089	-.511**	-.423*	**-.901****	.767**	0.432	-.775**	0.307	0.4	-0.178	-.414**
UV	***40***	0.001	0.007	0	0	0.236	0.001	-	0.251	0.066	-0.274	.752**	.509**	.409**	-.320*	-0.075	.483*	-0.009	0.014	-0.067	.742**
NH_4	***40***	0.048	0.429	0.802	0.446	0.043	0.049	0.118	-	0.046	-0.068	0.153	.478*	-0.278	.462**	0.357	0.032	0.114	0.232	-0.26	0.217
TN	***40***	0.499	0.025	0.578	0.428	0.073	0.337	0.684	0.779	-	.765**	.326*	.568**	.353*	-0.264	0.009	.615**	-.623**	**-.827****	-0.233	0.292
$NO_{2,3}$	***40***	0.498	0.394	0.19	0.274	0.18	0.583	0.087	0.678	0	-	0.025	.438*	0.188	-0.159	-0.234	.614**	-.665**	-.792**	0.101	0.114
TOC	***40***	0.001	0.061	0	0	0.985	0.001	0	0.344	0.04	0.879	-	**.971****	.602**	-.335*	0.278	.628**	-0.341	-.522*	-0.166	**.810****
DOC	***26***	0.043	0.034	0.059	0.023	0.121	0.031	0.008	0.013	0.002	0.025	0	-	.677**	-0.154	0.181	.678**	-0.444	-.631**	-0.212	**.832****
PO_4	***40***	0	0	0	0	0.371	0	0.009	0.083	0.026	0.246	0	0	-	-.745**	-0.149	.770**	-0.459	-.641**	-0.012	.561**
TP	***40***	0	0	0	0	0.007	0	0.044	0.003	0.099	0.326	0.035	0.454	0	-	0.466	-.633**	-0.056	0.386	-.659**	-0.225
Cd	***18***	0.049	0.274	0.158	0.105	0.347	0.074	0.769	0.145	0.972	0.349	0.264	0.472	0.555	0.051	-	-0.345	-0.09	-0.079	-0.466	0.126
Cu	***18***	0	0	0.003	0.001	0.24	0	0.042	0.899	0.007	0.007	0.005	0.002	0	0.005	0.161	-	-0.201	-.511*	0.282	.597**
Pb	***18***	0.311	0.123	0.376	0.318	0.1	0.215	0.97	0.653	0.006	0.003	0.166	0.065	0.055	0.826	0.722	0.424	-	.679**	.560*	-0.433
Ni	***18***	0.149	0.043	0.398	0.292	0.007	0.1	0.957	0.355	0	0	0.026	0.005	0.004	0.114	0.754	0.03	0.002	-	0.159	-.574*
Zn	***18***	0.416	0.642	0.66	0.624	0.207	0.479	0.793	0.298	0.351	0.69	0.512	0.397	0.961	0.003	0.051	0.257	0.016	0.529	-	-0.28
Q	***40***	0.01	0.021	0	0	0.83	0.008	0	0.178	0.067	0.483	0	0	0	0.162	0.619	0.009	0.073	0.013	0.26	-

* Correlation is significant at the 0.05 level (2-tailed).

** Correlation is significant at the 0.01 level (2-tailed).

Table 3. Correlation between the analyzed parameters in the sand filter effluent. Spearman correlation coefficients above the diagonal and significance (2-tailed) below the diagonal. Spearman correlations above 0.8 and below -0.8 are shown in bold. $NO_{2,3}$ stands for NO_2+NO_3 (nitrite and nitrate).

		TSS	**pH**	**EC**	**ALK**	**REDOX**	**TURB**	**UV**	**NH_4**	**TN**	**$NO_{2,3}$**	**TOC**	**DOC**	**PO_4**	**TP**	**Cd**	**Cu**	**Pb**	**Ni**	**Zn**	**Q**
	N	***38***	***38***	***38***	***38***	***38***	***38***	***38***	***38***	***38***	***38***	***38***	***26***	***38***	***38***	***17***	***17***	***17***	***17***	***17***	***38***
TSS	***38***	-	**.868****	0.178	-0.295	-.672**	**.931****	.505**	**.843****	0.239	0.23	-0.026	-0.187	-0.221	**.843****	-0.165	-.711**	.778**	.755**	-.708**	0.19
pH	***38***	0	-	-0.063	-0.279	-.689**	**.859****	.452**	.753**	0.102	0.075	-0.112	-0.098	-0.029	**.809****	-0.167	-.716**	.770**	**.809****	-.727**	0.268
EC	***38***	0.286	0.706	-	.579**	0.157	-0.024	.412*	-0.061	.352*	.339*	.395*	.557**	-0.248	0.063	0.242	0.337	-0.341	-0.264	0.125	-0.124
ALK	***38***	0.073	0.09	0	-	.481**	-.434**	-0.021	-.625**	-0.248	-0.256	.390*	.724**	.471**	-.397*	.537*	.491*	-0.407	-0.431	0.279	0.275
REDOX	***38***	0	0	0.346	0.002	-	-.638**	-0.118	-.696**	-.345*	-.344*	.443**	.612**	.356*	-.526**	0.407	**.826****	-.637**	-.710**	**.812****	0.172
TURB	***38***	0	0	0.888	0.006	0	-	.557**	**.843****	0.089	0.073	0.022	-0.091	-0.107	**.822****	-0.192	-.654**	**.807****	.784**	-.622**	0.292
UV	***38***	0.001	0.004	0.01	0.902	0.48	0	-	.333*	0.102	0.049	.522**	.451*	-0.053	.549**	0.156	-0.108	0.452	.562*	-0.156	0.269
NH_4	***38***	0	0	0.716	0	0	0	0.041	-	.437**	.434**	-0.243	-.720**	-.478**	**.822****	-0.456	-.718**	.724**	.696**	-.577*	-0.1
TN	***38***	0.149	0.544	0.03	0.134	0.034	0.594	0.542	0.006	-	**.991****	-0.252	-.759**	**-.912****	0.212	-.587*	-.521*	0.206	0.31	-0.365	**-.844****
$NO_{2,3}$	***38***	0.165	0.654	0.037	0.121	0.034	0.664	0.77	0.006	0	-	-0.283	-.789**	**-.917****	0.192	-.606**	-.512*	0.206	0.224	-0.337	**-.854****
TOC	***38***	0.879	0.502	0.014	0.015	0.005	0.896	0.001	0.141	0.127	0.085	-	**.911****	0.313	-0.047	0.463	.503*	-0.275	-0.126	0.442	.447**
DOC	***26***	0.36	0.632	0.003	0	0.001	0.66	0.021	0	0	0	0	-	.746**	-0.251	.606**	.568*	-0.254	-0.294	0.473	.672**
PO_4	***38***	0.182	0.861	0.133	0.003	0.028	0.524	0.754	0.002	0	0	0.056	0	-	-0.231	.573*	.497*	-0.22	-0.284	0.304	**.854****
TP	***38***	0	0	0.709	0.014	0.001	0	0	0	0.202	0.248	0.778	0.217	0.164	-	-0.314	-.708**	.613**	.626**	-.570*	0.162
Cd	***17***	0.527	0.522	0.35	0.026	0.105	0.46	0.55	0.066	0.013	0.01	0.061	0.01	0.016	0.219	-	0.287	-0.012	-0.157	0.234	0.402
Cu	***17***	0.001	0.001	0.185	0.045	0	0.004	0.68	0.001	0.032	0.036	0.04	0.017	0.042	0.001	0.264	-	-0.471	-.579*	**.901****	0.467
Pb	***17***	0	0	0.181	0.105	0.006	0	0.069	0.001	0.429	0.429	0.286	0.325	0.395	0.009	0.965	0.057	-	.565*	-0.368	0.028
Ni	***17***	0	0	0.305	0.084	0.001	0	0.019	0.002	0.226	0.388	0.63	0.252	0.269	0.007	0.547	0.015	0.018	-	-.708**	-0.026
Zn	***17***	0.001	0.001	0.633	0.278	0	0.008	0.549	0.015	0.149	0.186	0.076	0.055	0.236	0.017	0.366	0	0.146	0.001	-	0.284
Q	***38***	0.254	0.104	0.458	0.095	0.302	0.075	0.102	0.551	0	0	0.005	0	0	0.33	0.109	0.058	0.914	0.921	0.269	-

* Correlation is significant at the 0.05 level (2-tailed).

** Correlation is significant at the 0.01 level (2-tailed).